Susana Isabel Guerreiro Rodrigues

Development of polysaccharide-based carriers for pulmonary tuberculosis therapy

UAlg
UNIVERSIDADE DO ALGARVE

2019

Susana Isabel Guerreiro Rodrigues

Development of polysaccharide-based carriers for pulmonary tuberculosis therapy

PhD Programme in Mechanisms of Disease and Regenerative Medicine

Work developed under supervision of:
Prof. Doctor Ana M Grenha

2019

This page was intentionally left in blank

Development of polysaccharide-based carriers for pulmonary tuberculosis therapy

Declaração de autoria de trabalho

Declaro ser a autora deste trabalho, que é original e inédito. Autores e trabalhos consultados estão devidamente citados no texto e constam na listagem de referências incluída.

This page was intentionally left in blank

This work has been performed at:

Drug Delivery Laboratory
CBMR- Centre for Biomedical Research
CCMAR – Centro de Ciências do Mar
Faculdade de Ciências e Tecnologia – Universidade do Algarve
Campus Gambelas, 8005-139 Faro
PORTUGAL

Food and Drug Department, University of Parma, Italy

Martin-Luther-Universität Halle-Wittenberg
Halle (Saale), Germany

This work was supported by National Portuguese funding through FCT – Fundação para a Ciência e a Tecnologia, scholarship PD/BD/52426/2013 and projects PTDC/DTP-FTO/0094/2012, UID/Multi/04326/2013 and UID/BIM/04773/2013.

This page was intentionally left in blank

Acknowledgments

Este trabalho não seria possível sem o apoio da minha orientadora profª Ana Grenha, o meu muito obrigada por me ter guiado por estes longos anos de experiências pré e durante doutoramento, um grande Obrigada por todo o apoio e oportunidades criadas, foram mais de 8 anos de aprendizagem, de crescimento pessoal e profissional.

Quero agradecer às várias colaborações dentro da UAlg particularmente à Prof. Ana Costa por todo o apoio na purificação e marcação dos polímeros, à Prof. Leonor Faleiro pela ajuda nos ensaios com as bactérias, à Prof. Debora Power e às suas alunas Soraia e Liliana pela ajuda com as analises das amostras *in vivo*, aos técnicos do CBMR Maurícia Vinhas e Vítor Fernandes pelo apoio na citometria de fluxo.

Agradeço as oportunidades de colaboração com a Prof. Manuela Gaspar em Lisboa onde foi possível realizar o ensaio *in vivo* e a Prof Anabela Pinto Rolo em Coimbra onde foram analisados os soros dos animais.

Would like to thank Prof. Francesca Buttini from Parma University for let me be in her laboratory for 2 months and for all the help and knowledge shared. From Parma would like to thank also the support and friendship of Adryana, Irene and Judith.

Would like to thank Prof Lea Ann Dailey for open her laboratory to me in Martin-Luther-Universität Halle-Wittenberg for more than 3 months, for all the help, support and knowledge shared. Special thanks to Julia Kollan for the help with Cytation5 and cell culture, and Paola and Gabriela for sharing the office, for the personal help away from home and all the good moments shared.

Agradeço à Maria do CEDOC a disponibilidade de partilha da estirpe *M. Bovis* BCG para a realização dos ensaios na UAlg.

Um agradecimento especial a todos os colegas do 2.22 foram 8 anos de muito companheirismo a aprendizagem mútua. Marita Dionisio e André Santos colegas do início da vida laboratorial e amigos para a vida toda. Aos colegas Ana Alves, Filipa Guerreiro, Gisela Serrão, Jorge Pontes, Ludmylla Cunha, Tatiana Martins, Luis Brás, Flávia Musachio e Patricia Madureira.

Agradeço a todos os colegas ProRegeM mas especialmente ao grupo pioneiro 2014, Aline, André, Dino, Diogo Bitoque, Helena, João Cardeira, Margarida e Om, serão sempre os meus partners in crime.
Aos amigos que apesar dos meus muitos momentos de desanimo nunca desistiram de me puxar para cima: Alisson Ascenso, Ana Constantino, Andreia e Eduardo, Carina Tomás, Joana Apolónio, João Santos, Soraia Vitorino e em especial à prima Joana a companhia para todas as ocasiões.

Por último, mas um mais especial agradecimento ao apoio da família, especialmente aos pais Cidália e Armando Rodrigues, irmão Paulo André e aos avós Idalina e Manuel, o primeiro engenheiro da família apesar de não saber ler nem escrever. Sem eles nada disto seria possível.

Muito Obrigada por tudo,
Thank you all,

Susana Rodrigues

Resumo

A tuberculose é uma doença infeciosa provocada pelo *Mycobacterium tuberculosis*. A transmissão da bactéria ocorre por via inalatória, após o que a mesma se aloja nos macrófagos existentes na região alveolar. A bactéria tem a capacidade de sobreviver e multiplicar-se mesmo depois de fagocitada pelos macrófagos alveolares, podendo ficar em estado latente por vários meses e até anos. Apesar de existir uma vacina contra a doença, a denominada BCG, de *Bacillus Calmette-Guérin*, esta não é totalmente eficaz e muitas pessoas desenvolvem a doença apesar de imunizadas. A tuberculose continua a ser a principal causa de morte evitável a nível mundial e está a reaparecer na Europa, estando muito associada aos casos de co-morbilidade com o vírus da imunodeficiência humana (VIH). Segundo a Organização Mundial de Saúde (OMS), a terapia da tuberculose é obrigatoriamente combinada, para potenciar a eficácia do tratamento. Neste contexto, a isoniazida (INH) e a rifabutina (RFB) são dois dos fármacos de primeira linha utilizados, a última usada particularmente nos casos em que o doente apresenta também infeção por VIH. Estas moléculas apresentam características diferentes, nomeadamente em termos de massa molecular e afinidade aquosa. A INH é uma molécula hidrofílica com 137 g/mol, enquanto a RFB tem 847 g/mol e é hidrofóbica, exigindo solventes orgânicos ou soluções ácidas para dissolver.

Considerando a tuberculose pulmonar como a principal manifestação da doença, a administração direta de antibióticos ao pulmão e, particularmente, aos alvéolos, onde residem os macrófagos que atuam como hospedeiros da bactéria, compreende uma abordagem muito promissora, permitindo a entrega de fármacos no local primário da infeção. Esta estratégia implica o desenvolvimento de formulações para inalação, requerendo o uso de transportadores de fármacos que exibam propriedades aerodinâmicas adequadas para alcançar a região alveolar, onde residem os macrófagos que podem, assim, internalizar os fármacos. A literatura mostra que, para alcançar esta zona do pulmão, os transportadores devem ter um diâmetro aerodinâmico entre 1 e 5 μm. Na realidade, devido à geometria dos pulmões, as partículas a utilizar como transportadores precisam de ter um tamanho suficientemente pequeno para entrar nas vias aéreas inferiores, mas a sua massa deve ser suficiente para

impedir que sejam exaladas juntamente com o ar expirado, o que justifica o intervalo de diâmetros referido anteriormente e a frequente utilização de micropartículas para inalação. A opção pela utilização de transportadores como veículos dos fármacos requer também que a matriz constituinte das partículas seja o mais inerte possível, não induzindo toxicidade ou reações de inflamação. Neste sentido, os materiais de origem natural e, particularmente, os polímeros como os polissacáridos, são reportados como tendo maior probabilidade de exibir biocompatibilidade e biodegradabilidade, duas características essenciais para uma aplicação na área da administração de fármacos. Considerando que o agente patogénico se aloja nos macrófagos alveolares, os fármacos devem alcançar este compartimento intracelular antes de ocorrer a sua libertação a partir do transportador inalado, o que ficará facilitado pela internalização dos próprios transportadores pelas células. Para melhorar este processo de internalização, alguns trabalhos reportam a funcionalização da superfície das partículas com ligandos que são reconhecidos pelos recetores dos macrófagos. Alguns polímeros naturais apresentam uma importante vantagem a esse respeito, sendo compostos por unidades estruturais que são reconhecidas diretamente por vários recetores dos macrófagos. O sulfato de condroitina (ChS) e a k-carragenina (CRG) são dois exemplos desses polímeros naturais. O primeiro é composto por unidades alternadas de *N*-acetilgalactosamina e ácido glucurónico, enquanto o último contém resíduos de galactose-4-sulfato e galactose anidra. Ambos estão reportados como sendo reconhecidos especificamente pelos macrófagos, bem como por proporcionarem a ativação destas células.

Neste trabalho, foram produzidas micropartículas por um processo de atomização, as quais contêm os fármacos modelo (INH e RFB) de forma combinada, respeitando assim as indicações da Organização Mundial da Saúde. Os fármacos foram sempre associados às micropartículas numa razão de massa polímero/INH/RFB de 10/1/0.5. À formulação produzida com CRG, adicionou-se um outro polímero de matriz de forma a mitigar o potencial inflamatório que tem sido reportado para a CRG na literatura. As micropartículas foram, neste caso, preparadas com uma relação de massa de amido/CRG de 8/2. Esta formulação obteve um rendimento de produção de 70% e associou efetivamente 96% da INH e 74% da RFB. Ao analisar o diâmetro aerodinâmico foi verificado que este

variou entre 3.3 μm e 3.9 μm e obteve-se uma percentagem de partículas finas de 32% - 38%. Estes valores seriam satisfatórios não fosse a deposição de aproximadamente 50% das partículas na zona correspondente à garganta. Por esse motivo, identificou-se a necessidade de aperfeiçoamento desta formulação para utilização futura. Por outro lado, para as micropartículas compostas por ChS como material de matriz, foram testados dois solventes (etanol e ácido clorídrico) para solubilização da RFB, avaliando-se qual dos dois conduz à obtenção de partículas com melhores características. Ambas as formulações evidenciaram micropartículas de forma esférica, com uma superfície tendencialmente mais rugosa após a associação dos fármacos. Os rendimentos de produção foram bastante satisfatórios, na ordem dos 80%, e os fármacos foram associados com eficácia de 95% para INH e 59-69% para RFB. Apesar de ambas as formulações apresentarem diâmetros aerodinâmicos semelhantes (3.8 – 4.0 μm), as micropartículas produzidas com etanol demonstraram melhores resultados, registando uma maior percentagem de partículas finas (43% contra 35% nas micropartículas preparadas com HCl), o que reflete melhor capacidade para alcançar a região respiratória e uma maior dose de fármaco contida na fração de partículas finas que alcançarão a zona alveolar. Acresce que esta formulação permitiu ainda maior controlo sobre a libertação dos fármacos associados, nomeadamente da RFB. Desta forma, a formulação de micropartículas em que o etanol foi utilizado como solvente, foi selecionada para prosseguir os ensaios de biocompatibilidade em células. Na formulação de micropartículas com matriz à base de amido/CRG não foi possível testar a utilização de etanol, uma vez que o protocolo de preparação implica o recurso a um banho de água quente durante o processo de atomização, o qual levaria à evaporação do solvente. Assim se justifica que essas micropartículas tenham sido produzidas unicamente com ácido clorídrico como co-solvente.

A atividade inibitória dos fármacos modelo contra a *M. bovis* BCG foi mantida após o processo de microencapsulação por atomização em todas as formulações, independentemente dos materiais de matriz e dos solventes utilizados, o que indica a adequação do método de produção das micropartículas. Por forma a avaliar o perfil de citotoxicidade das micropartículas desenvolvidas, foram realizados ensaios em diferentes linhas celulares humanas, variando concentrações e tempos de exposição (até 24 h). As

micropartículas foram testadas em células epiteliais alveolares (A549) e em macrófagos derivados de monócitos (dTHP-1), ambos de grande relevância no contexto da tuberculose pulmonar. Verificou-se que as micropartículas compostas por amido/CRG podem apresentar algumas limitações, com algum nível de toxicidade indesejável, ao contrário das micropartículas com matriz de ChS, que mantiveram os níveis de viabilidade celular acima de 70% em todas as condições testadas. Os macrófagos derivados de monócitos foram ainda utilizados para testar quer a capacidade das células para capturar as micropartículas, quer a capacidade das últimas para induzir a ativação dos macrófagos. O ensaio de captura macrofágica demonstrou que, em comparação, as micropartículas de ChS conseguem um maior nível de internalização para um tempo de exposição e uma dose semelhante. Por outro lado, a produção de interleucinas (TNF-α e IL-8) pelas células foi mais pronunciada após contacto com as micropartículas de amido/CRG, indicando uma maior apetência destas para ativar os macrófagos mesmo a concentrações mais baixas.

Considerando os bons resultados obtidos com as micropartículas com matriz de ChS, a avaliação do seu perfil toxicológico foi aprofundada por meio da realização de um estudo multiparamétrico, o qual recorreu à utilização de macrófagos de ratinho (células J774A.1). O estudo envolveu a incubação das células com concentrações não tóxicas dos materiais, realizando-se posteriormente, por microscopia de fluorescência, uma análise de conteúdos específicos que indicam a resposta celular. Os parâmeros analisados foram a atividade mitocondrial, a área da célula, a área do núcleo, a permeabilidade da membrana, o conteúdo de fosfolípidos (fosfolipidose) e o conteúdo de lípidos neutros (esteatose). Após incubação com as micropartículas de ChS (produzidas com etanol), não foi verificada nenhuma alteração nos parâmetros estudados. Apenas para a RFB na forma livre se verificou uma alteração da quantidade de fosfolípidos existentes quando comparado com o controlo de células não expostas. Contudo, estas alterações apenas se verificaram em concentrações de fármaco muito mais elevadas do que as presentes nas micropartículas, pelo que se acredita que a níveis terapêuticos não ocorrerão as alterações verificadas, o que foi sugerido também quando se testaram as micropartículas com fármaco.

Foi realizado também um estudo preliminar *in vivo* em ratinhos BALB/c, no qual os animais foram expostos a micropartículas sem fármaco. Devido ao facto dos materiais de matriz utilizados neste trabalho, o sulfato de condroitina e o amido/CRG, não terem utilização reportada para via inalatória, considerou-se relevante fazer uma análise preliminar da resposta dos animais ao contacto com os mesmos. Foram testadas as micropartículas quer de ChS, quer de amido/CRG, as quais foram administradas aos ratinhos por inalação, num total de dez aplicações num intervalo temporal de duas semanas. Após o sacrifício dos animais foi avaliado o índice tecidular de diferentes órgãos, nomeadamente fígado, pulmão e rim, e realizada a análise de esfregaços sanguíneos, de modo a verificar o tipo de leucócitos presentes. Não foram observadas alterações do índice tecidular de nenhum dos órgãos analisados, nem se registaram modificações das percentagens dos vários leucócitos constituintes do sangue, para nenhuma das formulações de micropartículas. Os níveis séricos de ALT, AST e LDH, marcadores de alterações tecidulares, também não demonstraram alterações significativas, o que indica a tolerância dos animais ao contacto com as micropartículas e os seus materiais constituintes.

As formulações desenvolvidas ao longo deste trabalho demonstraram possuir características adequadas para a entrega de fármacos por via inalatória, com o propósito de alcançar a região alveolar e proporcionar um direcionamento para os macrófagos. No geral, a formulação com matriz de sulfato de condroitina (ChS/INH/RFB), produzida utilizando etanol como co-solvente, foi a que demonstrou melhores propriedades, sendo aquela identificada como tendo mais potencial.

Palavras chave: Atomização, k-carragenina, isoniazida, macrófagos alveolares, fagocitose, rifabutina, sulfato de condroitina, tuberculose

This page was intentionally left in blank

Abstract

Tuberculosis remains a leading cause of death, with therapeutic failure being mainly due to non-compliance with prolonged treatments, often associated with severe side-effects. New therapeutic strategies are demanded and, considering that the lung is the primary site of infection, direct lung delivery of antibiotics is an interesting and, possibly, effective approach. Therapeutic success in this context depends on suitable carriers that reach the alveoli where Mycobacterium hosts (macrophages) reside, as well as on their ability to promote macrophage capture and intracellular accumulation of drugs. In this work, we propose inhalable polymeric microparticles produced by spray-drying and tailored to suitable aerodynamic properties to reach the alveoli. Macrophage targeting will be driven by microparticle composition based on chondroitin sulphate or k-carrageenan. Both are sulphated polymers composed by moieties preferentially recognised by macrophage surface receptors. The spray-dried microparticles successfully associated two first-line antitubercular drugs (isoniazid and rifabutin). Furthermore, starch/CRG and ChS microparticles presented satisfactory aerodynamic properties, compatible with deep lung deposition. In ChS microparticles, ethanol and HCl were tested as co-solvents to aid the solubilisation of RFB and microparticles produced with ethanol general revealed the best features, being selected for further assessment. ChS-based formulations evidenced absence of toxicity in alveolar epithelial cells and macrophages (human and mouse). Starch/CRG formulation exhibited some toxicity, especially in mouse macrophages. The latter further elicited stronger production of interleukins from human macrophages, compared with the mild response to ChS microparticles, which reflects the ability to activate macrophages. ChS microparticles also evidenced better ability to undergo macrophage uptake and were, thus, further evaluated in a high content analysis (HCA) assay evaluating the response of mouse macrophages to exposure (lipid accumulation, nuclei area, etc.). The results revealed no subtoxic effects after 48 h exposure. Free RFB demonstrated some phospholipid accumulation, which was overpassed upon microencapsulation.

Considering the general trend of the results, good indications are given that encourage the continuation of the studies in order to establish the potential of these microparticles as inhalable carriers in tuberculosis treatment.

Keywords: alveolar macrophages, chondroitin sulphate, isoniazid, k-carrageenan, phagocytosis, spray-drying, rifabutin, tuberculosis

List of publications and communications

Patent:

Ana D Alves, Filipa S Pereira, **Susana Rodrigues**, Filipa Guerreiro, Ludmylla Cunha, Ana Grenha, Process for producing polysaccharide microparticles for alveolar macrophages targeting, microparticles obtained therein and use thereof. PCT/IB2016/052353 (under revision in the European Patents Office)

Publications:

Susana Rodrigues, Ana Grenha, 2015. Activation of macrophages: Establishing a role for polysaccharides in drug delivery strategies envisaging antibacterial therapy. *Current Pharmaceutical Design*, 21(33):4869-4887

Communications

Oral communications:

Susana Rodrigues, Francesca Buttini, Lea Ann Dailey, Leonor Faleiro, Ana M. Rosa-da-Costa and Ana Grenha. Chondroitin sulphate microparticles as antitubercular drug carriers, DDL2017 - Drug Delivery to the Lung, December 6-8, 2017, Edinburgh, Scotland

Susana Rodrigues, Francesca Buttini, Lea Ann Dailey, Ana M. Rosa-da-Costa, Ana Grenha. Tuberculosis treatment by macrophage targeting using chondroitin sulphate microparticles. 2nd CBMR/ProRegeM Annual Meeting, September 8, 2017, Faro, Portugal

Susana Rodrigues, Ana Grenha, “Encapsulation Technologies: a milestone of drug delivery”, 33rd Youth Science Meeting, July 29, 2015, Faro, Portugal

Posters in conferences:

Susana Rodrigues, Ana M. Rosa-da-Costa, Francesca Buttini, Ana Grenha, Starch/Carrageenan microparticles for lung delivery of antitubercular drugs, 21st International Symposium on Microencapsulation. September 27-29, 2017, Faro, Portugal

Susana Rodrigues, Ana M. Rosa-da-Costa, Francesca Buttini and Ana Grenha, Chondroitin sulphate microparticles for tuberculosis treatment: a way to target macrophages, Drug Delivery to the Lungs 27 (DDL27), December 7-9, 2016, Edinburg, UK

Susana Rodrigues, Ana M. Rosa-da-Costa and Ana Grenha, Inhalable starch/carrageenan microparticles: Macrophage targeting in tuberculosis therapy, The 2016 TB summit, June 21-23, 2016, London, UK

Susana Rodrigues, M Leonor Faleiro, Ana Grenha, Carrageenan microparticles: a tool for macrophage targeting in tuberculosis therapy. 3rd International TB-Meeting, inhaled therapies for tuberculosis and other infectious diseases. October 14-16, 2015, Parma, Italy

Ana D Alves, **Susana Rodrigues**, Ana Grenha, Proving a role for polysaccharides on activation of macrophages, 20th International Symposium on Microencapsulation, October 1-3, 2015, Boston, USA

Susana Rodrigues, Ana Grenha, K-Carrageenan Microcarriers for Lung Delivery of Antitubercular Drugs, RDD Europe 2015, May 5-8, 2015, Nice, France

Table of contents

List of figures

List of tables

This page was intentionally left in blank

Abbreviations

AE – Association efficiency

ACI – Andersen cascade impactor

ANOVA – One-way analysis of variance

BCG – Bacillus Calmette-Guérin

CCM – Cell culture medium

D_{aer} – Aerodynamic diameter

DMEM – Dulbecco's modified Eagle's medium

DMF – Dimethylformamide

DMSO – Dimethyl sulfoxide

dTHP-1 – macrophage derived from THP-1 cells

EDAC – *N*-(3-dimethylaminopropyl)-*N*′-ethylcarbodiimide hydrochloride

ELISA – Enzyme-linked immunosorbent assay

f_2 – similitude factor

FBS – Fetal bovine serum

FPD – Fine particle dose

FPF – Fine particle fraction

GSD – Geometric standard deviation

HCl – Hydrochloric acid

HIV – Human immunodeficiency virus

HPLC – High performance liquid chromatography

Ig – Immunoglobulin

IL – Interleukin

INH – Isoniazid

ISO – International Organization for Standardisation

LC – Loading capacity

LDH – Lactate dehydrogenase

LPS – Lipopolysaccharide

MD – Metered dose

MIC – Minimum inhibitory concentration

MMAD – Mass median aerodynamic diameter

MP – Microparticles

MTT – 3-(4,5-dimethylthiazol-2-yl)-2,5-diphenyltetrazolium bromide

OADC – Oleic acid, albumin, dextrose and catalase

PBS – Phosphate buffered saline

PDI – Polydispersity index

PMA – Phorbol 12-myristate 13-acetate

RFB – Rifabutin

SDS – Sodium dodecyl sulphate

SEM – Scanning electron microphotograph

TLR – Toll-like receptor

TNF – Tumor necrosis factor

WHO – World Health Organisation

Chapter I - General Introduction

The information presented in this chapter was partially published in the following publication:

S Rodrigues, A Grenha, 2015. Activation of macrophages: Establishing a role for polysaccharides in drug delivery strategies envisaging antibacterial therapy. *Current Pharmaceutical Design*, 21(33):4869-4887

This page was intentionally left in blank

1. General Introduction

1.1. Tuberculosis: epidemiology and current therapy

Tuberculosis is an infectious disease that is caused by a bacterium called *Mycobacterium tuberculosis* (*Mtb*), which is hosted by and multiplies inside alveolar macrophages, thus mostly affecting the lung. The *Mtb* ability to block phagosomal maturation contributes to the long-term survival and persistence of the bacterium in host macrophages (this topic will be further developed in section 1.3.2). Bacillus Calmette-Guérin (BCG) vaccine, derived from *Mycobacterium bovis*, exists for almost a century and covers close to 90% of new-borns worldwide, but is not effective in pulmonary forms of tuberculosis, responsible for transmission [1]. About 23% of the world's population is estimated to have latent tuberculosis infection, thus being at risk of developing active disease during their lifetime. Tuberculosis is one of the top 10 causes of death and the leading cause of death from a single infectious agent (above the human immunodeficiency virus (HIV)). This especially occurs in developing countries but is reappearing in Europe. According to the World Health Organization (WHO), about 10 million people developed this infectious disease in 2017 and tuberculosis caused an estimated 1.3 million deaths among HIV-negative people, while there were an additional 300 000 deaths among HIV-positive people [2]. Current therapy demands prolonged oral multi-drug antibiotherapy, frequently with strong side effects that decrease patient compliance [3]. It is estimated that, worldwide in 2017, 558 000 people developed tuberculosis that was resistant to rifampicin, the most effective first-line drug and, of these, 82% had multidrug-resistant tuberculosis (MDR-TB). The largest number of tuberculosis cases reported in 2017 occurred in South-East Asia, Africa and Western Pacific Region, as depicted in Figure 1.1. Despite the WHO's End TB Strategy launched in 2015, which aims at ending the global tuberculosis epidemic, a long way is still ahead before accomplishing the objective [4].

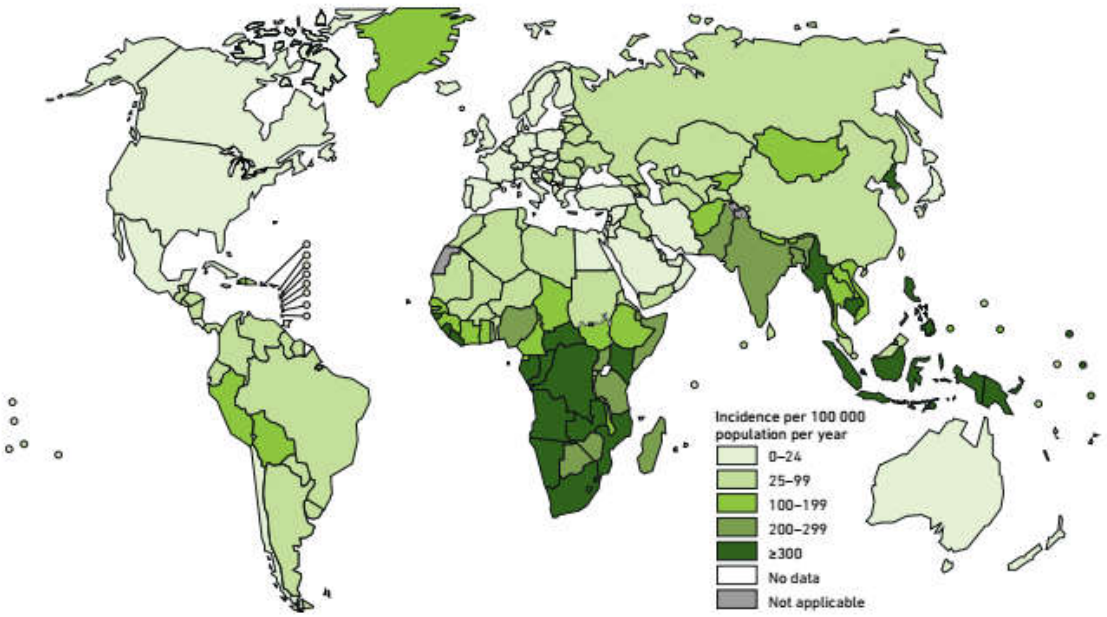

Figure 1.1 - Estimated tuberculosis incidence rates, 2017 [2].

In Portugal, as in many countries, there is still a reduction in reporting and incidence of the disease. Despite this reduction, there is an increase in cases of tuberculosis in children aged less than or equal to 5 years, particularly in the severe forms of the disease. This increase is mostly due to the fact that, in 2016, BCG vaccination strategy was changed from a universal strategy to a selective one [5]. Maintaining this strategy requires that appropriate identification of children who meet the eligibility criteria for vaccination is ensured. Currently, Lisboa and Porto are the Portuguese districts with the highest incidence of cases, as observed in Figure 1.2. In 2017, Portugal presented a mean incidence level of 15,6/100.000 persons, with 1244 new cases of pulmonary tuberculosis representing 71% of the total cases.

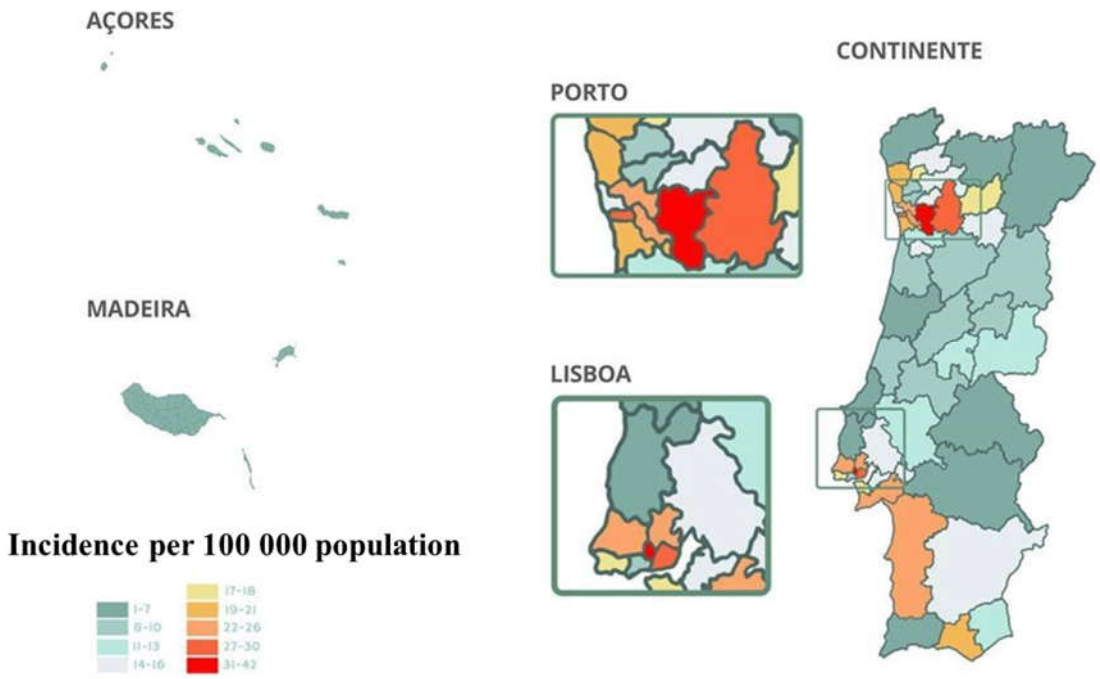

Figure 1.2 – Distribution in Portugal of tuberculosis incidence. Adapted from DGS [5].

Current WHO recommendations for the treatment of active tuberculosis include a combination of multiple drugs for long periods of time, in order to prevent the development of MDR-TB. Currently, the recommended treatment for new cases of drug-susceptible tuberculosis is a 6-month regimen of four first-line drugs: isoniazid (INH), rifampicin, pyrazinamide, and ethambutol. It involves an initial phase of a four-drug regimen for the first 2 months followed by a continuation phase of INH and rifampicin for the following 4 months. Up to 95% of people with drug-susceptible tuberculosis reach the cure with this four-drug regimen. In cases in which rifampicin resistance is suspected, other rifamycin derivatives, such as rifabutin (RFB) may be used. Moreover, RFB is the first-line antitubercular drug recommended for patients who follow therapeutic regimens involving drugs that are incompatible with rifampicin, such as antiretroviral drugs. Because of the emerging cases of MDR-TB and due to treatment regimens that are hard to follow, there is currently a great demand for new tuberculosis treatments. This can be either in the form of new drugs or focused on the development of alternative strategies to deliver drugs already in clinics. The latter approach can be highly beneficial if the strategy specifically addresses the intracellular character of the disease.

Considering the first-line antitubercular drugs, INH and RFB were selected for the present study as model drugs, taking into account the different molecular weight and solubility. Figure 1.3 displays the molecular structure of both drugs. INH is easily soluble in water (140 mg/mL), exhibits a molar mass of 137.14 g/mol and its chemical formula corresponds to $C_6H_7N_3O$. In turn, RFB has very low solubility in water (0.19 mg/mL), has a molar mass of 847.02 g/mol and its chemical formula corresponds to $C_{46}H_{62}N_4O_{11}$.

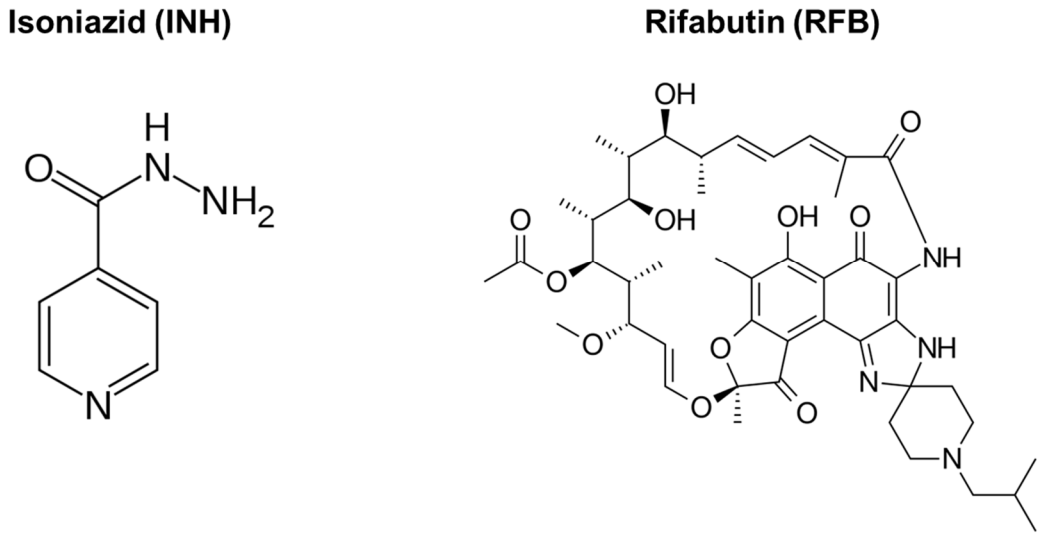

Figure 1.3 – Molecular structure of isoniazid and rifabutin.

The drugs present different mechanisms of action. While INH inhibits the synthesis of mycolic acid, an important component of bacterial cell wall [6], RFB acts by inhibiting the β-subunit-dependent DNA–RNA polymerase, leading to suppression of DNA formation by *Mtb* and, consequently, to death of bacteria *[7].*

1.2. Immune system and its relationship with tuberculosis

The human organism has developed, along millennia of evolution, several mechanisms of defence against external invading entities or as a response to internal danger signals. These mechanisms rely on both the innate and the adaptive immune systems and are responsible for avoiding damage on the multiple organic systems of the body caused by pathogens and foreign particles, or even cell debris [8]. Specialised phagocytes assuming important roles in this context include several types of white blood cells (leukocytes), such as

neutrophils, monocytes, macrophages, mast cells and dendritic cells, as depicted in Figure 1.4, which exist in different locations of the organism. Many of the defence mechanisms have their origin on monocytes, which circulate in the blood and differentiate into macrophages in the tissues. Together with antigen-presenting cells, these are the cell types known to play a major role in the defence against infections [9].

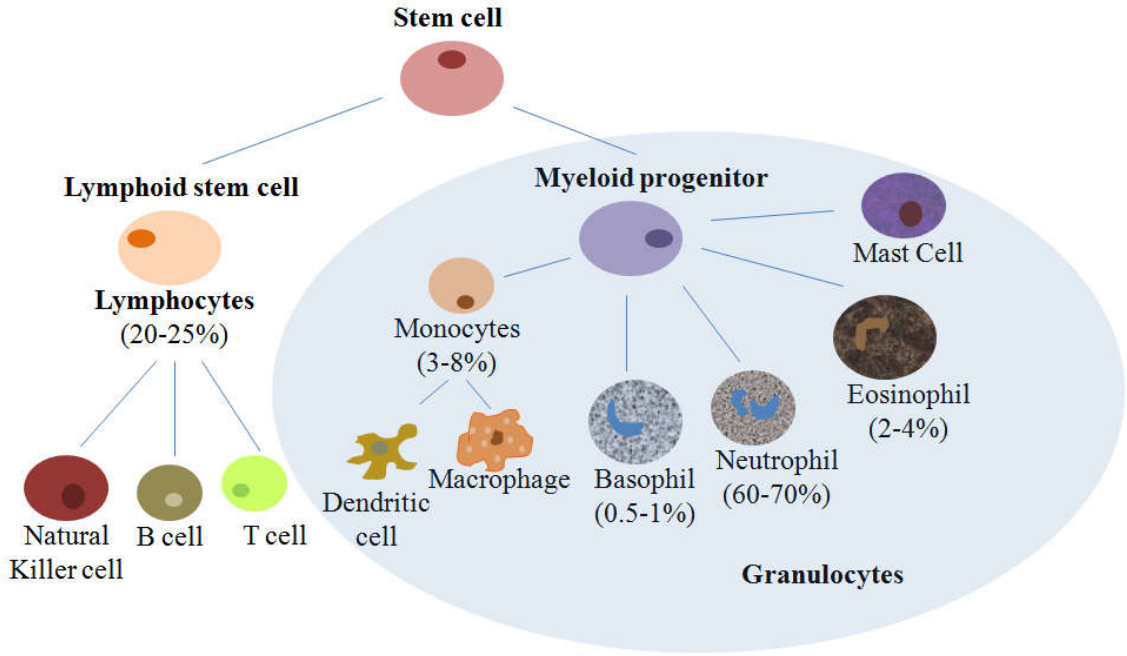

Figure 1.4 - Leukocyte development and indicative % in the blood. Reprinted with permission from Rodrigues, 2015 [10]. (consult supplementary page 164 for permissions)

When an infection occurs, the innate immune system initiates a protective inflammatory response that encompasses several phases, from initiation and full inflammation, to resolution and re-establishment of tissue integrity. After the elimination of the pathogen, the removal of dead and dying cells, damaged extracellular matrix and cell debris, takes place under the responsibility of macrophages, to end up with a recovery phase in which the tissue is repaired and restored, recovering its homeostasis (a state of normal morphology and function) [11]. The term ‘‘macrophage’’ was introduced back in the nineteenth century and translates from the Greek literally as ‘‘large eaters’’. The very first observations of the process of phagocytosis, which comes to be the main action of macrophages, were made around 1880, describing an uptake of foreign

objects in starfish larvae by amoeba-like cells, which were called phagocytes, ‘‘devouring cells’’ in a direct translation [12]. Macrophages are, thus, scavengers whose function is to maintain distinct places of the organism (blood, epithelial surfaces, etc.) clear of potentially prejudicial materials. They are mainly found in the spleen but their location is actually coincident with everyplace needing defence against pathogens. Therefore, the lungs and especially the intestine associated lymphoid tissue are areas of high macrophage population, given the privileged contact with external-born materials. Macrophage actions, therefore, mainly consist on engulfing infecting microorganisms and even infected cells, impeding the spreading and distribution of those agents. Additionally, macrophages also contribute directly to the containment of infections by secreting signals that mediate the orchestration of other cell responses, through the activation of other cell types that have prominent roles on the elimination of infection.

1.2.1 - Cells of the immune system

The immune system is a complex network of lymphoid organs, cells, humoral factors, and cytokines that work together to defend the organism against pathogens such as bacteria and virus, or other insults like tumour cells. When such a substance/material is discovered, several types of cells go into action in what is called an immune response. As depicted in Figure 1.4 there are different immune cells involved in the whole process, which will be briefly described below, along with the functions under their responsibility.

Lymphocytes and granulocytes are the main types of immune cells. An extensive and detailed description of their functions can be found in Rodrigues, 2015 [10].

Granulocytes are the cell family derived from the myeloid progenitor, comprising monocytes, basophils, eosinophils, neutrophils and mast cells. They are collectively termed either granulocytes, because of the cytoplasmic granules whose characteristic staining gives them a distinctive appearance in blood smears, or polymorphonuclear leukocytes, because of their irregularly shaped nuclei. They are blood circulating cells which enter the tissues only when recruited to sites of infection or inflammation. Mature circulating neutrophils have the shortest half-life among leukocytes as they undergo apoptosis constitutively. Neutrophil trafficking into inflamed tissues is associated with extended survival of

these cells due to delayed constitutive apoptosis, which allows them to effectively fulfil their microorganism-targeting effector function. On the other hand, prolonged neutrophil survival can also result in excessive tissue inflammation and damage, and macrophage-mediated elimination of apoptotic neutrophils from the inflamed area has been recognised as a crucial mechanism for promoting resolution of inflammation and tissue damage. Thus, neutrophil apoptosis must be tightly controlled to maximise bacterial elimination and minimise tissue damage. Whereas apoptosis is necessary to prevent the release of cytotoxic contents from neutrophils to the inflammatory site, extended survival is beneficial to pathogen elimination. Eosinophils and basophils are recruited to sites of allergic inflammation and appear to be involved in defending against parasites. Mast cells arise from precursors in bone marrow but complete their maturation in tissues, being essentially relevant in allergic responses. Monocytes arise from the bone marrow and have a circulating half-life of 1 - 3 days. If no recruitment occurs from a tissue, they die and are removed [11]. On the contrary, if monocytes are recruited, they first stick to blood vessel walls, squeeze between the cells of the vessel and, when entering the tissue, differentiate into macrophages or dendritic cells, contributing to host defence, along with tissue remodelling and repair [13]. Pro-inflammatory, metabolic and immune stimuli, all elicit the increased recruitment of monocytes to peripheral sites. Although with the same progenitor, macrophages and dendritic cells are anatomically different and are attributed with dissimilar functions. Dendritic cells interface with the adaptive immune system and modulate immune responses [14]. Immature dendritic cells travel via the blood to enter peripheral tissues, where they ingest antigens. When they encounter a pathogen, maturation occurs followed by migration to lymphoid tissues, where antigen-specific T lymphocytes are activated. Dendritic cells are known as the most efficient antigen-presenting cell type with the ability to interact with T cells and initiate an immune response [15]. In turn, macrophages are generally assumed as a key component of the innate immune system, being the main tissue-resident phagocytic cells of the innate immune system [14]. Macrophages have, thus, a prominent role in tuberculosis and will be described in more detail in the next section.

The immune response elicited in each case is a coordinated effort, as all the immune cells work together towards a common objective [16]. Therefore,

intercellular communication is a refined skill, mediated by the secretion of special protein molecules called cytokines, which act on other cells [17]. A wide variety of cytokines is described, including interleukins, interferons, tumour necrosis factors, and colony-stimulating factors [18, 19].

Immunity as a whole is usually divided in two distinct types, the division being determined by the speed and specificity of the elicited reactions: innate immunity and adaptive immunity. The term innate immunity is sometimes used to include physical, chemical, and microbiological barriers, but more usually encompasses the elements of the immune system (neutrophils, monocytes, macrophages, complement, cytokines, and acute phase proteins) which provide immediate host defence. The highly conserved nature of the response, which is seen even in the simplest animals, confirms its importance in survival. Adaptive immunity is the hallmark of the immune system of higher animals. This response consists of antigen-specific reactions through T lymphocytes and B lymphocytes. Whereas the innate response is rapid but sometimes damages normal tissues through lack of specificity, the adaptive response is precise, but takes several days or weeks to develop. Additionally, the adaptive response has a “memory”, so that a subsequent exposure leads to a more vigorous and rapid response, although this is not immediate [15]. Worth to mention is the fact that, in spite of the division, the two types of immunity share many processes and are in strong interaction with each other [15].

1.2.2 - The macrophage as a cell entity

As understood from the above description, the origin of tissue-resident macrophages has long been attributed to circulating monocytes, which are considered their precursors. However, there is now evidence that some tissue macrophages possess a substantial potential for autonomous self-renewal and that they can populate tissues before birth, deriving from early hematopoiesis in the yolk sac [11, 20]. In fact, major macrophage populations were found to originate on embryonic progenitors and to renew independently of hematopoietic stem cells in a process that may not require progenitors, as mature macrophages can proliferate in response to specific stimuli indefinitely and without transformation or loss of functional differentiation [20]. So far, the reason why

some tissue macrophages are partially replenished by monocytes, whereas other populations are independent on circulating monocytes, is still unclear.

Despite that evolution on the concept of macrophage origins, the functions of these cells are already well-established. Macrophages are resident phagocytic cells in virtually all tissues of adult mammals, either lymphoid or non-lymphoid tissues, where they can represent up to 10-15% of the total cell number in quiescent conditions in a determined tissue [11]. Hallmarks of their specialised properties include proficient phagocytosis, motility and biosynthetic capacity [21]. With such features, macrophages are mainly involved in steady-state tissue homeostasis via the clearance of senescent cells, as well as in the remodelling and repair of tissues [22-24]. Additionally, macrophages are key players in tissue development, by shaping the tissue architecture, are responsible for the generation of immune responses to pathogens and also have a role in surveillance and monitoring of tissue changes, by acting as sentinel and effector cells [11, 22, 23]. For instance, in the respiratory epithelium alveolar macrophages have a crucial role in the maintenance of the tissue homeostasis by defending the airways from air-borne infections [22]. Macrophages are known to survive for several months *in vivo* and are thought to be capable of multiple phagocytic episodes. Possibly, following the ingestion of a number of microorganisms or an amount of material, the macrophage ceases to ingest and redirects its efforts to the production of proinflammatory cytokines. Alternatively, when pathogens are the captured material, these may induce apoptosis in macrophages [21]. Importantly, in the case of tuberculosis it was recently described that, depending on the virulence of *Mtb*, necrosis of the infected phagocytic cells may be induced instead of the desired apoptosis, with consequences at the level of bacterial containment [25].Macrophages are characterised by high heterogeneity, reflecting the specialisation of their functions in different anatomical regions, which confers a variety of phenotypes resulting from a diverse pattern of gene expression. Indeed, several tissue macrophage subsets are described including alveolar macrophages, microglia, Kupffer cells and osteoclasts, just to mention some. In the referred cases, their location corresponds to the alveolar surface, central nervous system, hepatic tissue and bone tissue, respectively [13]. A good description of macrophage subsets and the inherent functions can be found in [11, 13].

Structurally, macrophages usually assume stellar or ameboid morphology, along with high vacuolation [12] and the exhibition of pseudopodia [21]. Macrophages are described as extremely dynamic cells, with intensive membrane trafficking, fusion and fission associated with endocytosis, phagocytosis and ruffling [21]. The process of phagocytosis requires the utilisation of large amounts of plasma membrane, especially when considering how phagocytes are able to rapidly ingest a large number of particles and even particles that are of similar size to the cell itself [26]. As a reference, alveolar macrophages have been reported to have around 21 μm [27], while in general macrophage size varies within 10-20 μm.

A very relevant set of structures in the macrophage concerns cell membrane surface receptors. A wide range of these receptors has been described to be present and, in some cases, represents the key for the very specific activities performed by these cells. The surface receptors assume various functions, determining the control of macrophage activities, which involve growth, differentiation, activation, recognition, endocytosis, migration and secretion. The list is long and the functions of some of the receptors are still unknown. Within the list, a categorisation in three main groups is frequently assumed: Toll-like receptors (TLR), non-TLR and opsonic receptors (Figure 1.5). The latter include complement receptors (integrins) and Fc receptors (immunoglobulin superfamily). These opsonic receptors work towards the phagocytosis and endocytosis of complement- or antibody-opsonised particles, respectively [21]. As an example of the immunoglobulin superfamily receptors, the CD44 receptor can be mentioned, while a popular receptor of the integrins family is CD11b [28]. The family of Toll receptors has been conserved throughout evolution from flies to humans and plays a central role in the initiation of cellular innate immune responses [29]. TLR do not mediate phagocytosis/endocytosis, but are important sensors of bacteria, fungi and viruses [30, 31]. TLR are located both in cell membrane and within vacuoles and play a role in the recognition of intracellular pathogens. In cooperation with phagocytic receptors they can trigger a pathogen-specific response. Non-TLR are involved in phagocytosis and endocytosis, and include the family of scavenger receptors [32] and the C-type lectins [33].

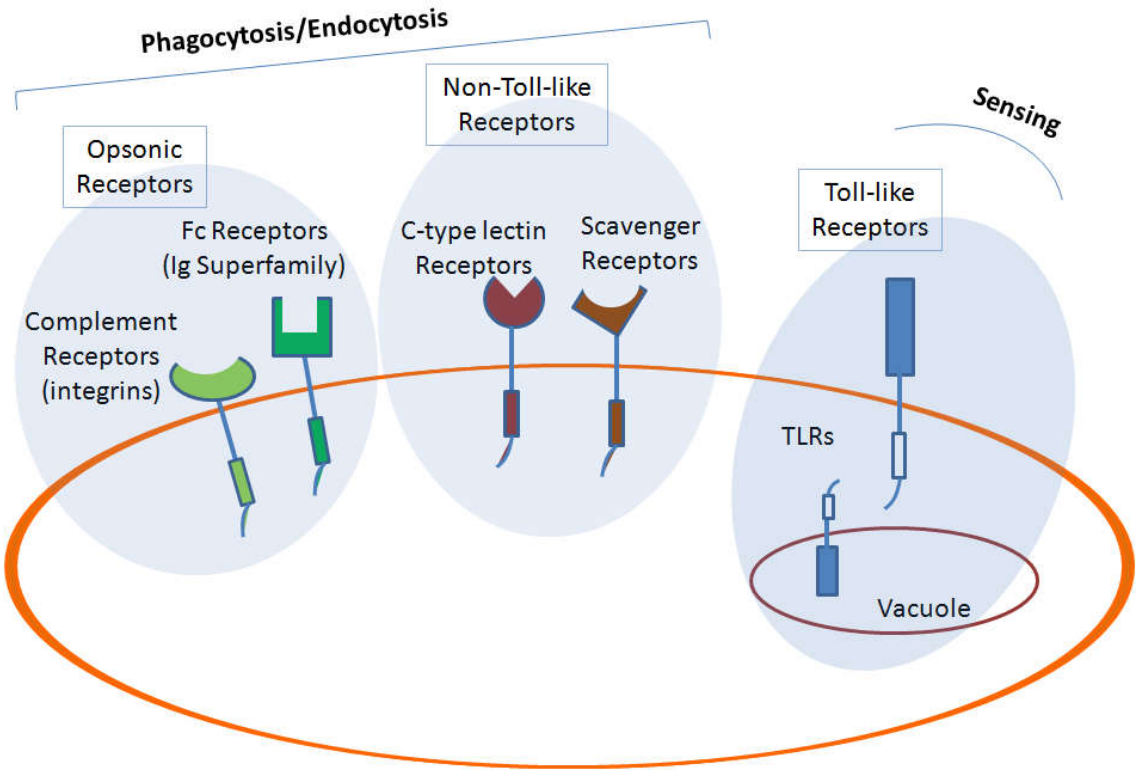

Figure 1.5. - Categories and localisation of macrophage recognition receptors. Macrophages express many receptors that mediate their diverse functions, as for example the recognition of extracellular and intracellular pathogens. Reprinted with permission from Rodrigues, 2015 [10].

Of the several classes of scavenger receptors (8 classes from A to H), the class A is considered to be of high importance in antimicrobial host defence. This class is composed of three different receptors, namely the scavenger receptor A (CD204), the macrophage receptor with collagenous domain (MARCO), and a recently identified protein scavenger receptor with C-type lectin [34, 35]. C-type lectin receptors are a much larger family. These are carbohydrate binding proteins belonging to a super family characterised by the presence of one or more C-type lectin-like domains. C-type lectins and proteins with C-type lectin-like domains are found in all organisms and the super family includes 17 different categories that are distinguished by their domain architecture [36, 37]. Most of these groups have a single C-type lectin-like domain. Macrophages only present C-type lectins of group II, V and VI, but the mannose receptor (group VI), also known as CD206, has eight of the mentioned domains [36]. Despite the presence

of a highly conserved domain, C-type lectins are functionally diverse and have been implicated in various processes, including cell adhesion, tissue integration and remodelling, platelet activation, complement activation, pathogen recognition, endocytosis and phagocytosis [37]. Many C-type lectins act in receptor-mediated endocytosis to deliver bound, soluble ligands to lysosomes, leading to receptor accumulation and degradation in phagolysosomes or to recycling of the receptor to the cell surface. Regarding the ligand affinities, C-type lectin receptors recognise conserved carbohydrate structures, including mannose and galactose, found on the surface of many respiratory pathogens, such as *Yersinia pestis*, *Mycobacterium tuberculosis*, *Streptococcus pneumoniae* and influenza viruses, among others [38]. The mannose receptor, specifically, is reported as capable of recognising mannose, fucose, *N*-acetylglucosamine units and sulphated sugars [33, 39]. Dectin receptors are other examples of C-type lectins, Dectin-1 recognises β-glucan units [33, 40, 41] and Dectin-2 binds to mannose [33]. Galactose and *N*-acetylgalactosamine (GalNAc) residues are also reported to bind to three receptors in the C-type lectin family: the Kupffer cell receptor, the macrophage galactose lectin and the scavenger receptor C-type lectin [42].

In summary, differentiating characteristics of macrophages such as the variety of expressed receptors, along with the natural ability for phagocytosis, will possibly be the driving force for the consideration of these cells as potential targets in drug delivery strategies.

1.2.3 - Microbial recognition and macrophage responses

Through their ability to clear pathogens/invading material and instruct other immune cells, macrophages have a central role in protecting the host, but also contribute to the pathogenesis of inflammatory and degenerative diseases. Tissue-resident macrophages are those establishing the first contact with invading materials. Once a macrophage recognises a substance (usually assumed as a particle) as a foreigner, the phagocytic process starts envisioning the elimination of the said substance. The recognition by macrophages might involve different processes but is mainly mediated by the receptors existing in the membrane surface, which have different affinities for molecular groups or residues, as exposed in the previous section. Of the exhibited receptors depend

many of the responses that macrophages might provide. In turn, the presence or absence of the receptors strongly depends on the microenvironment surrounding the cells in each singular situation. In fact, macrophages are remarkably plastic and in response to various environmental cues (microbial products, damaged cells, etc.) or under different pathophysiological conditions (hypoxia, for instance), they can assume distinct functional phenotypes via undergoing different phenotypic polarisation [43]. This polarisation is frequently referred to as activation, giving rise to expressions such as “the macrophages were activated”. Basically, the state of activation encompasses a cascade of events initiated by the macrophages upon contact with certain substances, in a skilled communication with the surrounding environment and structures, which is personalised by specifically released chemical factors. Indeed, one of the most fascinating aspects of macrophages is their promptness to *de novo* synthesise and release a large variety of cytokines (i.e. IL-1, IL-1ra, IL-6, IL-8, IL-10, IL-12, TNF-α, IFN-α, IFN-γ) upon activation [17, 44]. Cytokines are small glycoproteins that regulate a number of physiological and pathological functions including innate immunity, acquired immunity and a plethora of inflammatory responses. Induction of leukocyte migration is the main function of chemokines, a specific group of cytokines, but they also affect angiogenesis, collagen production and the proliferation of haematopoietic precursors [11]. There is compelling evidence that some chemokines are also involved in polarised immune responses. Tissue-resident macrophages, the typical macrophages found in tissues in steady-state conditions, are reported to not being activated (assumed as M0 activation state) [45]. Based on their function, activated macrophages are divided broadly into two categories: classical M1 and alternative M2 macrophages [46], which describe the opposing activities of killing and repairing [43]. A coordinate action of various inflammatory modulators, signalling molecules and transcription factors is involved in regulating macrophage polarisation. The M1 phenotype is typically stimulated by microbial products or pro-inflammatory cytokines such as IFN-γ or TLR ligands [43]. Macrophages holding this phenotype express numerous pro-inflammatory mediators including TNF-α, IL-1, IL-6, reactive nitrogen and oxygen intermediates, which display a strong microbicidal and tumoricidal activity, along with cell proliferation inhibitory capacity. Additionally, the typical characteristics of M1 macrophages include high antigen presentation ability [47, 48]. This feature

is mediated by the peptide fragments resulting from the endosomal digestion of phagocytosed material, which combine with major histocompatibility complex class II molecules for presentation to T lymphocytes [49]. In contrast, the M2 phenotype is characterised by the upregulation of Dectin-1, mannose receptor, scavenger receptors A and B and IL-10 [46, 47]. Instead of generating reactive nitrogen and oxygen intermediates, M2 macrophages produce ornithine and polyamines through the arginase pathway [47]. This M2 phenotype is associated with parasite infestation, tissue remodelling and tumour progression (immunoregulatory functions) [23, 48, 50, 51]. These M1 and M2 phenotypes are interchangeable, thus being potentially converted into each other in specific microenvironments [52].

Macrophages are therefore considered a plastic cell type because, as described, in a given moment they can modulate their activation state and, consequently, the proper cytokine and receptor expression profiles [43], as depicted in Figure 1.6.

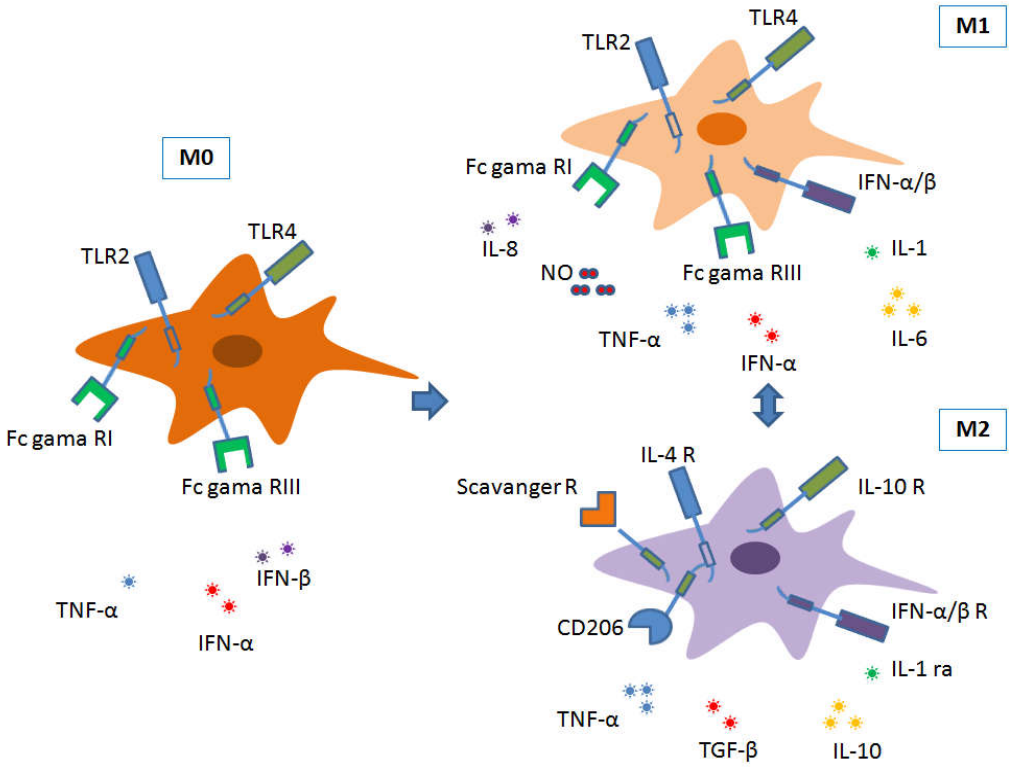

Figure 1.6. - Macrophage different activation states, M0, M1 and M2, along with the respective receptor and cytokine profiles. Reprinted with permission from Rodrigues, 2015 [10].

Regarding the macrophage recognition abilities, there are examples of well-studied situations. For instance, yeasts and bacteria are known to be recognised by Dectin-1, the β-glucan receptor, and by TLR2 [53], while the bacterial lipopolysaccharide (LPS), the major structural component of the outer wall of Gram-negative bacteria, is recognised by CD14, TLR4 and the myeloid differentiation protein-2 [54]. Non-biological particles lack specific opsonins, preventing a classic opsonin-dependent phagocytosis. Nevertheless, macrophages have been described to phagocytose non-opsonised particles, in a process that is mainly mediated by the scavenger receptors, namely class A scavenger receptor (CD204) and the MARCO [49]. In spite of this ability, there is evidence that phagocytosis is in fact enhanced by opsonisation, as demonstrated in a work studying the phagocytosis of *Streptococcus pneumonia* by alveolar macrophages [55].

Bacteria, dead tissue cells and small mineral particles are all examples of entities potentially undergoing phagocytosis. The process starts with the binding of the ligands present at the material surface to macrophage receptors, being followed by the engulfment of the material that, inside the macrophage, is located in an internal vesicle known as phagosome [56, 57]. The phagosome is then fused with a lysosome to form a phagolysosome, where the acid hydrolase enzymes present into the lysosome usually ensure the digestion of the pathogen/foreign particle. Along with this process, the activation of the macrophage occurs and the cell either remains in the concerned tissue or is removed via the lymphatic system to regional lymph nodes. Going back to particle digestion performed by the macrophage, it is remarkable that bacteria, for instance, have evolved to acquire specialised mechanisms to evade the macrophagic elimination mechanisms. In fact, after being phagocytosed the fate of bacteria can assume three distinct possibilities: 1) escape from phagosome, 2) prevent phagosome-lysosome fusion or 3) survive inside phagolysosomes [58-60]. These possibilities are exemplified in Figure 1.7. Concrete example of bacteria exhibiting these abilities is *Mycobaterium tuberculosis* that impedes phagosome maturation [61-63]; *Legionella pneumophila* that modifies the phagosome [64]; and *Coxiella burnetti* that replicates inside phagolysosomes [65]. From the listed pathogens,

Mycobacterium tuberculosis is the one raising more concerns, as mentioned in section 1.1.

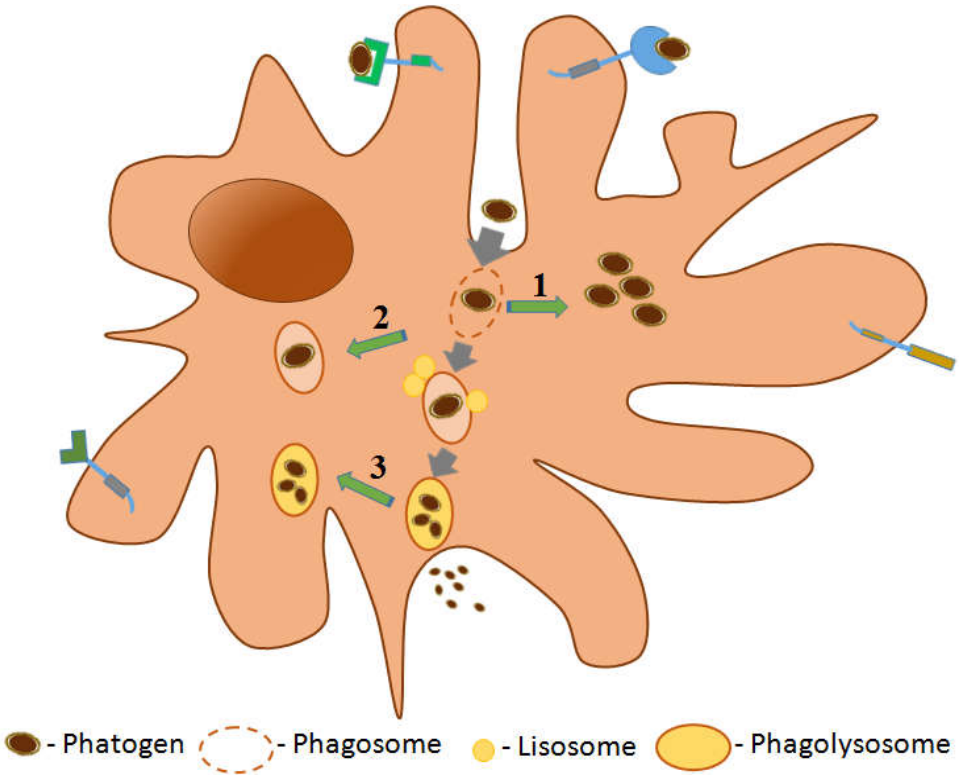

Figure 1.7. - Macrophage phagocytosis and digestion of pathogens (grey arrows) and the three different mechanisms developed by the pathogen developed in order to escape from digestion: 1) escaping from phagosome, 2) preventing phagosome-lysosome fusion or 3) survive inside phagolysosomes. Reprinted with permission from Rodrigues, 2015 [10].

When a bacterial infection is occurring, macrophages generally activate towards an M1 phenotype in the early stage of the infection. When macrophage receptors recognise the bacteria, the activation leads to the production of a large amount of pro-inflammatory mediators (TNF-α, IL-1, reactive oxygen species, etc), which promote the elimination of the invading organisms and activate the adaptive immunity. In order to counteract the excessive inflammatory response, macrophages undergo apoptosis or activate to an M2 phenotype to protect the host from excessive injury and facilitate wound healing. The macrophage approach to viral and fungal infections is also mediated by both activation states

[19]. By capturing invading particles through the whole body, macrophages are active in the prevention of infections in general.

In spite of their natural ability for the phagocytosis of particulate matter, which was previously highlighted, macrophages have a preference for certain particles/materials, not only regarding their composition and the inherent affinity for different receptors, but also as a function of their size and even the concentration. The size described to favour phagocytosis the most is around 1 μm. In turn, submicron particles in the lower nano scale (200 nm) and particles with size greater than 10 μm are known to escape phagocytosis or at least delay the process [66, 67]. It is also generally thought that the large surface area per unit concentration of particles having less than 2.5 μm, as compared to larger particles, potentiates stronger cellular interactions and a downstream biological response [49].

As a whole, the mentioned activation of macrophages refers to a state of different receptor expression, cytokine production, effector function and chemokine repertoires. In this regard, these differentiating characteristics might comprise an opportunity for the development of drug delivery strategies, as will be highlighted in the following sections.

1.2.4. - Macrophages as therapeutic targets

Many are the pathogens described to be hosted by macrophages upon invasion of the human organism. Under the normal function of these cells in the ambit of the immune system, it is expected that the elimination of captured microorganisms takes place. However, a diverse range of naturally occurring pathogens, including virus, bacteria, parasites, which are encountered by the host early in the course of infection, are able to exploit, subvert or exacerbate the innate immune response [21], as mentioned above, which results frequently in the development of diseases. Table 1.1 congregates several examples of these pathogens and indicates the disease that usually develops as consequence of the infection. Focus has been placed in bacterial infections, honouring the objective of the present work, but other microorganisms have the same behaviour, such as for example the human immunodeficiency virus (HIV) [68, 69].

As previously described, the first contact between host and pathogen is mediated by the macrophage receptors. Phagocytosis-related receptors, which are located

in large number on macrophage surface [70], are thus optimal structures for a macrophage-targeted therapy. This happens because 1) these receptors reflect the physiological function of macrophages (activated M1 or M2 states) and 2) because they are used for pathogen internalisation by macrophages. Therefore, therapeutic carriers targeting a certain receptor can lead to accumulation of important amounts of therapeutic molecules in the same intracellular niches where microorganisms develop, even if the endocytosis usually requires simultaneous interaction of several receptors. In the case of tuberculosis, for instance, alveolar macrophages uptake inhaled *Mycobacterium tuberculosis* cells (as well as other air-borne pathogens) upon a contact that is mediated by the complement receptors CR1, 3 and 4, and the mannose receptors. Additionally, it has been demonstrated that the uptake is enhanced in the presence of non-immune serum, a source of the complement proteins [71], although the binding of *M. tuberculosis* also occurs in the absence of serum.

Table 1.1. - Examples of microorganisms described to be hosted by macrophages and diseases developed as consequence of pathogen infection. Reprinted with permission from Rodrigues, 2015 [10].

Pathogenic agent	Disease	References
Mycobacterium tuberculosis	Human tuberculosis	[61, 72, 73]
Mycobacterium bovis	Bovine tuberculosis	[74]
Mycobacterium avium	Tuberculosis-like disease (birds, rodents and humans)	[75]
Mycobacterium leprae	Leprosy (Hansen's disease)	[76]
Leishmania	Leishmaniasis (hyraxes, canids, rodents and humans)	[77]
Staphylococcus aureus	Impetigo, cellulitis, food poisoning, toxic shock syndrome, necrotizing pneumonia and endocarditis	[78]
Listeria monocytogenes	Listeriosis	[79]
Salmonella typhi	Typhoid fever	[80]
Salmonella enterica	Gastroenteritis	[81]
Chlamydia	Sexual transmitted infection	[82]
Shigella	Bacillary dysentery	[83]
Yersinia pestis	Bubonic plague or, less frequently, septicaemic plague	[84]
Helicobacter pylori	No specific disease described (several might appear as consequence, i.e. gastric ulcer)	[85]
Trypanosoma cruzii	Chagas disease	[86]
Brucella suis	Brucellosis, a zoonotic infection affecting ruminants, pigs, dogs, rodents, and cetacean	[87]
Legionella pneumophila	Legionnaires' disease	[88]
Streptococcus pneumoniae	Pneumonia	[89]

Mycobacteria display phosphatidylinositol anchored molecules on their cell wall, including lipoarabinomannan (LAM) [90] which, in virulent strains, includes mannose oligosaccharides at the terminus of the molecule (ManLAM) [61, 62]. The presence of this mannose terminus increases the attachment of LAM to macrophages and suggests a vital role of macrophage receptors in *M. tuberculosis* phagocytosis [91]. However, ManLAM provides other important abilities to the bacteria, being responsible for the phagosome maturation arrest, which, as was said above, is the main resistance mechanism of *Mycobacterium tuberculosis* against macrophage bactericidal effect [61, 92]. Mannose has been reported as a functional group that can mediate the direct targeting of carriers to macrophages. Based on these observations, and other of similar nature that are described in the literature, macrophages have been identified as candidate therapeutic targets with potential interest in the establishment of drug delivery strategies for tuberculosis and several other disease conditions [93-95], many of them described in Table 1.1. In tuberculosis, mannosylated carriers, either at nano or micro scale have been proposed to successfully deliver antitubercular drugs to alveolar macrophages, enabling dose reduction and a consequent improvement of patient compliance. Mannosylated gelatin microspheres were reported to deliver isoniazid (INH) to alveolar macrophages, maintaining therapeutic concentrations for a prolonged period of time even upon the administration of a reduced clinical dose [96]. Gelatin nanoparticles [97] and solid lipid nanoparticles composed by stearic acid [98] were also proposed for the same objective. In both cases, macrophage uptake was increased comparing with non-mannosylated particles, while a higher reduction of bacterial levels was observed compared to free drug, upon intravenous injection in mice. The pulmonary delivery of antibiotics in this context is being currently proposed as strong alternative, under the argumentation that it would result in more effective drug concentration in the target site, enabling a decrease in the whole administered dose, accompanied by decreased systemic side effects [99]. Our group has been working in this field and we have observed *in vitro*, in macrophage-differentiated THP-1 cells, that microparticles composed of polymers bearing residues of saccharides potentially recognised by macrophages, such as mannose and fucose, are taken up by macrophages to very high levels [100, 101].

However, the strategy of macrophage targeting is not restricted to tuberculosis therapy, also being proposed under the scope of other bacterial diseases. Polyanhydride nanoparticles functionalised with mannose and galactose, residues referred above to exist on the surface of many respiratory pathogens, were reported to target macrophage C-type lectin receptors, with a consequent activation of the cells, which triggered an immune response. The appearance of the activated phenotype of macrophages was found to be dependent upon nanoparticle internalisation. Mannose and galactose functionalisation enhanced the expression of the macrophage mannose receptor and the macrophage galactose lectin, respectively, as well as increased the production of the pro-inflammatory cytokines IL-1β, IL-6 and TNF-α [38].

Apart from the interest raised by situations where macrophages host pathogens, leading to the development of diseases that can be therapeutically approached by macrophage targeting, other diseases exist that might benefit from the direct targeting of therapeutic molecules to these cells. Cancer therapy, for instance, also attracts attention in this context [51, 94, 102], as polarised M2 macrophages have been suggested to support tumour growth and development [51, 103]. Diabetes is another example, as the typical M2 polarisation occurring as consequence of the disease, which is mediated by a specific protein (peroxisome proliferator-activated receptor - PPAR), might be decreased by PPAR inhibitors, improving insulin sensitivity [19]. Gaucher disease is another relevant example of the application of macrophage targeted therapy which, interestingly, counts already with commercialised products. It is a lysosomal storage disease [104], being caused by mutations in the glucocerebrosidase gene that lead to a decrease in enzymatic activity and accumulation of the enzyme substrates (glucosylceramide and glucosylsphingosine) inside the lysosomes of macrophages in various tissues. In the commercial approaches, a mannose-terminated form of the enzyme is efficiently recognized by macrophage mannose receptors and is then targeted to macrophage lysosomes for substrate catabolism [105, 106]. Interestingly, a study on the effect of mannose chain length on targeting abilities concluded that larger mannose structures induce increased binding to receptors [106]. Although very interesting, these approaches are out of the scope of this work and will not be further explored. The interest of

macrophage drug targeting in the ambit of several diseases like atherosclerosis, obesity and diabetes, tumours and asthma is well addressed in [19].

As was evidenced above, saccharide units are those mostly used to provide a specific targeting to macrophages. In fact, the information exposed above indicates that materials bearing some specific units, including mannose, fucose and acetylglucosamine, among others, might provide a privileged contact with macrophages. The mentioned units are the main components of many polysaccharides, thus suggesting that these materials might have an important role in the design of drug delivery carriers intended for an application in macrophage targeting and, particularly, in tuberculosis. The following section describes several polysaccharides evidencing a targeting ability.

1.3 Application of polysaccharides in antitubercular drug delivery strategies

Almost 30 years ago, Chong and Parish revealed the potential marker for macrophage subsets of the cell surface receptors for sulphated polysaccharides [107]. The published work evaluated the capacity of a different range of sulphated polymers for macrophage interaction and further determined whether polymers undergone phagocytosis. From the studied range, several were the polymers demonstrating binding ability, including glycosaminoglycans, chondroitin-4-sulphate, chondroitin-6-sulphate and dermatan sulphate. However, heparin, fucoidan and kappa-carrageenan were the polysaccharides being specifically endocytosed. In spite of these findings, and others commenting on the ability of macrophages to favourably recognise sugar units, natural polymers, and particularly polysaccharides, seem to be nearly forgotten in the conducted researches. In fact, the majority of works exploring the application of carriers for macrophage targeting usually describes the use of synthetic polymers (i.e. polyesters) to produce the core carriers. These are subsequently decorated with adequate targeting ligands by surface functionalisation approaches [96, 108-110]. The referred polyesters are biocompatible, but that feature is not displayed by most synthetic materials. Natural polymers are extracted from natural resources and present the advantage of being generally more prone to biocompatibility, biodegradability and non-toxicity, which are cumulative requisites of drug delivery systems [111]. The use of natural polymers for

pharmaceutical applications is further attractive because they are economical, readily available and non-toxic. Additionally, polysaccharides present an incomparable advantage regarding macrophage targeting ability, many of them being composed of basic units potentially undergoing direct recognition by macrophage mannose- and galactose-type receptors. Examples of these units include mannose, fucose, *N*-acetylglucosamine, galactose and *N*-acetylgalactosamine residues [98, 108, 112]. Therefore, polysaccharides might be clear adjuvants in drug delivery formulations [113]. As said, works reporting the use of natural-based carriers in the ambit of macrophage targeting are scarce, but it has been referred that future research will mostly rely on these carriers.

Polysaccharides are polymeric carbohydrate molecules composed of long chains of monosaccharide units linked by glycosidic unions. The composing monomers are normally mannose, glucose, galactose and fucose, with different linkages and sulphate or amine substitutions. An interesting example of different monomer arrangement that results in polysaccharides having different functions in the human body is the one behind the definition of blood groups. In the surface of red blood cells, glycoproteins and glycolipids have attached carbohydrates. As depicted in Figure 1.8, for each type of blood group, one of the three different structures, termed A, B, and O, may be present. These substances have in common an oligosaccharide structure called the O antigen. The A and B antigens differ from the O antigen only by the presence of one extra monosaccharide. This can be either *N*-acetylgalactosamine (for A) or galactose (for B), which binds through an α-1,3 linkage to a galactose moiety of the O antigen. This leads to different antigen presenting profile and, consequently, to a different protein binding (opsonisation).

Carbohydrate antigens have been shown to be expressed in bacteria cell wall [114], as well as in a variety of different cell types and at high levels in many tumours of epithelial origin, including those of colon, breast, lung, prostate and ovary [115].

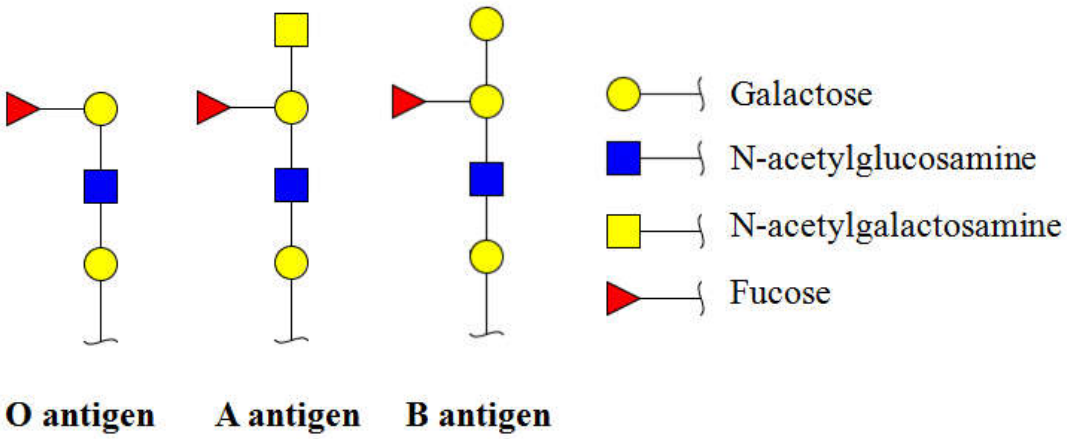

Figure 1.8. - Carbohydrate sequence of blood antigens O, A and B. Reprinted with permission from Rodrigues, 2015 [10].

Polysaccharides have a composition similar to that of these antigens, as is exemplified in Figure 1.9, which depicts the structural units of various polysaccharides of interest. In the figure, all polysaccharides were structured with 10 monomers for a matter of coherence within the proper figure, but different size chains might apply inter- and intrapolymer, as in many cases different molecular weights can be obtained for the same molecule.

It is worth mentioning that having a composition based on polysaccharides, provides the drug carriers with the incomparable advantage of ensuring degradation within the body. This degradation will be mediated by natural biological processes that include enzymatic breakdown into monosaccharide units. This eliminates concerns on the removal of the carrier after release of the active agent and is the premise for biodegradability. Nevertheless, on proposing any material for an application involving a determined route of administration, it is required that specific local biodegradability is ensured.

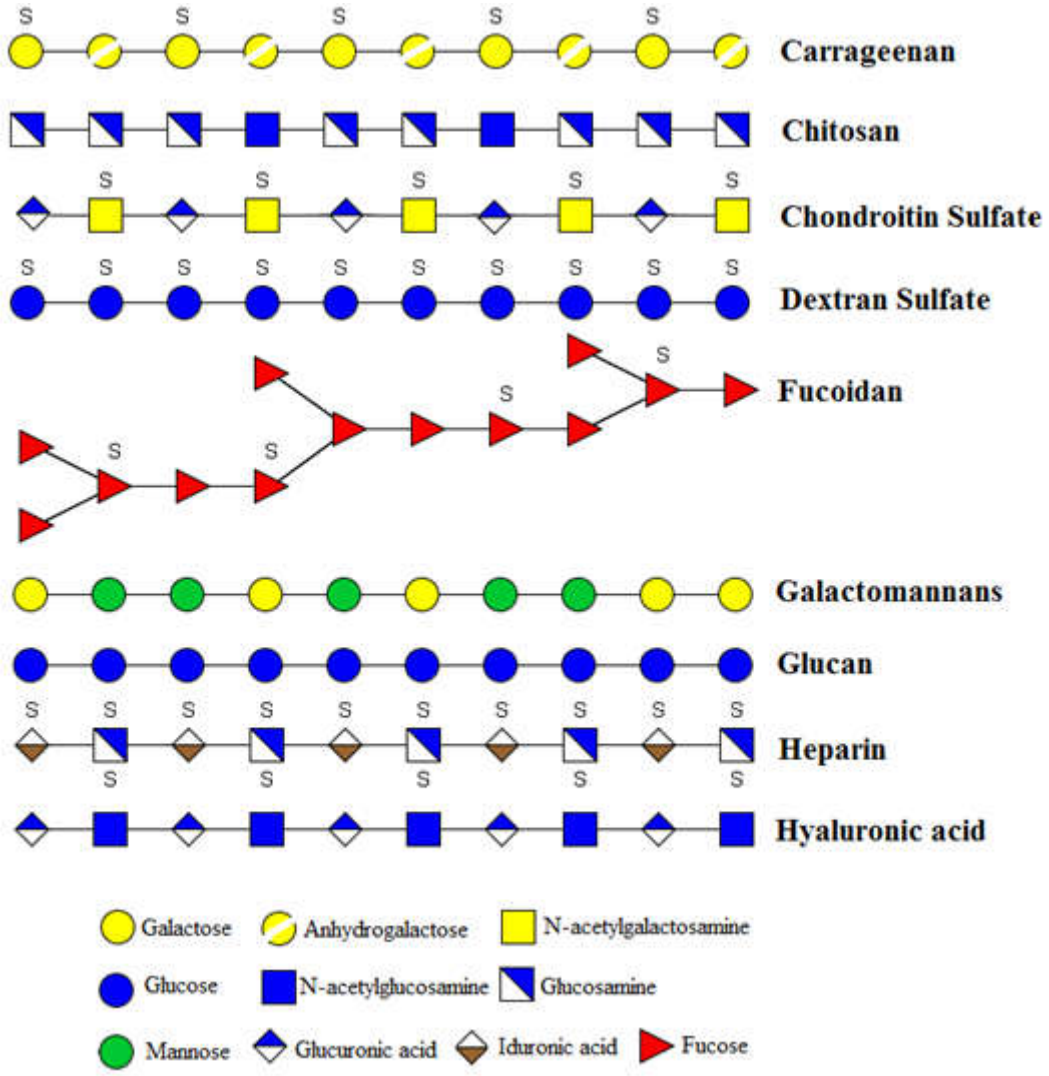

Figure 1.9. - Carbohydrate sequence of some polysaccharides evidencing ability for macrophage targeting via receptor recognition. *S* represents sulphate groups. Reprinted with permission from Rodrigues, 2015 [10].

The present thesis developed drug carriers that intended to explore the potential of two polysaccharides in the context of tuberculosis therapy, chondroitin sulphate and carrageenan. Their specific characteristics are, thus, detailed below.

1.3.1. Carrageenan

Carrageenan (CRG) is extracted from red edible seaweed, being mainly used as thickener in food industry (EU approved additive - E407), but also evidencing gelling and stabilising properties. CRG main application is in dairy and meat products, due to the strong binding to food proteins. Different pharmacopoeias

(British, United States and European) include CRG as pharmaceutical excipient. Its use is reported in a variety of non-parenteral dosage forms, including suspensions (wet and reconstitutable), emulsions, gels, creams, lotions, eye drops, suppositories, tablets, and capsules [116]. Several works report its potential application in drug delivery [117]. Antiviral and antibacterial properties have been reported for this polysaccharide [118-120], while some ongoing clinical trials report its ability for interaction with viruses [121-123].CRG market worldwide sales are estimated to be around $525 million/year [124]. The type of seaweed from which carrageenan is extracted is common in the Atlantic Ocean near Britain, Europe and North America. First discovered by the British pharmacist Stanford in 1862, CRG is a complex group of linear polysaccharides made up of repeating galactose-related monomers [125], some of them bearing sulphate groups. CRG might be of three main types: lambda, kappa and iota. Kappa CRG is the one with higher gel strength and is the most commonly used type, congregating about 70% of the worlds' total production of the polymer. Kappa CRG is composed of galactose-4-sulphate and anhydrogalactose units. On the contrary, lambda-type is highly sulphated and the only of the three types not presenting gelling ability, thus being the less used in drug delivery applications. In turn, iota CRG has a sulphate content intermediate between kappa and lambda CRG, forming an elastic gel with good freeze-thaw and re-healing properties [126].

CRG can cause reproducible inflammatory reaction and remains a standard irritant for examining acute inflammation and the behaviour of anti-inflammatory drugs. With specific interest regarding the ambit of this work, CRG is reported to alter the binding, phagocytosis and killing abilities of macrophages [127]. CRG-macrophage interactions are still under characterisation, but knowledge produced so far indicates that the interaction is mediated by scavenger receptor class A [128]. In parallel, there is some controversy about the involvement of TLR-4, as some works defend its affinity for lambda carrageenan [129], while other works report no affinity [130].

Importantly, some studies report CRG as macrophage depleting agent [131-133], but the cytotoxic effect has been referred to be restricted to short length chains appearing upon degradation [134]. Molecular size seems to be the key parameter regarding the toxicological effect. In this regard, 1.7 *k*Da CRG is reported to

stimulate the induction of IL-10 in human- and in mice-blood cells in a concentration-dependent way, while the stimulation with the original polysaccharide molecule (400 *k*Da) does not induce a concentration-dependent effect [135]. In agreement, several works, including those from our team, have referred an absence of toxicity or inflammatory response in different cells (HEK293 cells [130], A549 and Calu-3 cells [136, 137]) upon contact with CRG (polymer). It is a fact that no cytotoxic effect was observed in the respiratory epithelial cells at concentrations of up to 1 mg/mL, but it is also true that the studies did not include the effect of the degradation products of CRG [136, 137]. Although some reports indicate an apparent toxicity, low molecular weight CRG (1.7 *k*Da) was, in 2003, associated with antitumor activity [138], providing an indication on another possible application. Recently, the polymer was in fact presented as food supplement candidate, as an alternative approach to metastatic human colon cancer therapy. The treatment with carrageenan enhanced the intracellular mitochondrial ROS levels in HCT-116 (human colon cancer) but not in HEK293 (human embryonic kidney) and L6 (rat myoblast) cells, leading to the apoptosis of colonic cells only [139]. A very recent study performed in preweaning piglets, in turn, has demonstrated no adverse effects of CRG administered at a daily dose of 2250 ppm for 28 days, ruling out any effect from degradation products. The authors inclusively propose a safe dose for infants (0 - 12 weeks) equivalent to 430 mg/kg/day [140]. As understood, data on the safety of this polymer results in some controversy. Although the polymer is certainly one of those requiring more tests to confirm or clear the toxicity concern, it has been proposed several times in drug delivery. Proposed applications include the delivery of anti-tubercular drugs and address pulmonary delivery [141-143], which is considered a sensitive route, compared with others that are more robust, such as the oral. However, no reports are available so far for an application in macrophage targeting. In order to avoid this CRG toxicity concern, starch was selected to complement the matrix, as it is a low cost polymer, abundantly available, degradable and is approved as excipient in several pharmaceutical applications [144, 145].

1.3.2. Chondroitin sulphate

Chondroitin sulphate (ChS) is a sulphated polymer and, as happens for most of the sulphated polymers reported as macrophage activators, it belongs to the family of proteoglycans. Proteoglycans are macromolecules composed of a central core protein to which one or more glycosaminoglycan chains are covalently attached. The latter are large carbohydrates that are composed of repeating disaccharide units and exist in four forms: 1) heparan sulphate and heparin, 2) ChS (mainly ChS A and ChS C, and dermatan sulphate, ChS B), 3) keratan sulphate and 4) hyaluronic acid (HA). The first three occur predominantly as protein-bound glycosaminoglycans and contain sulphate, while only HA is a free glycosaminoglycan and lacks the sulphate groups.

ChS chain is composed of alternating sugars (*N*-acetylgalactosamine and glucuronic acid) and might has over 100 monomers, each of which having the possibility to be sulphated in varied positions and quantities. ChS is an important structural component of cartilage and provides much of its resistance to compression. Along with glucosamine, it has become a widely used dietary supplement for the treatment of osteoarthritis. ChS A and dermatan sulphate are structurally related, since both are 4-sulphated, whereas the form C of chondroitin is 6-sulphated. Soluble proteoglycans constitute a class of molecules produced by human monocytes and macrophages upon stimulation, among other classes of pro- and anti-inflammatory cytokines, prostaglandins, leukotrienes, and reactive oxygen metabolites. ChS proteoglycans have been reported to be the predominantly soluble proteoglycan produced by cells of the monocyte/macrophage lineage. From these, 80% to 90% correspond to chondroitin 4-sulphate (ChS A or dermatan sulphate) [146]. Relevant information in the ambit of this work is the fact that chondroitin 4-sulphate chains have been reported to be recognised by several macrophage structures. These include the extracellular portion of mannose receptor, the membrane-distal cysteine-rich domain Cys-Macrophage receptor [147], and the CD44 receptor [146]. In turn, chondroitin 6-sulphate units do not undergo a direct recognition. The scavenger receptors are also reported to mediate chondroitin recognition [128]. Several studies evidence the anti-inflammatory effect of chondroitin [148-151]. Indeed, this polysaccharide demonstrated selective inhibition of inflammatory cytokines released by LPS stimulated murine macrophages [152] and from monosodium

urate crystal induced human macrophages [153]. Furthermore, it was shown to influence the phagocytic activity of latex beads and the release of reactive oxygens species in guinea-pig peritoneal macrophages [154].

1.4. Pulmonary delivery of antitubercular drugs

In tuberculosis, the infectious bacteria enter the organism through the lung and alveolar macrophages act as pathogen hosts. In that case, the administration of drug carriers directly to the lung, by means of inhalation, might be an effective therapeutic approach and the delivery of dry powder formulations adequate.

Targeting drugs to macrophages in this context has the great advantage of delivering therapeutically effective concentrations of drugs to the primary site of infection. Moreover, there is the additional benefit of bypassing first-pass metabolism when lung delivery is envisaged [99].

In most of the current approaches of drug delivery, the drugs are incorporated in carriers that frequently assume particulate forms, either at the nano- or the microscale, and which are usually of a polymeric base. The use of carriers for the strategy of macrophage targeting might has a dual benefit. On one side, macrophages have an innate ability for unspecific uptake of particulate matter (phagocytosis). On the other side, the carriers can be properly designed to have a composition that favours both the interaction with these cells and the consequent internalisation, which will ensure the localisation of drugs inside the infected niche. The uptake of particles by macrophages has been reported to be maximal for sizes of 1-2 μm [108, 155], thus showing a benefit of using microparticles instead of nanoparticles. Shape also affects internalisation, spherical particles being more prone to phagocytosis than irregular shaped particles [156]. Polysaccharides might be easily processed to obtain particles of that dimension, as several methods are available to permit so, including spray-drying or emulsification-based techniques, for instance. It might be argued, though, that hydrophobic materials are those reported to favour phagocytosis the most [108]. However, polysaccharides although not hydrophobic, have the recognition provided by specific receptor interactions, as detailed above.

Successful administration of drugs to the lungs, however, requires suitable carriers that must be rigorously designed to exhibit the adequate properties to reach the desired zone. This is highly dependent on the therapeutic objective. In fact, the lung route may be very useful both for the delivery of systemically acting drugs, such as proteins, and for drugs intended to treat local diseases of the lung. In the case of tuberculosis, as was already referred, therapeutic carriers must reach the alveolar zone, where macrophages hosting *Mtb* reside. The fate of particles administered by inhalation is highly dependent on several parameters, including the deposition pattern and the mechanisms of lung clearance. The deposition of aerosol particles in a particular region of the respiratory tract depends on their aerodynamic properties, namely the aerodynamic diameter (Daer), and on the patient's breathing pattern. Daer of an irregular particle is equivalent to the diameter of a sphere with unit density (1g/cm^3) which has the same settling velocity as the particle that is to be characterised [157]. As indicated in Figure 1.10, carriers with a Daer higher than 10 µm will collide and settle in mouth and throat, higher than 5 µm are mainly deposited in the upper airways, while sizes below 5 µm can be distributed to the lower airways [158].

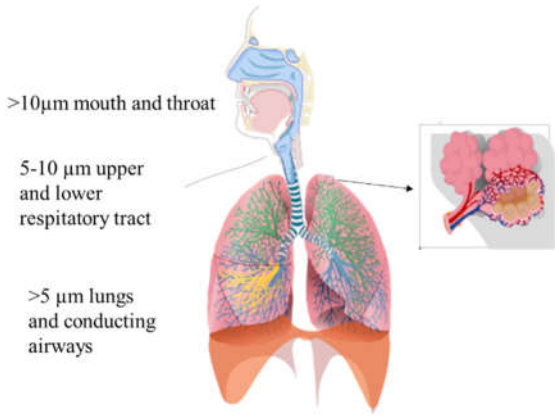

Figure 1.10 – Particle deposition in the lungs according to the aerodynamic diameter, adapted from [159].

Inhalable therapy of tuberculosis requires carriers that reach the respiratory zone, generally accepted to exhibit aerodynamic diameter between approximately 1 and 5 µm. Importantly, particles with a very small size (Daer < 0.5 µm) have been reported to face a high risk of exhalation, because their low mass prevents

effective deposition in the mucosal surface [159]. Additionally, holding the breath during inhalation is known to favour the deeper penetration of particles and the sedimentation on airway surface [160].

Lung delivery of drugs promoted by the use of carriers has several advantages, potentially increasing drug residence time and providing protection from local degradation, as well as possibly promoting stability during aerosolisation. Among the various systems mediating the delivery of drugs by inhalation, dry powders are one of the most used nowadays. Comparing with liquid counterparts, they present the great advantage of being in the solid state, which confers extra stability [161]. Inhalable dry powders can be prepared by different techniques, but spray-drying is one of the most common and popular. Briefly, the polymer is first dissolved in a suitable solvent and the drug is then dispersed/solubilised in the polymer solution. This dispersion is then atomised in a stream of hot air, leading to the formation of small droplets. This happens in a drying chamber where temperature is set to enable instantaneous solvent evaporation, which results in the formation of microparticles. In the end, these are separated from the hot air by means of a cyclone separator. Spray-drying is described as highly reproducible, even on an industrial scale. It is in fact relatively easy to scale up, it is simple, fast, inexpensive and usually provides a regular distribution of particle size, as well as ensures uniformity of drug distribution even when used at lower doses [162]. Furthermore, it is a unique single step method for microencapsulation of drugs in polymeric carriers and is frequently used for the production of dry powders [163].

This page was intentionally left in blank

Chapter II - Motivation and Objectives

This page was intentionally left in blank

2. Motivation and objectives

Tuberculosis is one of the leading causes of death worldwide and demands a more efficient treatment. Despite the existence of a vaccine, this is not completely efficient, and the prevalence of the disease is increasing in many countries, especially associated with the co-infection with HIV. The existing therapy is effective but prolonged and associated with side effects. Moreover, the available antibiotics are increasingly facing issues of drug resistance, which is raising serious concern in the WHO. Extra efforts are, thus, being endeavoured worldwide in the search of alternatives [164]. Finding a therapeutic approach that permits the use of lower doses ideally associated with a shorter treatment, would certainly be beneficial.

New cases of tuberculosis predominantly start as pulmonary tuberculosis, due to the propagation of the disease via inhalation. Alveolar macrophages host the infectious bacteria and should sustain the progression of the disease, but the bacteria have the mechanisms to survive and replicate inside these cells. Endowing the antitubercular drugs with the proper means to target macrophages would, thus, lead to better therapeutics, enabling drug accumulation in the infection site. Specific receptors present in the surface of macrophages could be explored for this targeting purpose. In this context, several polysaccharides are constituted by moieties that resemble the natural ligands of those receptors. CRG and ChS are two sulphated polysaccharides constituted by alternated residues of sulphated galactose/anhidrogalactose and glucuronic acid/sulphated *N*-acetylgalactosamine respectively. Both have been reported to interact with macrophage receptors.

Considering the basics of tuberculosis physiopathology, the recommendations of the WHO for combined therapy and the reported macrophage targeting ability of the referred polymers, it was hypothesised that developing a polysaccharide-based carrier with suitable properties for inhalation, aimed at pulmonary tuberculosis therapy, would be a valuable alternative for the treatment of this disease. Therefore, taking into account the motivations referred above, the main objective of this work was to explore the potential of CRG and ChS as matrix materials of lung drug delivery carriers, in the context of tuberculosis therapy. INH and RFB, two first-line drugs in tuberculosis treatment, were chosen as model

drugs considering the different molecular sizes, aqueous affinity and mechanism of action.

In order to accomplish the referred general objective, several partial objectives were considered:

- To produce ChS- and CRG-based microcarriers by a technique of spray-drying and evaluate the effect of different solvents on the characteristics exhibited by the microparticles;
- To determine the capacity of microparticles to simultaneously associate the selected model drugs, and to characterise their release profile;
- To assess the aerodynamic properties of the developed microparticles and establish their potential to reach the alveolar zone where macrophages hosting the bacteria reside;
- To evaluate the effect of the microencapsulation process on the antibacterial activity of drugs against a strain of mycobacteria;
- To estimate the cytotoxicity of the developed drug carriers in human pulmonary epithelial (A549) cells and macrophage-like cells (human differentiated THP-1 cells and mouse J774A.1 cells);
- To evaluate the capacity of the carriers to interact with the alveolar macrophages, especially regarding to the ability of these cells to uptake the proposed carriers;
- To perform a preliminary *in vivo* assay to elucidate on the safety of the microparticles for an application via inhalation, searching for signs of allergic or inflammatory responses.

In this manner, it was expected to develop polymeric carriers which efficiently associate antibiotics, retain the inhibitory activity after encapsulation, present adequate aerodynamic properties to reach the alveolar zone after inhalation and display the ability to target alveolar macrophages without inducing toxicity.

Chapter III - Development of polysaccharide microparticles and evaluation of biological interactions: Materials and methods

This page was intentionally left in blank

3. Development of polysaccharide microparticles and evaluation of biological interactions: Materials and methods

3.1. Materials

k-CRG was obtained from FMC Biopolymer (Norway). Starch (C*pharmGel 12012) was a kind gift from Cargill (USA). ChS was acquired from Creative Biomart (USA). Dimethylformamide (DMF), dimethyl sulfoxide (DMSO), Dulbecco's modified Eagle's medium (DMEM), fluorescein sodium salt, HCl, isoniazid (INH), L-glutamine solution (200 mM), non-essential amino acids solution and penicillin/streptomycin (10000 units/mL, 10000 g/mL), *N*-(3-dimethylaminopropyl)-*N*′-ethylcarbodiimide hydrochloride (EDAC), phorbol 12-myristate 13-acetate (PMA), phosphate buffered saline (PBS) tablets pH 7.4, sodium dodecyl sulphate (SDS), trypan blue solution (0.4%), trypsin-EDTA solution (2.5 g/L trypsin, 0.5 g/L EDTA), Tween 80® and thiazolyl blue tetrazolium bromide (MTT) were purchased from Sigma-Aldrich (Germany). APC-CD11b antihuman antibody was obtained from BioLegend (USA). Rifabutin (RFB) was supplied by Chemos (Germany) and fetal bovine serum (FBS) by Gibco (Life Technologies, USA). RPMI 1640 was obtained from Lonza Group AG (Switzerland). Lactate dehydrogenase (LDH) kit was supplied by Takara Bio (Tokyo, Japan). Middlebrook 7H9 (M7H9; 4.7 g/L) and oleic acid, albumin, dextrose and catalase supplement (OADC) were purchased from Remel (Lenexa, KS, USA). Cellular stains Hoechst 33342 from Thermo Fisher Scientific Inc (USA) and HCS CellMask Deep Red, HCS LipidTOXTM Phospholipid Red, HCS LipidTOXTM Green and Image-iT® DEAD™ Green were obtained from InvitrogenTM (UK). Ultrapure water (MilliQ, Millipore, UK) was used throughout. All other chemicals were reagent grade.

3.2. Preparation of microparticles

Two formulations of microparticles were prepared by spray-drying, either containing ChS or a mixture of starch/CRG. The specific protocols are detailed below:

Starch/CRG microparticles

Starch/CRG microparticles, without drug and containing an association of the antitubercular drugs INH and RFB, were prepared according to a previously

reported protocol [165]. The total concentration of the polymers in the final dispersion was 2% (w/v), of which 80% corresponded to starch and 20% to CRG. The dispersion of the polymers was placed on a water bath at 85 ºC under slow stirring for 30 min to enable solubilisation of both materials. Drug-loaded microparticles were produced at polymer/INH/RFB mass ratio of 10/1/0.5 and while INH was solubilised in water, 10 mL of HCl at 0.01M were used to enable the solubilisation of RFB. Due to the gelling ability of CRG, the spraying solutions were maintained at 85 ºC during the spray-drying process. This was performed using a laboratory mini spray dryer (Büchi B-290, Büchi Labortechnik AG, Switzerland) operating in open mode and equipped with a high-performance cyclone. Protection from light was ensured during the whole process. The operating parameters were: inlet temperature: 170 ± 2 ºC; aspirator setting: 90%; feed rate: 0.7 ± 0.1 mL/min; and spray flow rate: 473 L/h. These conditions resulted in outlet temperature of 110 ± 2 ºC.

Fluorescent (unloaded) microparticles of CRG were further prepared, to be used in the assay of macrophage capture. Fluorescein was covalently bound to CRG in the presence of EDAC, which is an activator of the fluorescein carboxyl group. To do so, 1 g of CRG was dissolved at 1% (w/v) in 10^{-4} M HCl. Fluorescein sodium salt (23.5 mg dissolved in 2 mL of ethanol) and EDAC (16.3 mg dissolved in 30 mL of 10^{-4} M HCl) were previously mixed and added to the former solution. The reaction mixture was kept under stirring in the dark for 72 h and afterwards dialysed (2000 Da Mw cut-off) against distilled water, protected from light. The dialysate was frozen and freeze-dried (FreeZone Benchtop Freeze Dry System, Labconco, Kansas City, MO, USA). The fluorescently-labelled polymers were stored in a desiccator until further use, under light protection. Fluorescent microparticles were produced by spray-drying, as described above.

Chondroitin sulphate microparticles

The commercial polymer was not of pharmaceutical grade and contained 5.52% (w/w) of protein. A purification of ChS was, thus, performed by ethanol precipitation. To do so, commercial ChS was solubilised in water at 5% (w/w, 200 mL) and poured over 250 mL of ethanol. This was left to rest at 4 ºC overnight. After that, the dispersion was centrifuged (22 000 g, 4 ºC, 1 h). The polymer was

recollected from the pellet, freeze-dried and stored in a desiccator for further use. All the experiments described below were performed with the purified ChS.

ChS microparticles were prepared by spray-drying, either unloaded or containing an association of the antitubercular drugs INH and RFB. ChS was used at 2% (w/v) in all cases and the drug-loaded microparticles were produced at ChS/INH/RFB mass ratio of 10/1/0.5, similar to what was established for starch/CRG microparticles. While INH was solubilised in water, the hydrophobic character of RFB required the use of a co-solvent. Ethanol 70% (v/v) and HCl 0.01 M were tested for this end and the obtained RFB solution was then added to the previously formed ChS/INH solution. When ethanol was used, final water/ethanol ratio of 80/20 (v/v) was applied in the spraying solution, while HCl was used at a final concentration of 0.002 M. The solutions were spray-dried in a laboratory mini spray-dryer (Büchi B-290, Büchi Labortechnik AG, Switzerland) operating in open mode and equipped with a high-performance cyclone. The operating parameters were similar to those used for starch/CRG microparticles, which the exception of an inlet temperature of 175 ± 2 ºC. The applied conditions resulted in outlet temperature of 110 ± 2 ºC.

Similarly to starch/CRG microparticles, fluorescent microparticles of ChS were also produced for the assessment of microparticle uptake by macrophages, using an adaptation of the described protocol. In this case, 1 g of ChS was dissolved at 2% (w/v) in water. Fluorescein sodium salt (15 mg dissolved in 1.5 mL of ethanol) and EDAC (11.4 mg dissolved in 30 mL of milli-Q water) were previously mixed and added to the former solution. The reaction mixture was kept under stirring in the dark overnight and afterwards dialysed (2000 Da Mw cut-off) against distilled water, protected from the light. The dialysate was frozen and freeze-dried (FreeZone Benchtop Freeze Dry System, Labconco, Kansas City, MO, USA). The fluorescently-labelled polymers were stored in a desiccator until further use, under light protection. Fluorescent (unloaded) ChS microparticles were prepared under the same conditions described above.

In all cases, microparticles were collected after spray-drying and placed in a dark flask, being stored inside a desiccator until further use.

The spray-drying yield was calculated by gravimetry, comparing the total amount of solids initially added with the resultant weight of microspheres after spray-drying [166].

3.3. Characterisation of microparticles

The morphology of microparticles was characterised by field emission scanning electron microscopy (FESEM; FESEM Ultra Plus, Zeiss, Germany), after sputter-coating (model Q150T S/E/ES, Quorum Technologies, UK) the samples with iridium (5 nm thick).

The particle size distribution of microparticles was determined by laser light scattering (Spraytec, Malvern Panalytical, UK). To do so, approximately 15 mg of dry powder were dispersed in 15 mL of 2-propanol and sonicated for 5 min. Various parameters were calculated automatically in the Spraytec software (Malvern Panalytical, UK) to establish the volume-based size distribution. The particle sizes below which 10%, 50% and 90% of the spray lies, were determined, being expressed as Dv(10), Dv(50) and Dv(90). From these values, span was calculated as follows:

$$\text{Span} = \frac{Dv(90) - Dv(10)}{Dv(5\ 0)} \quad (3.1)$$

The analyses were carried out in triplicate with an obscuration threshold of 10%.

3.4. Determination of drug association and release

In order to determine the drug content, drug-loaded microparticles were completely dissolved in HCl 0.1 M (30 min magnetic stirring). Samples were then centrifuged (16000 g, 10 min; Heraeus Fresco 17 centrifuge, Thermo scientific, USA) and filtered (0.45 µm). Drug content was determined by HPLC (Agilent 1200 series, Germany) using an adaptation of previously reported methods [167-169]. A gradient of acetonitrile in 50 mM potassium dihydrogen phosphate eluted isoniazid and rifabutin sequentially after a single injection. A LiChrospher® 100 RP-18 (5 µm) column of 4 mm i.d.×250 mm length with security guard cartridge

was used. The eluent was a mixture of 50 mM potassium dihydrogen phosphate (A) and acetonitrile (B) at a flow rate of 1 mL/min. The used chromatographic conditions were: A:B starting at 95:5 and kept in the first 5 min, changed afterwards to 20:80 in 3 min and kept in this 20:80 during additional 6 min. Detection was performed by a diode array detector at 275 nm. INH was eluted at 3.8 min and RFB at 12.6 min. A linear calibration plot for INH and RFB was obtained over the range of 10-400 µg/mL (n = 3).

Drug association efficiency (AE) and microparticle (MP) loading capacity (LC) were estimated as follows (n = 3):

AE (%) = (Real amount of drug on MP / Theoretical amount of drug on MP) x 100 (3.2)

LC (%) = (Real amount of drug on MP/ Weight of MP) x 100 (3.3)

The determination of drug release was performed in PBS pH 7.4 added of 1% (v/v) Tween 80®. The assay respected sink conditions, as the maximum amount of drug was always below 30% of its maximum solubility [170]. INH solubility was considered 274 ± 4.79 mg/mL [171], while that of RFB was 0.496 mg/mL [165]. A determined amount of microparticles (30 mg) was incubated with the medium (10 mL), at 37 °C, under mild shaking (100 rpm, orbital shaker OS 20, Biosan, Latvia). Samples (1 mL) were periodically collected and the amount of each drug quantified as indicated above (n = 3).

The release profiles of both drugs were compared using the similarity factor (f_2), according to the following equation:

$$f2 = 50 \times \log\left([1 + (1/n)\sum_{t=1}^{n}(R - T)^2]^{-0.5} \times 100\right) \quad (3.4)$$

R is the mean of the dissolved drug from the reference batch at time t, T is the mean of the drug dissolved from the test batch at time t, n is the number of time points. f_2 values between 50 - 100 represent less than 10% difference between

released drugs at each time point (i.e. similarity) and values <50 are considered dissimilar [172].

3.5. Aerodynamic characterisation of microparticles using an Andersen cascade impactor (ACI)

HPMC size 3 capsules (Quali-V-I, Qualicaps, Spain) were filled with 30 mg of drug loaded microparticles. The content of three capsules was discharged in each aerodynamic test using the medium resistance RS01® inhaler (Plastiape Spa, Italy) and experiments were performed in triplicate. The device was connected to the Andersen cascade impactor (ACI, Copley Scientific, UK) which operates at 60 L/min, ensuring a pressure drop of 4 kPa through the device. This was activated for 4 s in order to let 4 L of air passing through the system, thus complying with the standard procedure described by USP 38 and Ph.Eur.8 [173, 174].

The ACI separates particles according to their aerodynamic diameter and it was assembled using the appropriate adaptor kit for the 60 L/min air flow test. Cut-offs of the stages (-1 to 6) at the air flow rates adopted in this work are reported in Table 3.1. A glass fibre filter (Whatman, Italy) was placed right below stage 6 in order to collect particles with diameter lower than that of stage 6 cut-off.

Table 3.1. Cut-off aerodynamic diameter (μm) for stages of Anderson cascade impactor (ACI) used at 60 L/min.

Stage -1	Stage -0	Stage 1	Stage 2	Stage 3	Stage 4	Stage 5	Stage 6
8.60	6.50	4.40	3.20	1.90	1.20	0.55	0.26

The plates of the impactor were coated with a thin layer of ethanol containing 1% (w/v) Tween 20® to prevent particle bounce. The drugs were recovered from the apparatus with water/acetonitrile mixture (50/50, v/v) and quantified by HPLC (Agilent 1200 series, Germany) as described above. The quantification of drug deposited inside the impactor allows calculating different aerodynamic parameters. Emitted dose (ED), metered dose (MD), mass median aerodynamic

diameter (MMAD), fine particle dose (FPD) and fine particle fraction (FPF) were calculated as described elsewhere [100].

The recovery (%) is the percentage of MD versus the labelled dose. The recovery ranged between 77-91% in all the experiments, generally complying with the pharmacopeial requirements [175].

3.6. In vitro determination of antitubercular activity

The *in vitro* antitubercular efficacy of microparticles was evaluated against *Mycobacterium bovis* bacillus Calmette-Guérin (BCG). The Minimum Inhibitory Concentration (MIC) of free and microencapsulated INH and RFB was determined by the microdilution method [176]. Drug loaded microparticles and the powders of free drugs were exposed to UV light for 10 min to provide sterilisation. Then, a solution of each dry powder was prepared at 1 mg/mL and diluted to the desired drug concentrations. First, 1 mg/mL stock solution of INH was prepared by dissolving the drug in the M7H9 supplemented medium. RFB was previously solubilised in DMSO (1 mg/mL) and then diluted with M7H9 broth. Drug stock solutions were mixed to reach concentrations corresponding to drug loadings. Two-fold dilutions of the antibiotics/microparticles were performed to obtain final concentrations of RFB from 0.001 to 0.125 µg/mL and of INH from 0.008 to 1 µg/mL. A 1/10 dilution of a McFarland 1.0 turbidity standard suspension of *M. bovis* BCG was inoculated (20 µL of inoculum in 180 µL of medium or test solution) with a multichannel pipette, delivering approximately 10^4 CFU per well. The outside lane of wells (a frame-like) was filled with sterile distilled water to avoid the evaporation of microplate content. The plates were covered with the lid, sealed with parafilm and incubated at 37 °C (Binder, USA) for 7 days. Afterwards, 30 µL of MTT sterile solution were added to each well, followed by 4 h of incubation at 37 °C. Then, 50 µL of DMSO were added into the wells to solubilise the tetrazolium blue crystal that was produced, which is proportional to the growth rate of mycobacteria. The absorbance was measured by spectrophotometry (Infinite M200, Tecan, Austria) at 540 nm. The assays were performed in triplicate. The MIC value was considered the lowest that inhibited mycobacteria growth by 95 – 100% [177, 178].

3.7. *In vitro* evaluation of the toxicological profile of microparticles

3.7.1. Cell lines

A549 cells (human alveolar epithelium) and J774A.1 cells (mouse macrophages) were obtained from the American Type Culture Collection (ATCC, USA) and used in passages 27-37 and 30-40, respectively. THP-1 cells (human monocytes) were obtained from the Leibniz-Institut DSMZ (Germany) and used in passages 10-20. Cell cultures were grown in humidified 5% CO_2/95% atmospheric air incubator at 37 ºC (HerAcell 150, Heraeus, Germany). Cell culture medium (CCM) for A549 cells and J774A.1 was DMEM supplemented with 10% (v/v) FBS, 1% (v/v) L-glutamine solution, 1% (v/v) non-essential amino acids solution and 1% (v/v) penicillin/streptomycin.

THP-1 cells were grown in suspension and cell culture was maintained between 2 x10^5 and 1.0 x 10^6 cells/mL. When reaching the latter, cells were sub cultivated in new passage at the concentration of 2 x 10^5 cells/mL. Differentiation of THP-1 monocytes to provide the macrophage phenotype (dTHP-1) was performed using PMA. The specific conditions are described below, whenever applicable.

3.7.2. Cell viability evaluation by MTT test

The evaluation of cell viability upon exposure to microparticles was performed by the MTT assay, using three cell lines of high relevance within the scope of tuberculosis infection, A549, J774A.1 and dTHP-1 cells. A549 cells were seeded at a density of 1 x 10^4 cells/well on 96-well plates (Orange Scientific, Belgium), in 100 µL of complete DMEM. J774A.1 cells were seeded at a density of 2.4 x 10^4 cells/well on 96-well plates (Orange Scientific, Belgium), in 200 µL of complete DMEM. Cells were incubated for 24 h at 37 ºC in 5% CO_2 atmosphere before use. THP-1 cells were differentiated before the experiments to acquire the macrophage-phenotype. To do so, cells were seeded on 96-well plates (3.5 x 10^4 cells/well) in 100 µL of RPMI supplemented with PMA and incubated for 48 h at 37 ºC in 5% CO_2 atmosphere. After that time, CCM was renewed for other 24 h, before the experiments.

Microparticles and polymers at the concentrations of 0.1, 0.5 and 1.0 mg/mL were incubated with the cells in the form of a suspension prepared in pre-warmed CCM without FBS and evaluated for 3 h and 24 h. Free INH (0.1, 0.05 and 0.01 mg/mL)

and free RFB (0.05, 0.025 and 0.005 mg/mL) were also tested as controls in a similar protocol, the tested concentrations corresponding to those theoretically present in microparticles.

MTT solution (0.5 mg/mL in PBS, pH 7.4) was added after the exposure time (in A549 and J774A.1 cells, samples were previously removed; in dTHP-1 cells no removal was applied). Incubation was allowed for 2 h, after which formazan crystals were solubilised with DMSO (A549 and J774A.1 cells) or 10% SDS in a 1:1 mixture of DMF:water (dTHP-1 cells). The absorbance was measured by spectrophotometry (Infinite M200, Tecan, Austria) at 540 nm and background correction was applied at 650 nm. The viability of untreated cells was assumed to correspond to 100% of cell viability, and that of treated cells was compared to this control. The assay was replicated at least three times, each with six replicates.

3.7.3. Determination of cell membrane integrity

The integrity of cell membrane after exposure to microparticles was determined by the quantification of LDH released by cells. The assessment was performed in A549 and dTHP-1 cells upon 24 h exposure to a concentration of 1 mg/mL of unloaded and drug-loaded microparticles. The chosen concentration corresponds to the maximum concentration tested in the MTT assay.

Cells were cultured in 96-well plates in the conditions described above for the MTT assay (the assays were performed simultaneously). Upon exposure, cell culture supernatants were collected, centrifuged (1 000 x g, 5 min, 4 ºC) and processed using a commercial kit. Absorbances were measured by spectrophotometry (Infinite M200, Tecan, Austria) at a wavelength of 490 nm (background correction at 690 nm).

A negative control of LDH release was performed incubating cells only with the respective CCM and a positive control corresponded to the lysis solution (Triton-X 10% (v/v) in CCM). Released LDH (%) upon incubation with each sample was determined by comparison with the 100% of the positive control. All measurements were performed in triplicate.

3.7.4. High content analysis of the responses of J774A.1 cells to ChS microparticles

J774A.1 cells were seeded at a density of 1.5 x 10^4 cells/well on µClear® bottom black 96-well plates and incubated overnight to adhere to the plates. Different concentrations of ChS polymer, unloaded ChS microparticles and drug-loaded ChS microparticles produced with ethanol (20-1400 µg/mL), INH (10-1000 µg/mL) and RFB (1-100 µg/mL) were incubated with the cells for 48 h. Amiodarone (10 µM) was used as a phospholipidosis control, carbonyl cyanide-4-(trifluoromethoxy)phenylhydrazone (FCCP; 200 µM) was used as a mitochondrial activity control, and 0.5% (v/v) Triton-X was used as a membrane permeability control. The staining procedure was adapted from the one used in Hoffman et al, 2017 [179]. After the 48 h incubation time, cells were stained with a dye cocktail containing Hoechst 33342 10 µg/mL, MitoTracker Red 300 nM and Image-iT® DEAD™ Green 25 nM (Invitrogen, Renfrewshire, UK) for 30 min. Cells were washed once with 100 µL PBS and fixed with 3.7% w/v paraformaldehyde for 15 min. Cells were then washed once more with PBS prior to imaging. For the determination of lipid content, cells were incubated with HCS LipidTOXTM Phospholipid Red (Invitrogen, Renfrewshire, UK) diluted 1:2000 for 48 h, then fixed with 3.7% w/v paraformaldehyde containing Hoechst 33342 (10 µg/mL) for 20 min, followed by one wash step with PBS. The fixed cells were then incubated with HCS LipidTOXTM Green (Invitrogen, Renfrewshire, UK) diluted 1:2000 for 30 min at room temperature for detection of neutral lipids. Images were captured using the Cytation5 (BioTek® Instruments, Inc., USA) with a 20x objective in standard 2D imaging mode with the following settings; DAPI 377/447 Filter Cube PN 1225100, 365nm LED PN 1225007; GFP 469/525 Filter Cube PN 1225101, 465nm LED PN 1225001 and RFP 531/593 Filter Cube PN 1225103, 523nm LED PN 1225003; and Texas Red 586/647 Filter Cube PN 1225102, 590nm LED PM 1225002. The experiment was performed in triplicate with different passage numbers. Image analysis was performed using Gen5 3.03.14 analysis (BioTek® Instruments, Inc., USA). For cell health and morphology analysis, Hoechst 33342 cell nuclear staining was used to identify nucleated cells and to calculate the number of cells. MitoTraker Red dye is an established cell delineation tool for cellular imaging and was used to highlight the cytoplasmic regions within the cells

identified. This dye detects the changes in the mitochondrial membrane potential and accumulates in active mitochondria. Image-iT® DEAD™ Green is an impermeant dye to healthy cells that becomes permeant when the plasma membrane of cells is compromised. For lipid content analysis, Hoechst 33342 was again used to identify nucleated cells and to calculate the number of cells. HCS LipidTOXTM Green, which has high affinity for neutral lipids, was used to identify and quantify neutral lipid accumulation (steatosis) in cells. The intercellular accumulation of phospholipids (phospholipidosis) was detected and quantified by cell incubation with phospholipids conjugated to fluorescent dye – LipidTOXTM Red Phospholipidosis.

Six quantitative measurements were generated from the analysis, namely mitochondrial activity, cell area, nuclear area, cell permeability, phospholipid content per cell and neutral lipid content per cell, which characterised cell health and lipid content. Data represented 9–12 different experiments, n = 6 wells per experiment, for untreated cells and 3 different experiments, n = 1 well per experiment, for ChS-exposed cells. Exposure conditions that reduced the total number of cells imaged to less than 50% of the number of untreated cells (control) were excluded.

The high content image analysis methodology described by Hoffman et al. 2017 captures multiple parameters for individual cells, enabling analysis of a subset of the population of cells that respond to the drug stimulus [179]. J774A.1 cells were selected following the same criteria from the flow cytometry assay. Profiles describing the cell population were generated to describe cell health, morphology and lipid content characteristics that were elevated from untreated cells. Dead/dying cells were eliminated as described above and mean nuclear area ± two standard deviations of the untreated cell population was used as exclusion criterium to remove cells with partial or double nuclei (dividing cells). The remainder of cell health, morphology and lipid profile descriptors were classified as those that were elevated from untreated controls. ‘Elevated’ responses were defined as being greater than two standard deviations above the mean of the untreated control cell population. Multi-parameter profile analysis of the elevated

population characteristics revealed an impact on elevated phospholipid content and cell health markers as expected for the controls.

3.8. Study of the interaction of microparticles with macrophages

3.8.1. Assessment of the uptake of microparticles by macrophages

Flow cytometry analysis

The determination of macrophage ability to uptake microparticles was performed *in vitro* using dTHP-1 cells. THP-1 cells (3.5 x 10^5 cells/mL) were suspended in RPMI supplemented with 50 nM PMA to allow differentiation and seeded at 3 mL/well in an individual dish for cells in suspension (growth area of 8 cm^2).

Flow cytometry (FacScalibur cell analyser, BD Biosciences, Belgium) was used for the assessment upon exposure to fluorescently-labelled microparticles (100 and 250 µg/cm^2). For this step, CCM was removed and only a residual amount of medium was kept, ensuring the hydration of cell surface. Particles were aerosolised onto the macrophage layer using the Dry powder Insufflator™ (Model DP-4, Penn-Century™, USA) and an incubation of 2 h at 37 ºC was allowed. The phagocytic process was stopped by the addition of a cold solution of PBS with 3% FBS (PBS.3% FBS, 5 mL, two applications). Cells were scraped and centrifuged (800 x g, 2 min, room temperature) in 2 mL of PBS supplemented with 3% FBS. The cell pellet was resuspended in 5 mL PBS.3% FBS and centrifugation/resuspension was repeated thrice. As some microparticles might remain in the cell pellet, APC-CD11b antihuman antibody was incubated with the cells to ensure a double stain, eliminating the interference of non-phagocytosed microparticles in the final reading. An antibody dilution of 1:100 in PBS.3%FBS was incubated in the cell pellet (50 µL) for 1 h on ice. At the end, cells were washed 3 more times and re-suspended in 1 mL of PBS.3% FBS, transferred to cytometry tubes (BD Biosciences, Belgium) and maintained at 4 ºC until the analysis.

In the flow cytometer, FSC-H and SSC-H channels were used, respectively, to measure size and granularity of cells, while side scatter light was used to identify the population of viable cells. The number of cells exhibiting a double fluorescent signal (APC from the antibody and FITC from fluorescent microparticles) was

considered to have phagocytosed microparticles. The assay was replicated at least three times for each dose.

Cell imaging of microparticle uptake

The ability of macrophages to uptake microparticles was further assessed by imaging techniques, using J774A.1 cells and selecting ChS microparticles as reference. The cells were seeded at a density of 1.5 x 10^4 cells/well on µClear® bottom black 96-well plates and incubated overnight for adherence. Different concentrations (0.125; 0.250; 0.500 and 1.00 mg/mL) of fluorescent ChS microparticles were incubated with the cells for 24 h, at 37 ºC. After this time, 100 µL of Hoechst 33342 at 10 µg/mL were added to the wells and incubated for 30 min at 37 ºC. The medium was then discarded and cells washed with 100 µL of PBS. Next, cells were fixed with 3.7% (w/v) paraformaldehyde for 15 min at room temperature. New PBS washing step was performed before the staining with HCS CellMask deep red diluted 1:2000 for 90 min at room temperature, followed by two washing steps with PBS. Finally, 100 µL PBS were added to each well for the analysis of the plates. The fluorescence intensity of each well was measured for the different fluorochrome wavelengths (excitation-emission; FITC: 479-520 nm, Hoechst: 360-460 nm and deep red HCS CellMask: 640-681 nm). Images of the wells were taken using the Cytation5 equipment (BioTek® Instruments, Inc., USA) with a 20x objective and three different filter cubes (GFP 469/525 Filter Cube PN 1225101, 465nm LED PN 1225001; DAPI 377/447 Filter Cube PN 1225100, 365nm LED PN 1225007 and Cy5 628/685 Filter Cube PN 1225105, 623nm LED PN 1225005). The experiment was performed in triplicate.

3.8.2. Interleukin release by macrophages

To evaluate the capability of microparticles to induce the release of pro-inflammatory interleukins by macrophage-like cells, dTHP-1 cells (96 well plates, 3.5 x 10^5 cells/well) were incubated with ChS polymer and ChS/INH/RFB microparticles at 1 mg/mL and starch, CRG and starch/CRG/INH/RFB microparticles at 0.5 mg/mL in CCM. After 24 h of incubation, cell-free supernatants were collected and TNF-α and IL-8 quantified with ELISA kits according to the manufacturer protocol. The amount of each cytokine was expressed in pg/mL based on reference standard curves. Cytokines released

from cells treated with LPS (100 µg/mL) and untreated cells were used as control values. The absorbance of samples was determined by spectrophotometry (Infinite M200, Tecan, Austria) at 450 nm and corrected for background absorbance at 540 nm.

3.9. Statistical analysis

The student t-test and the one-way analysis of variance (ANOVA) with the pairwise multiple comparison procedures (Holm-Sidak method) were performed to compare two or multiple groups. All analysis was run using the GraphPad Prism (version 6.07) and differences were considered to be significant at a level of $p < 0.05$.

Chapter IV - Starch/CRG microparticles: Results and discussion

This page was intentionally left in blank

4.Starch/CRG microparticles: Results and discussion

4.1. Preparation and characterisation of starch/CRG microparticles

Unloaded starch/CRG microparticles were successfully produced by spray-drying with a yield of 58%, which increased significantly to 71% ($p < 0.05$) when the model drugs were associated to the formulation (Table 4.1). This difference in the yield may be explained by the addition of HCl in the drug-loaded formulation, which was visually observed to decrease the viscosity of the solution, as reported elsewhere [180], improving the spraying characteristics. A small amount of HCl was in fact required to dissolve RFB. A possible explanations for the decreased viscosity may be the occurrence of some depolymerisation of CRG [181], although the amount of HCl involved in the experiment is possibly too low for that. On the other hand, CRG used in this work is a mixture of potassium and sodium salt forms. Potassium has been reported to lead to double-helix conformation associated with increased viscosity. It is possible that the addition of HCl in the drug-loaded formulation interfered in the total ionic concentration, consequently altering hydrogen bonds in the double-helix and decreasing the viscosity of the solution [182, 183]. The influence of HCl in the viscosity of polymeric solutions was reported in a previous work of our group regarding locust bean gum, a very viscous polymer [165].

As depicted in Figure 4.1, the morphological analysis of starch/CRG microparticles suggested an increase in the number of small particles upon the inclusion of INH and RFB in the formulation. In fact, this was demonstrated in the characterisation of particle volume diameter, evidencing a decrease from 11.3 μm in the unloaded particles to 7.0 μm ($p < 0.05$) in drug-loaded microparticles (Table 4.1). The microparticles corresponding to both dry powders exhibited dimpled surface morphology. Drugs were successfully associated to microparticles, with efficiencies of 96% for INH and 74% for RFB. The significantly lower value obtained for RFB ($p < 0.05$) is possibly a consequence of its low water solubility (125 mg/mL for INH and 0.19 mg/mL for RFB). Although a solution was previously prepared for spray-drying, when the spray is formed, water starts to evaporate and a phase separation may occur, depending on drug solubility [162]. In fact, after the atomisation process, the walls of the drying chamber assumed a reddish hue, which indicates a certain deposition of RFB.

Table 4.1 – Spray-drying production yield, volume diameter - Dv50 and span, drug association efficiency and loading capacity of starch/CRG microparticles (mean ± SD, n = 3). Different letters represent significant differences in each parameter ($p < 0.05$).

Microparticles (Mass ratio)	Production Yield (%)	Dv50 (μm)	Span	Association Efficiency (%)	Loading Capacity (%)
Starch/CRG (80/20)	58.2 ± 5.0[a]	11.3 ± 0.3[c]	2.3 ± 0.5[e]	n. a.	n. a.
Starch/CRG/INH/RFB (80/20/10/5)	71.0 ± 1.7[b]	7.0 ± 0.7[d]	2.5 ± 0.2[e]	INH: 96.3 ± 3.4[f]	INH: 8.4 ± 0.3[h]
				RFB: 74.4 ± 11.9[g]	RFB: 3.2 ± 0.5[i]

CRG: carrageenan; INH: isoniazid; n.a.: not applicable; RFB: rifabutin

The reported association efficiency corresponded to loading capacities of 8.4% for INH and 3.2% for RFB, which compare with the theoretical values of 8.6% for INH and 4.3% for RFB.

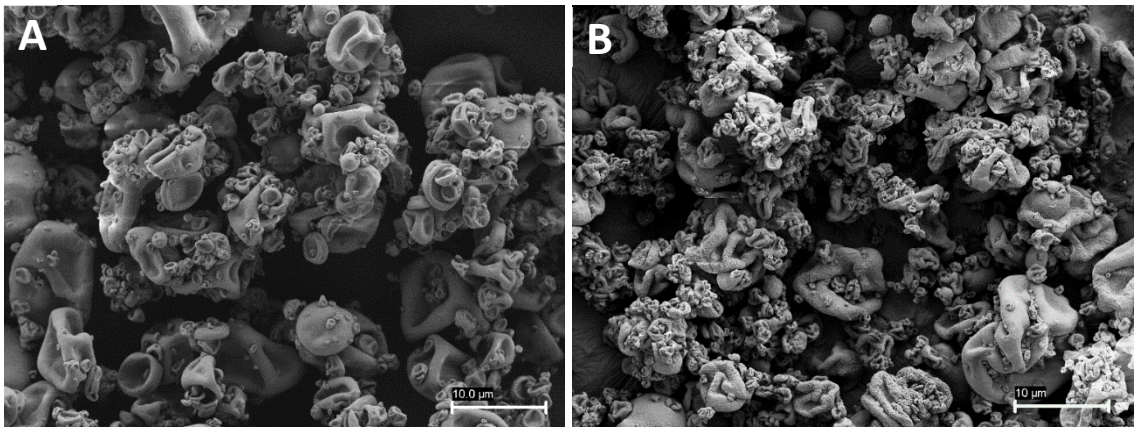

Figure 4.1 - Microphotographs of unloaded starch/CRG microparticles (A) and starch/CRG/INH/RFB microparticles (B) as obtained by scanning electron microscopy. Scale bar is 10 µm.

In order to evaluate the potential of starch/CRG microparticles for inhalation purposes, their aerodynamic properties were characterised using an Andersen cascade impactor, Figure 4.2. Although some differences were observed in drug loading, the deposition profiles showed an even distribution of the two drugs through the stages, which indicates that the drugs were homogeneously distributed through the particles, without a size-dependent preferential allocation.

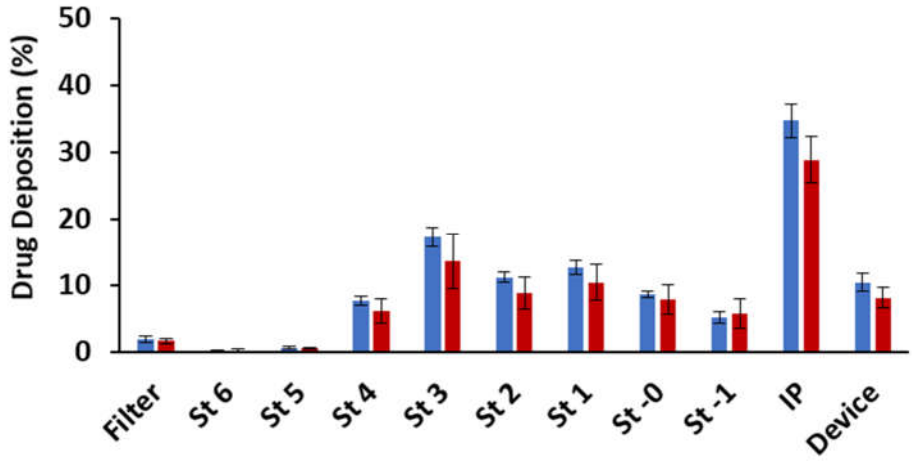

Figure 4.2 – Stage-by-stage deposition profiles of isoniazid (INH, blue) and rifabutin (RFB, red) inside the Andersen cascade impactor after aerosolisation with RS01 inhaler at 60 L/min, inhalation volume of 4L (values are mean ± SD, n = 3). IP: induction port; St: stage.

The mass deposition profiles allowed the calculation of other aerodynamic parameters, detailed in Table 4.2. As a consequence of the homogeneous distribution of both drugs, already referred above, no significant differences were found in the aerodynamic parameters when using INH or RFB as the reference. The calculated MMAD is within 3.3 – 3.9 μm and the determination of FPF indicated that 32% - 38% of microparticles have less than 5 μm, having suitable properties to reach the respiratory zone. This value is in agreement with those usually determined for high dose antibiotic powders formulated without lactose as carrier [100, 184, 185]. The emitted dose is also satisfactory, 91%. Nevertheless, an optimisation of the formulation is envisaged to mitigate the high deposition in the induction port (almost 50%). This area represents the throat, which is difficult to overcome for particles of large size [186] and the high deposition that was observed concords with the determined Dv50 of 7.0 μm.

Table 4.2 - Aerodynamic properties of starch/CRG/INH/RFB (8/2/1/0.5, w/w) microparticles (mean ± SD, n = 3). Different letters represent significant differences in each parameter ($p < 0.05$).

Emitted dose (%)	Drug	MMAD (μm)	GSD (μm)	FPD (mg)	FPF< 5 μm (%)
91.0 ± 3.8	INH	3.9 ± 0.3^{a}	2.2 ± 0.1^{b}	2.3 ± 0.6^{c}	32.1 ± 9.4^{d}
	RFB	3.3 ± 0.4^{a}	2.2 ± 0.1^{b}	1.4 ± 0.3^{c}	37.9 ± 8.0^{d}

FPD: fine particle dose; FPF: fine particle fraction; GSD: geometric standard diameter; MMAD: mass medium aerodynamic diameter.

4.2. Release of INH and RFB from starch/CRG microparticles

The *in vitro* release of INH and RFB encapsulated in starch/CRG/INH/RFB microparticles was assessed in PBS pH 7.4 added of 1% (v/v) Tween 80®. The pH resembles that of the lung lining fluid [187] and the addition of Tween 80® intends to mimic the surfactant content [188]. The registered release profiles are depicted in Figure 4.3. INH release was faster than that of RFB, reaching 100% in 60 min, while RFB took 240 min to reach the same value. Differences in the release profiles started to be statistically significant at 15 min, remaining as such until 180 min. This difference was confirmed by a calculation of the similarity factor (*f2*), which reached 33 and, being lower than 50, indicates the existence of differences in the release patterns. The observations were expected in some way, because of the lower water solubility and higher molecular weight of RFB. Additionally, similar behaviours were reported for the same drugs when other polymers with gelling ability, as occurs for CRG, were used as microparticle matrix [100, 189].

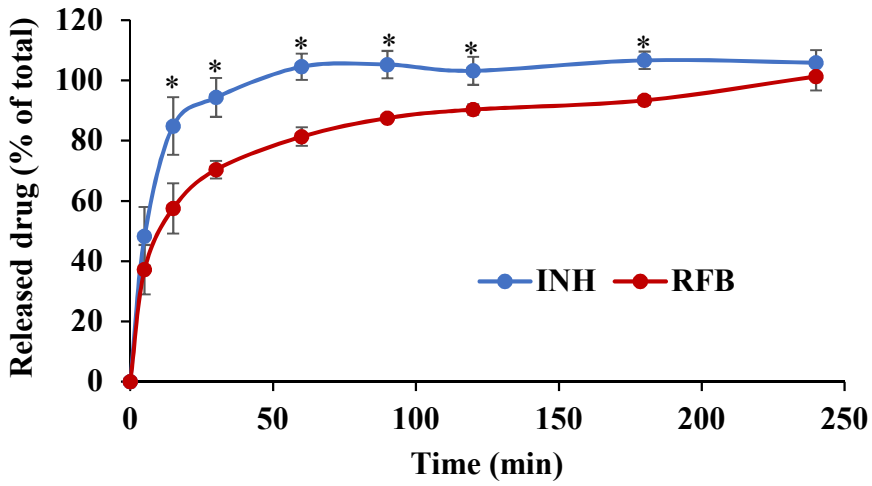

Figure 4.3 - *In vitro* release profile of isoniazid (INH) and rifabutin (RFB) from starch/CRG/INH/RFB (8/2/1/0.5, w/w) microparticles in PBS pH 7.4-Tween 80®, at 37 °C (mean ± SD, n = 3). * $p < 0.05$ comparing INH and RFB at a given time point.

Overall, the release rate of RFB was slower than that of INH, although sustained release is not considered to occur, as 80% of the drug releases within 60 min. The solubility difference between both drugs may explain the faster release of INH. Nevertheless, a fitting to the Korsmeyer–Peppas equation [190] results, for RFB, in r^2 of 0.991 and a n value of 0.245, which may result from a polydisperse particle size distribution evident in Figure 4.1. Different particle size distributions, geometries and aspect ratios may affect the diffusional exponent. The present study suggests that the rate of RFB diffusion (Fickian diffusion or quasi-Fickian diffusion) through the microparticle matrix is mostly governing the release [191].

4.3. Effect of spray-drying on antitubercular activity of drugs

M. bovis BCG constitutes a live attenuated vaccine against tuberculosis, which is one of the most commonly administered vaccines worldwide, being also frequently used in experiments as a surrogate for virulent *M. tuberculosis* [192]. For this reason and because *M. bovis* BCG is a slow growing strain with similarities to *M. tuberculosis*, it was selected to test the effect of spray-drying on the antibacterial activity of the drugs.

The MIC value of free and encapsulated drugs was determined by exposing *M. bovis* BCG to different concentrations of drugs for 7 days. The MIC values obtained for the free drugs were 0.125 µg/mL for INH and 0.004 µg/mL for RFB, indicating higher sensitivity of *M. bovis* BCG to RFB than to INH. The literature reports variable values, depending on the bacterial strains and determination methods that are used, but the values obtained herein were similar to those reported in other studies [192, 193]. A 2/1 ratio of INH/RFB was tested in combination in the form of free drugs, respecting the ratio present in the microparticles. In that case, RFB ruled the inhibition effect and the same 0.004 µg/mL concentration (0.004 µg/mL RFB and 0.008 µg/mL INH) led to inhibition of the growth of *M. bovis* BCG. Drug-loaded starch/CRG microparticles evidenced the same MIC value observed for the corresponding free RFB concentration and to the concentration of RFB in the mixture of INH/RFB. This indicates that the spray-drying process did not affect the antimicrobial effect of the drugs, as reported in other similar works [101, 194, 195]. In summary, *in vitro* susceptibility

of *M. bovis* BCG was observed towards drug-loaded starch/CRG microparticles with considerable growth inhibition.

4.4. Biocompatibility assessment

Considering the purpose of inhalation and the fact that the proposed materials have not been frequently explored for such an application, the biocompatibility of the developed carriers is a relevant matter. The evaluation of cell metabolic activity upon 3 h and 24 h exposure to microparticles and their individual components was performed in three different cell lines using the MTT test. The chosen cells are relevant for the application, representing the human alveolar epithelium (A549 cells) and macrophages (human: dTHP-1 cells and mice: J774A.1 cells). Different concentrations were evaluated, between 0.1 and 1.0 mg/mL. For the effects of the discussion, a toxic effect was considered to exist when cell viability was below 70%, the threshold indicated by ISO 10993-5 [196]. The results obtained upon exposure to starch/CRG microparticles and polymers are depicted in Figure 4.4 for A549 cell line. Figure 4.5 depicts the results corresponding to dTHP-1 and J774A.1. Free drugs, also tested as controls, lead to the results presented in Figure 4.6.

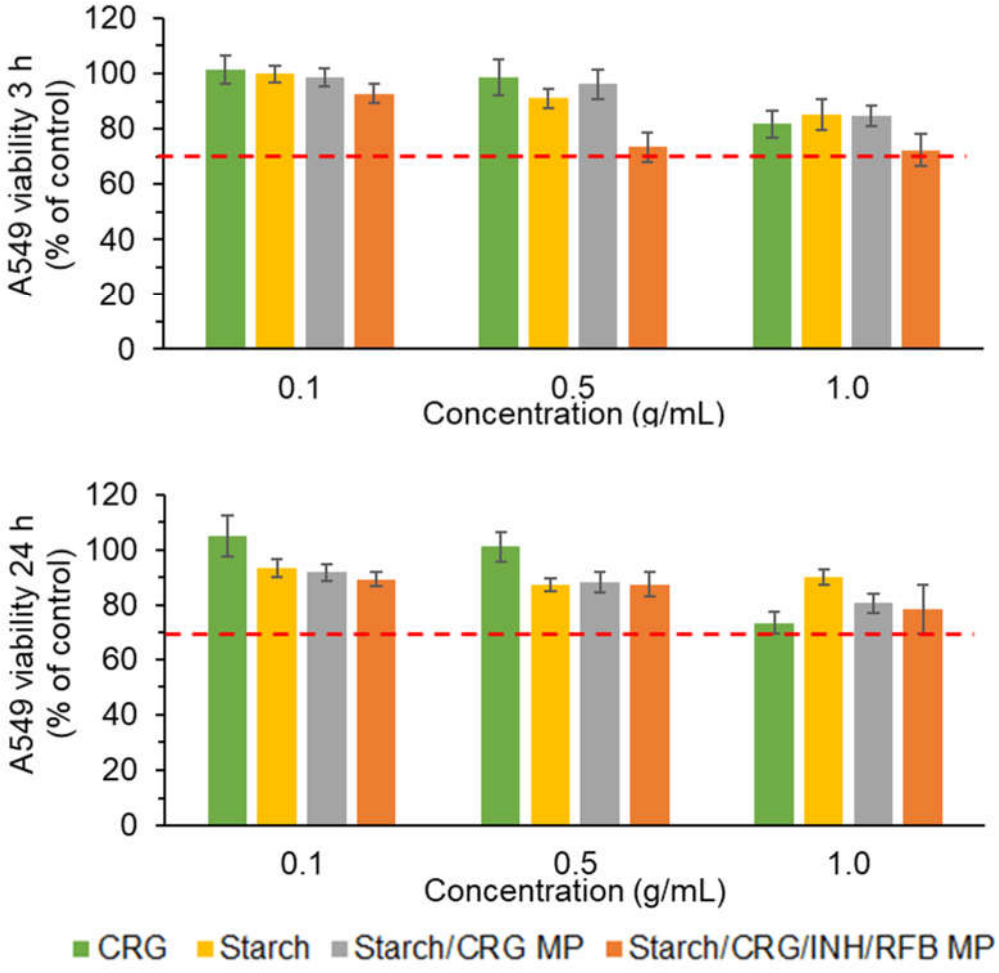

Figure 4.4 - Viability of A549 cells after 3 h and 24 h incubation with carrageenan (CRG) polymer, starch polymer, starch/CRG unloaded and drug-loaded (starch/CRG/INH/RFB) microparticles (MP). Dashed line indicates 70% cell viability. Data represent mean ± SEM (n = 3).

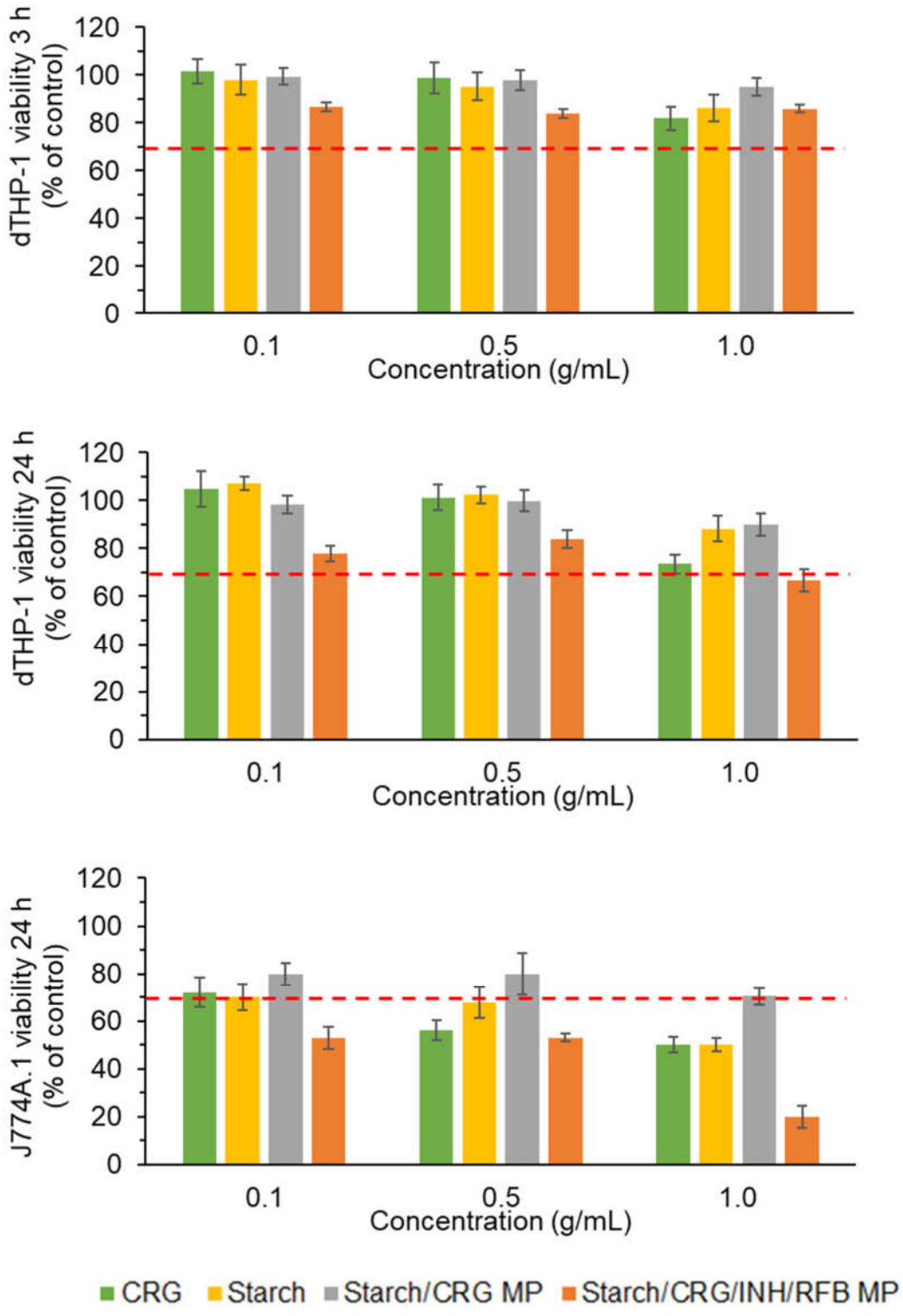

Figure 4.5 - Viability of dTHP-1 and J774A.1 cells after incubation with carrageenan (CRG) polymer, starch polymer, starch/CRG unloaded and drug-loaded (starch/CRG/INH/RFB) microparticles (MP). Dashed line indicates 70% cell viability. Data represent mean ± SEM (n = 3).

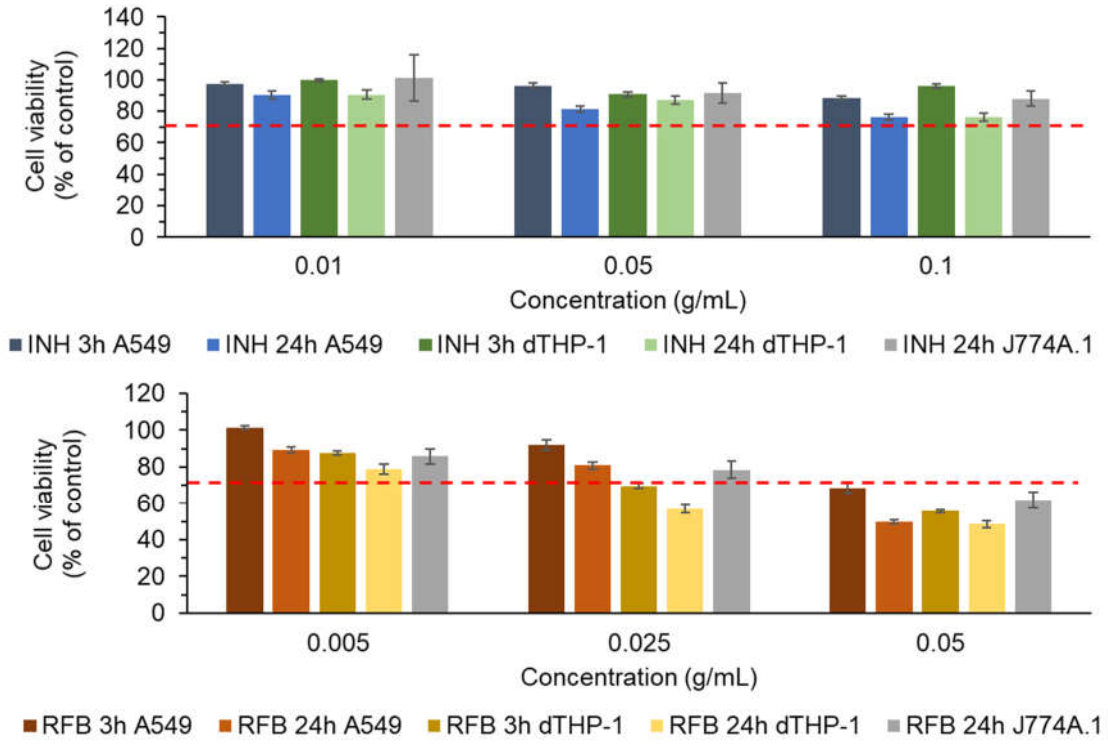

Figure 4.6 - Viability of A549, dTHP-1 and J774A.1 cells after incubation with free isoniazid (INH) and rifabutin (RFB). Dashed line indicates 70% cell viability. Data represent mean ± SEM (n = 3).

Free RFB was the only tested sample reducing cell viability clearly beyond 70% in all cell lines, particularly at the highest tested dose, reaching values of 49% (Figure 4.6). Despite this observation, the toxic effect was considerably overcome by drug microencapsulation, as the 24 h exposure to starch/CRG/INH/RFB microparticles induced cell viability of 67% and 78%, in A549 and dTHP-1 cells, respectively ($p < 0.05$, Figure 4.4 and 4.5). The same trend of toxicity reversal by microencapsulation was observed in other works [100, 101, 189]. Lower concentrations and the incubation for 3 h shower absence of toxicity, with cell viabilities between 83% and 107% (Figure 4.4 and 4.5).

The observations were somewhat different in mouse macrophages (J774A.1 cells), as these were found to have lower tolerability to the microparticle formulation or composing materials. In this case a period of 24 h was tested and observation of Figure 4.5 and 4.6 indicates that INH was the only sample inducing

cell viability above 70% at the highest dose tested. For this reason, no further studies were performed with starch/CRG microparticles in this cell line.

The metabolic activity assay was complemented with the determination of the release of cytoplasmic enzyme LDH, upon 24 h exposure to the samples at a concentration corresponding to the highest tested in the MTT assay. The results are shown in, Figure 4.7.

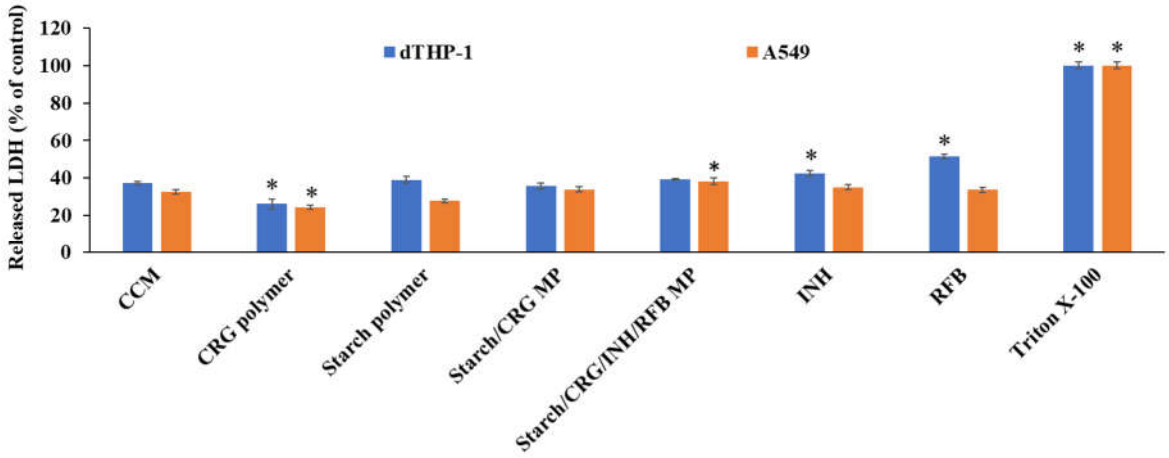

Figure 4.7 – LDH released by A549 and macrophage-differentiated THP-1 (dTHP-1) cells after 24 h exposure to CRG and starch as polymers, starch/CRG unloaded and drug-loaded microparticles, and free drugs. Triton X-100 was the positive control and cell culture medium (CCM) the negative control. The released LDH was calculated based on 100% assumed for positive control. Data represent mean ± SEM (n = 3). * $p < 0.05$ compared to respective CCM.

Surprisingly, the exposure to CRG led to the release of a significantly lower amount of LDH, when compared to CCM ($p < 0.05$). The exposure to free drugs (INH and RFB) affected LDH release from dTHP-1 cells, inducing a significant increase ($p < 0.05$) that was not perceived in A549 cells. Although this correlates with the MTT results in the case of RFB, the same was not observed for INH. Starch and starch/CRG microparticles did not induce alterations in LDH release, while drug-loaded microparticles led to increased release only in A549 cells. Nevertheless, the latter was a very slight alteration of less than half of that presented for the positive control.

Although the observed responses are not exactly coincident, the general indication is of low toxicity of the system. Nevertheless, the need to deepen the analysis with complementary assays is identified, in order to reach more robust conclusions.

4.5. Study of microparticle-macrophage interaction

Bearing in mind the application proposed in this work, where macrophages are the target cells of the prepared microparticulate systems, the evaluation of the potential interaction occurring between the carriers and the cells is of utmost importance. Different concentrations of fluorescently-labelled starch/CRG unloaded microparticles were aerosolised onto a monolayer of dTHP-1 cells and the capacity of microparticles to undergo macrophage uptake established. Unexposed cells (incubated with CCM only) were taken as negative control (0% of phagocytosis) and the increase in fluorescence was considered to correspond to cells that phagocytose microparticles.

Figure 4.8 displays the obtained results, showing that there is affinity of starch/CRG microparticles for macrophages, with the level of phagocytosis varying between 36% and 65%, in a dose-dependent process. In comparison, a similar dose of fucoidan microparticles was reported to reach a lower level of phagocytosis [101], while locust bean gum, a polymer with mannose moieties, reached practically 100% [165]. Nevertheless, the experimental conditions in these cases present some differences, making a direct comparison difficult. Moreover, it should be stressed that while in the above-mentioned formulations, fucoidan and locust bean gum were the only excipients present in the tested microparticles, in the present study CRG composes only 20% of the carriers' matrix material. CRG sulphate groups and galactose units are believed to drive macrophage recognition, leading to phagocytosis. However, old studies also report the uptake of starch-based materials by macrophages [197], thus indicating the need to deepen this uptake study, perhaps using individual polymers as controls, in order to establish more rigorously the existing affinities. Additionally, using as control a material devoid of units potentially recognised by macrophages and complementing cytometry data with confocal microscopy

images, would be beneficial in corroborating the data obtained so far. Finally, perhaps testing different amounts of CRG in the microparticles could provide a hint on the best option towards effective macrophage targeting.

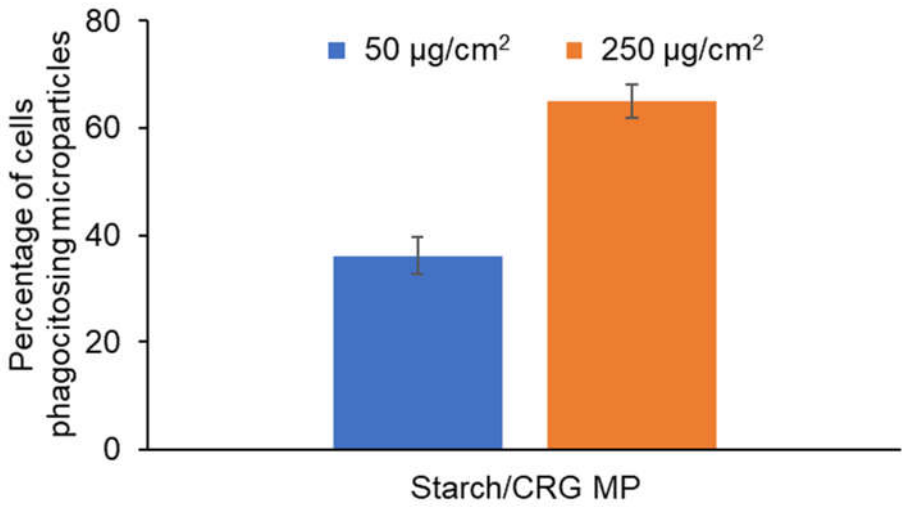

Figure 4.8 – Percentage of dTHP-1 cells phagocytosing fluorescently-labelled unloaded starch/CRG microparticles after 2 h exposure, as obtained by flow cytometry. Data represent mean ± SEM (n = 3).

Alveolar macrophages are cells programed to process and remove inhaled particulate matter from the airways. After internalisation of bacteria like *M. tuberculosis*, activation of macrophages normally occurs and the phagocytosis of other particulate matter has been reported to result in similar activation states [49, 198, 199]. It has been argued that this leads to increased ability for bacteria elimination, for instance, as the bactericidal activity of macrophages is reported to increase upon activation [200]. One of the hallmarks of this activation process is the release of pro-inflammatory cytokines. Two of the cytokines involved in the process are TNF-α and IL-8 [201, 202]. These cytokines were also reported to be the most predominant in the supernatant of THP-1 macrophages [203]. Therefore, the secretion of TNF-α and IL-8 to cell supernatant was analysed after 24 h exposure of dTHP-1 cells to the samples. Negative control consisted of cells incubated only with CCM and positive control comprised an exposure to LPS, which is known to induce activation of macrophage cells, thus resulting in

cytokine expression. The obtained results are displayed in Figure 4.9, showing different outcomes for the exposure of dTHP-1 cells to the samples and controls. Despite the concern about CRG inflammatory capacity, the polymer did not increase cytokine secretion comparing with the negative control. On the contrary, the exposure to starch led to increased production of both cytokines (IL-8≈$6.2x10^3$ pg/mL and TNF-α≈$1.5x10^3$ pg/mL) ($p < 0.05$). This could be a consequence of the incomplete solubilisation of starch in the incubation medium, which led to the presence of some insoluble granules in the micro size range that possibly undergone phagocytosis by dTHP-1 cells, inducing activation, despite the reported absence of inflammatory properties of starch [204]. When comparing starch/CRG/INH/RFB microparticles with starch (polymer), the level of released TNF-α was similar, but a statistically significant increase was observed for IL-8 ($p < 0.05$). Most of this induction is certainly caused by the presence of starch, but a possible effect from the drugs should also be ascertained in future tests. In this context, however, a study has shown that the particulate forms of drugs rather than the solutions, are those contributing to higher induction of cytokine secretion [205].

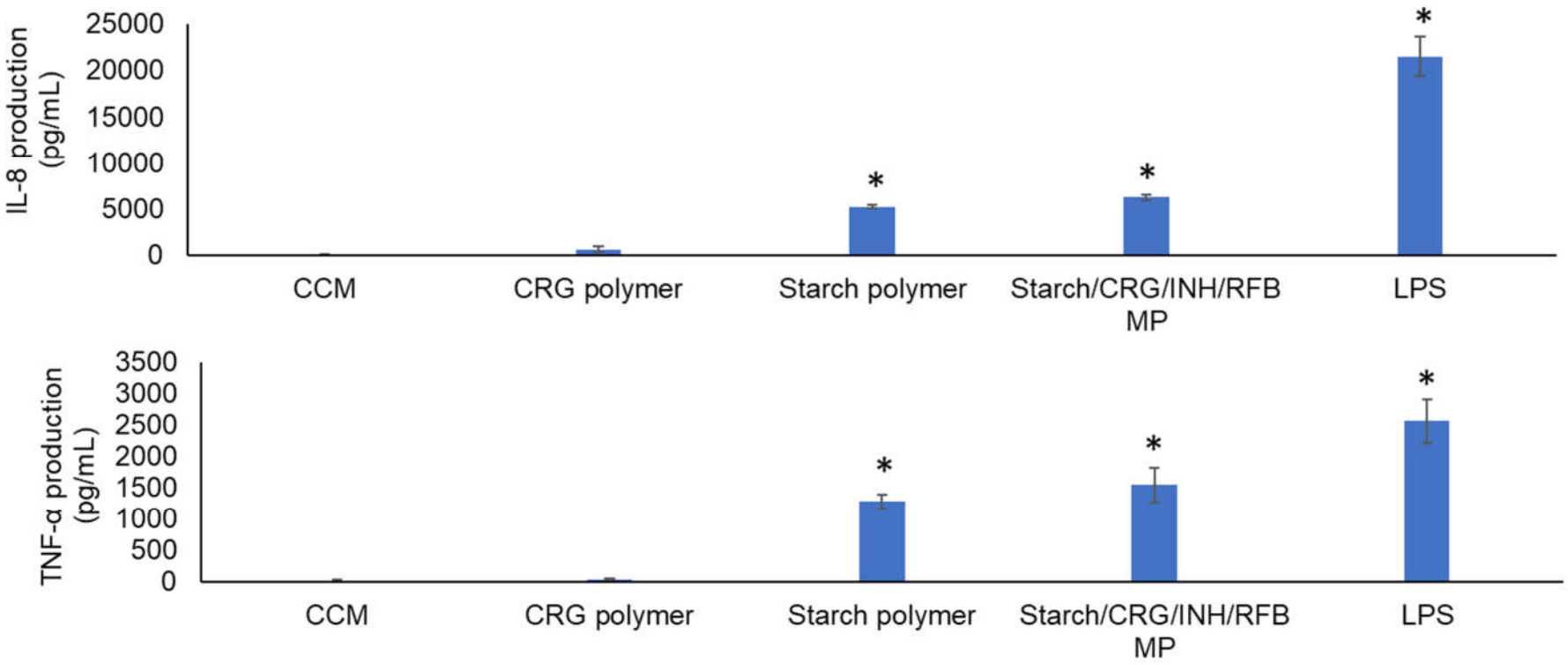

Figure 4.9 – IL-8 and TNF-α secretion after 24 h incubation with CRG polymer, starch polymer and starch/CRG/INH/RFB (8/2/1/0.5, w/w) microparticles. Cell culture medium (CCM) was used as negative control and lipopolysaccharide (LPS) as positive control. Data represent mean ± SEM (n = 3). * $p < 0.05$ compared to CCM.

Despite the general indication that macrophage activation may result in improved bactericidal activity, recent findings in the field of tuberculosis pathogenesis have indicated that typical inflammatory markers, such as reactive oxygen species, induce the necrosis of polymorphonuclear cells infected with mycobacteria, consequently promoting bacterial escape from cell antimicrobial effectors and allowing bacterial growth [25]. Therefore, the results require a cautious analysis and need to be considered in the light of the continuous advancement of findings in the field of tuberculosis pathogenesis. Nevertheless, the performed assays demonstrate a favourable interaction of starch/CRG microparticles with macrophages.

4.6. Conclusions

Starch/CRG/INH/RFB microparticles were successfully produced, efficiently associating the model drugs, which antibacterial effect was not affected by the microencapsulation process. The aerosolisation properties were satisfactory, with emitted doses of 91% and MMAD of 3.3 – 3.9 μm, although optimisation is required to improve FPF, an important parameter regarding the objective of reaching lower zones of the lung. Low toxic effect was observed in alveolar epithelial cells and human macrophages, but further testing is needed to reinforce the potential of the system, particularly if more prolonged treatment schedules are envisaged. Starch/CRG microparticles demonstrated some ability to interact with macrophages and induced moderate activation of these cells. As a whole, this work provides indications on the potential of the carriers to interact with macrophages, thus providing a platform for drug delivery in the context of macrophage intracellular diseases. Additionally, if tuberculosis is focused, these microparticles can be used as inhalable drug carriers.

This page was intentionally left in blank

Chapter V - Chondroitin sulphate microparticles: Results and discussion

This page was intentionally left in blank

5. Chondroitin sulphate microparticles: Results and discussion

5.1. Preparation and characterisation of ChS microparticles

ChS undergone an initial step of purification in order to maximise the polymer content and avoid the presence of proteins. The purified polymer was used to prepare microparticles associating a combination of INH and RFB. As far as we know, this is the first time that ChS is being proposed as platform for the inhalable therapy of tuberculosis. The microparticles were prepared by spray-drying, resulting in yields of approximately 85% (Table 5.1), which were deemed very satisfactory [206]. INH is a hydrophilic drug, but RFB has hydrophobic character, thus requiring solvents other than water to solubilise. Despite spray-drying permits processing a suspension, not requiring the solubilisation of all components of the spraying dispersion, it was decided to provide the complete solubilisation of both drugs in order to ensure a higher level of homogeneity in the final product. Ethanol and HCl were, then, tested as co-solvents of RFB, being mixed with water.

Disregard of the used solvent, the obtained microparticles generally exhibited a spherical shape, as observed in Figure 5.1. Moreover, the association of the drugs translated into the production of more wrinkled and corrugated microparticles (Figures 5.1B and 5.1C) comparing with the unloaded microparticles (Figure 5.1A). Objectively, the use of different solvents had no effect on microparticle morphology. The literature reports already several formulations of ChS microparticles, although none was produced by spray-drying and different co-excipients were included in all cases. Nevertheless, it was interesting to notice that the spherical shapes and smooth surfaces observed in the unloaded microparticles reported herein, were common characteristics [207-209]. The microphotographs suggest that the size of drug-loaded particles tends do decrease, having a higher number of small particles comparing with unloaded particles. Comparing de Dv50 of the produced microparticles, a significant decrease ($p < 0.05$) from 9.6 μm of the unloaded particles to 4.1 μm of the drug loaded counterparts was observed (Table 5.1). This size range is reported as adequate to potentiate phagocytosis by macrophages [210], which could be advantageous in the treatment of intracellular diseases or vaccination approaches [211, 212].

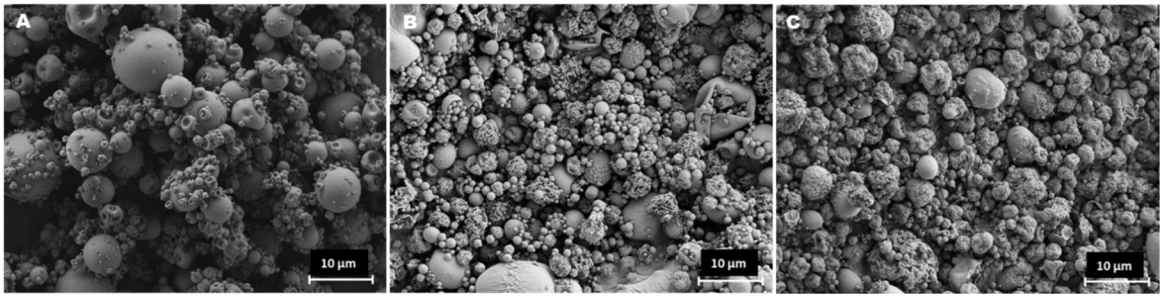

Figure 5.1. - Microphotographs of unloaded ChS microparticles (A) and ChS/INH/RFB microparticles produced with water-ethanol (B) and water-HCl (C) as solvents, as obtained by scanning electron microscopy. Scale bar is 10 µm.

The tap density was determined to be around 0.5 – 0.6 g/cm^3 for the dry powders corresponding to unloaded microparticles and microparticles produced with HCl, decreasing to 0.3 g/cm^3 for microparticles produced with ethanol. A lower density has been correlated with less cohesive powders and better flowability [213]. INH was associated to microparticles with an efficiency around 95%, independently of the used solvent. However, a significant difference was observed in RFB association, which was 59% when ethanol was used *versus* 67% when HCl was the solvent ($p < 0.05$). The loading capacity was 8.2% for INH, varying within 2.6% and 2.9% for RFB, values that compare with the theoretical 8.6% for INH and 4.3% for RFB.

Table 5.1. Production yield (PY), Feret's diameter, tap density, drug association efficiency (AE) and loading capacity (LC) of ChS microparticles (mean ± SD, n = 3). Different letters indicate statistically significant difference within the same parameter.

	PY (%)	Dv50 (µm)	Span	Tap density (g/cm^3)	AE%	LC%
ChS	73.3 ± 4.4[a]	9.6 ± 0.2[c]	2.0 ± 0.0[e]	0.50 ± 0.01[g]	n. a.	n. a.
ChS/INH/RFB (ethanol)	83.4 ± 1.0[b]	4.1 ± 0.1[d]	2.9 ± 0.1[f]	0.32 ± 0.03[h]	INH: 94.9 ± 5.7[i]	INH: 8.2 ± 0.5[l]
					RFB: 59.0 ± 6.9[j]	RFB: 2.6 ± 0.3[m]
ChS/INH/RFB (HCl)	84.9 ± 1.1[b]	4.1 ± 0.0[d]	3.1 ± 0.1[f]	0.58 ± 0.02[h]	INH: 94.6 ± 4.0[i]	INH: 8.2 ± 0.3[l]
					RFB: 67.6 ± 1.4[k]	RFB: 2.9 ± 0.1[n]

AE: association efficiency; LC: loading capacity; n.a.: not applicable; PY: production yield;

Figure 5.2 shows the stage-by-stage deposition profile of both drugs encapsulated in the tested microparticles. The similarity of the profiles (INH *vs* RFB) indicates that the two drugs were equally distributed in the various stages, as was also observed for starch/CRG microparticles. This reinforces the adequacy of spray-drying as technique to produce microparticles with drug combination, resulting in homogeneous composition independently of particle sizes, which led to co-deposition of drugs. A statistically significant difference in the deposition of both formulations was found in the induction port, and in stages 2 and 3 ($p < 0.05$). This translated into differences in the calculated aerodynamic characteristics, which are displayed in Table 5.2. The dose emitted from the inhaler was very satisfactory in all cases, reaching 90%. This is indicative of the suitability of ChS to be used as microparticle matrix material in spray-drying, producing microparticles with good flowing capacity with any of the tested solvents. Similar MMAD values (3.8 – 4.0 μm) were obtained for both formulations. This aerodynamic diameter fits the range considered suitable to reach the respiratory zone, which is 1–5 μm [214, 215], thus being adequate for an approach in tuberculosis therapy approach. Moreover, FPF of 34% - 44% was determined, indicating that this fraction of the microparticles has the necessary conditions to reach the respiratory zone of the lung, with aerodynamic diameter below 5 μm. This value is in agreement with those usually determined for high dose drug powders formulated without lactose as carrier [184, 185].

Despite having very similar MMAD, microparticles produced using ethanol as solvent provided higher FPF, as a consequence of higher deposition on stages 2 and 3, enabling deep lung delivery of 1.5 mg of RFB and 3.1 mg of INH. The presence of ethanol apparently benefited the formulation, resulting in a less cohesive powder with better flowing properties. Despite the slightly lower drug association efficiency, the resulting aerodynamic properties provide increased drug accumulation in the respiratory zone comparing with that enabled by microparticles produced with HCl.

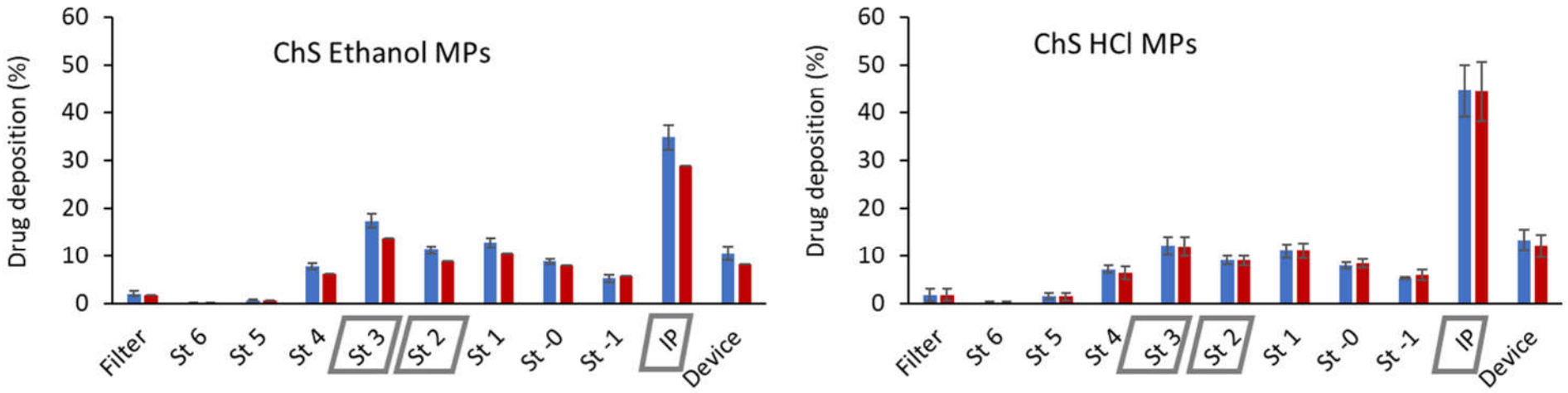

Figure 5.2. Stage-by-stage deposition profiles of isoniazid (blue) and rifabutin (red) inside the Andersen cascade impactor after aerosolisation of chondroitin sulphate (ChS) microparticles (MPs) with RS01 medium resistance inhaler operated at 60 L/min (values are mean ± SD, n = 3). Grey boxes in X axis represent $p < 0.05$ comparing the same stage between the two formulations. IP: induction port; St: stage.

Table 5.2. Aerodynamic characteristics of ChS/INH/RFB (10/1/0.5, w/w) microparticles (mean ± SD, n = 3).

Microparticles	Powder Emitted dose (%)	Drug	MMAD (μm)	GSD (μm)	FPD (mg)	FPF (%)
ChS/INH/RFB (ethanol)	90.9 ± 1.0[a]	INH	3.8 ± 0.1[b]	1.9 ± 0.1[c]	3.1 ± 0.3[d]	43.7 ± 2.4[g]
		RFB	3.9 ± 0.1 [b]	2.0 ± 0.1[c]	1.5 ± 0.1[e]	42.6 ± 1.7[g]
ChS/INH/RFB (HCl)	89.6 ± 1.8[a]	INH	4.0 ± 0.2 [b]	2.0 ± 0.0[c]	2.9 ± 0.1[d]	35.0 ± 1.7[h]
		RFB	4.0 ± 0.3 [b]	2.1 ± 0.1[c]	1.2 ± 0.1[f]	34.0 ± 3.7[h]

FPD: Fine particle dose; FPF: Fine particle fraction; GSD: geometric standard deviation; MMAD: Mass median aerodynamic diameter.

5.2. Release of INH and RFB from ChS microparticles

Similarly to the study performed with starch/CRG microparticles, drug release profiles were determined in PBS pH 7.4 added of 1% Tween 80®. The results are displayed in Figure 5.3 and evidence rapid release of the drugs, as 100% release was registered within 60 min for INH and 120 min for RFB, in both formulations. The surface irregularities of microparticles, commented in section 5.1., certainly contributed to the rapid release, due to the increased contact with the release medium. Additionally, the high solubility of the polymeric matrix was another factor with similar contribution, with the hydrophilic character of ChS resulting in rapid dissolution of the particle matrix and permitting a fast release of the drugs. Nevertheless, RFB tends to exhibit slower release than INH ($p < 0.05$). The similarity factor *f2* was used to compare the release of both drugs in each formulation along with the release of each drug in the two different formulations. The comparison between INH and RFB resulted in f_2 factor of 30 for microparticles produced with ethanol and 43 for microparticles produced with HCl. As f_2 values are lower than 50, it is concluded that differences exist in the release profiles, of both drugs, independently of the microparticle formulation. This is possibly a consequence of the higher molecular weight of RFB, along with its hydrophobicity, which contrasts with the hydrophilic character of INH.

When comparing the release of each drug from both formulations, no differences were observed for INH, as this follows a similar release pattern from both microparticles, which is reinforced by an f_2 factor of 64. In contrast, Figure 5.3 evidences a difference in RFB release profile when the two microparticle formulations are compared. In this context, microparticles produced with ethanol provided somewhat slower release comparing with those produced with HCl ($p < 0.05$). A f_2 factor of 46 confirms the dissimilar profiles. Considering the results of the rheological study (please consult supplementary information page 159), no differences in the characteristics of the polymer were found comparing the two spray-dried microparticle formulations, that could justify this behaviour. Therefore, one possible explanation for this effect could be that HCl remaining in the formulation after spray-drying facilitated RFB solubilisation afterwards, by providing a certain degree of protonation [216]. Another reason could be the existence of a different pattern of dispersion of RFB within the microparticle matrix in each formulation. If RFB is located more at the surface in microparticles

produced with HCl, comparing with those produced with ethanol, this could justify the observed profiles. Nevertheless, further studies would be needed to study this possibility.

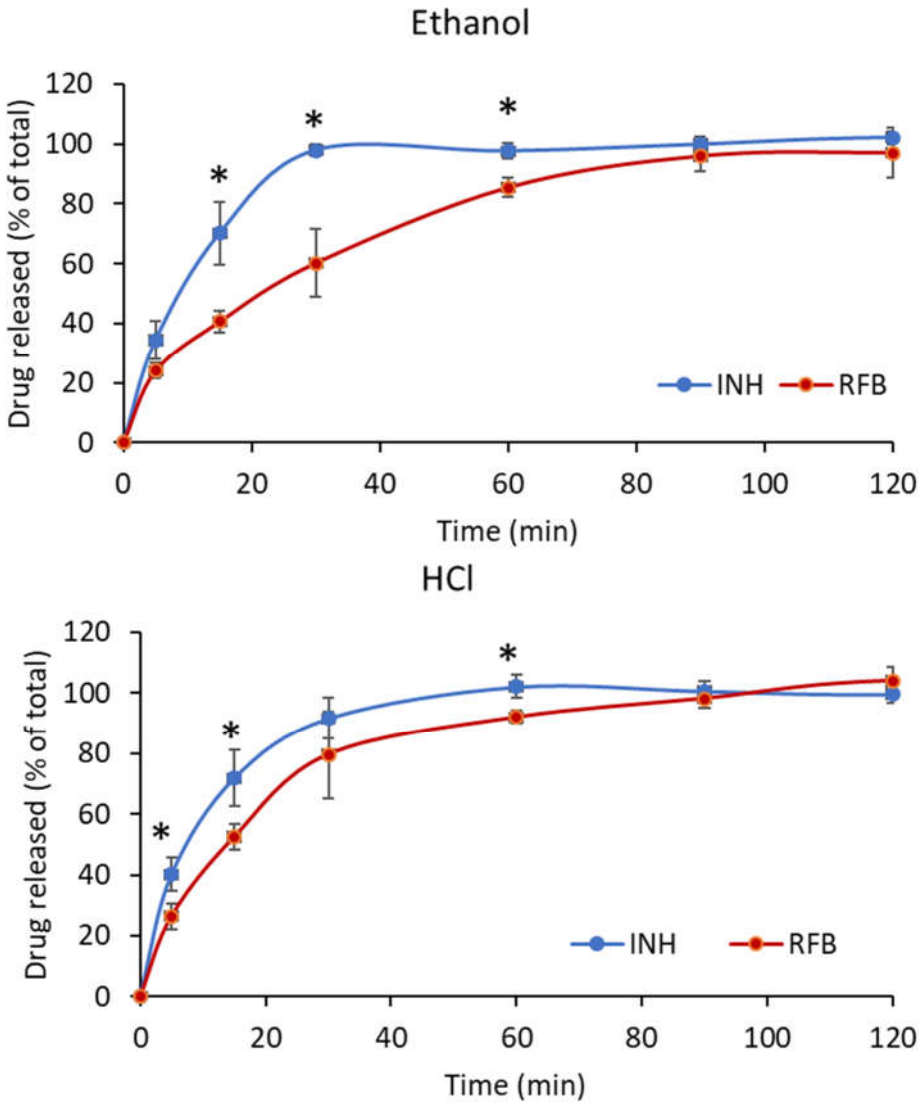

Figure 5.3. - *In vitro* release of isoniazid (INH) and rifabutin (RFB) from ChS/INH/RFB (10/1/0.5, w/w) microparticles in PBS pH 7.4-Tween 80®, at 37 °C (mean ± SD, n = 3). * $p < 0.05$ comparing INH and RFB at a given time point.

The encapsulation of the same pair of drugs was reported in other works that used different microparticle matrix materials. The comparison of release profiles supports the conclusion that the matrix rules the release pattern. Although ChS is a hydrophilic polymer, it was able to provide slower release of these drugs in comparison with microparticles composed of fucoidan, another hydrophilic polymer, which has shown total release of INH and RFB in 30 min [101]. Locust

bean gum, in turn, provides more viscous solutions and, thus, sustained the release of INH until 120 min and RFB up to 240 min [100], while low molecular weight chitosan microparticles released completely INH and RFB in 120 min [195]. Another work reporting chitosan microparticles, but using chitosan with higher molecular weight, indicated more sustained release of INH, up to 40-60 h, which was demonstrated to be influenced by the polymer properties and crosslinking degree [217]. In fact, polymeric particles devoid of crosslinking agents typically show a faster release of the associated drugs [218].

It should be stressed that this assay does not mimic *in vivo* conditions, as it is well known that the alveolar epithelium is covered by a thin layer (~0.2 μm) of lung lining fluid [219]. Therefore, microparticles are expected to be only partially in contact with the fluid, and not immersed in it, as in this assay. Consequently, we anticipate that the drug release *in vivo* will show slower kinetics, allowing microparticle internalisation by macrophages before particle dissolution and complete drug release.

5.3. Antibacterial activity of drugs after microencapsulation

The MIC value of INH and RFB was determined and the effect of spray-drying on this parameter was evaluated. MIC value of free and encapsulated drugs was determined by exposing *M. bovis* BCG to different concentrations of free drugs, association of free INH and RFB (at INH/RFB = of 2/1, to mimic the ratio present in the microparticles) and at the two different microparticle formulations for 7 days. As already reported in section 4.4, the MIC value observed for the free drugs was 0.125 μg/mL for INH and 0.004 μg/mL for RFB, similar to what was reported in other studies [192, 193] and indicating higher sensitivity of M. bovis to RFB than to INH. The combination of both drugs resulted in MIC of 0.004 μg/mL (0.004 RFB and 0.008 INH). ChS-based drug-loaded microparticles evidenced the same MIC value observed for the free drugs in combination, disregard the formulation. This provides a dual indication: 1) that the spray-drying process does not affect the antitubercular effect of the drugs, as was also observed when starch/CRG were used as matrix materials and 2) that the used solvent has no effect on this property of microparticles.

5.4. Toxicological profile of ChS microparticles by evaluation of cell viability and cell membrane integrity

As reported in section 4.4. for starch/CRG microparticles, the toxicological profile of ChS-based microparticles was performed in three cell lines that are relevant for the context of an application in tuberculosis therapy, representing both the alveolar epithelium (human A549 cells) and macrophages, (human dTHP-1 cells and J774A.1 cells from mice). The metabolic assay MTT was performed upon 3 h and 24 h exposure to different concentrations of microparticles and controls, between 0.1 and 1.0 mg/mL. The exception was the cell line representing mouse macrophages (J774A.1 cells), which were tested only for 24 h.

The results observed for the free drugs were already described in section 4.4 and are repeated in this section to simplify the comparison of results (Figure 5.4). As commented before, free RFB was the only tested sample reducing cell viability beyond 70%, reaching values of 49-62% depending on the cell line under examination. Again, the observed toxicity was overcome by the microencapsulation of the drug and ChS/INH/RFB microparticles induced cell viability between 79% and 85%, in line with observations reported in other studies [100, 101, 189]. As depicted in Figures 5.5 and 5.6, none of the tested conditions (different cells, microparticle formulations and concentrations) resulted in a cytotoxic effect, as cell viability remained above 70% in all cases. As was referred in section 4.4, this is the threshold indicated in ISO 10993-5 to consider a cytotoxic response to occur [196]. The exposure to lower concentrations was observed to generate cell viability above 75%.

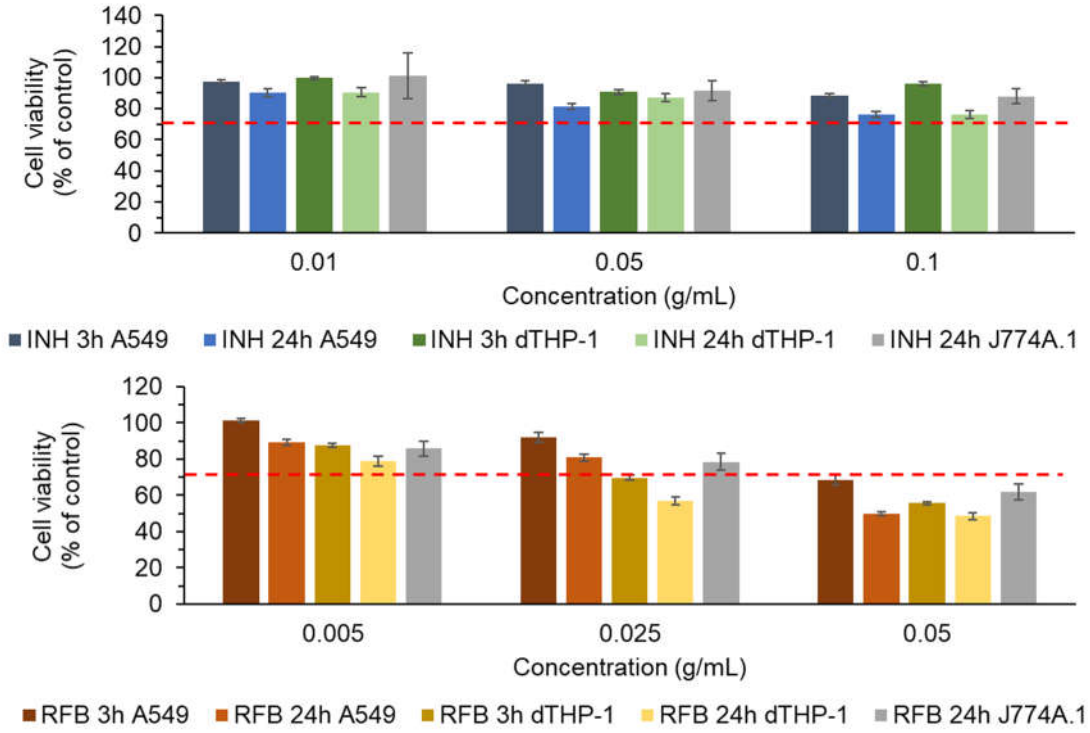

Figure 5.4 – Viability of A549, macrophage-differentiated THP-1 (dTHP-1) and J774A.1 cells after 3 and 24 h incubation with free isoniazid (INH) and rifabutin (RFB). Dashed line indicates 70% cell viability. Data represent mean ± SEM (n = 3). Note: this figure replicates the results of Figure 4.4 and is included in this chapter to simplify the comparison of results.

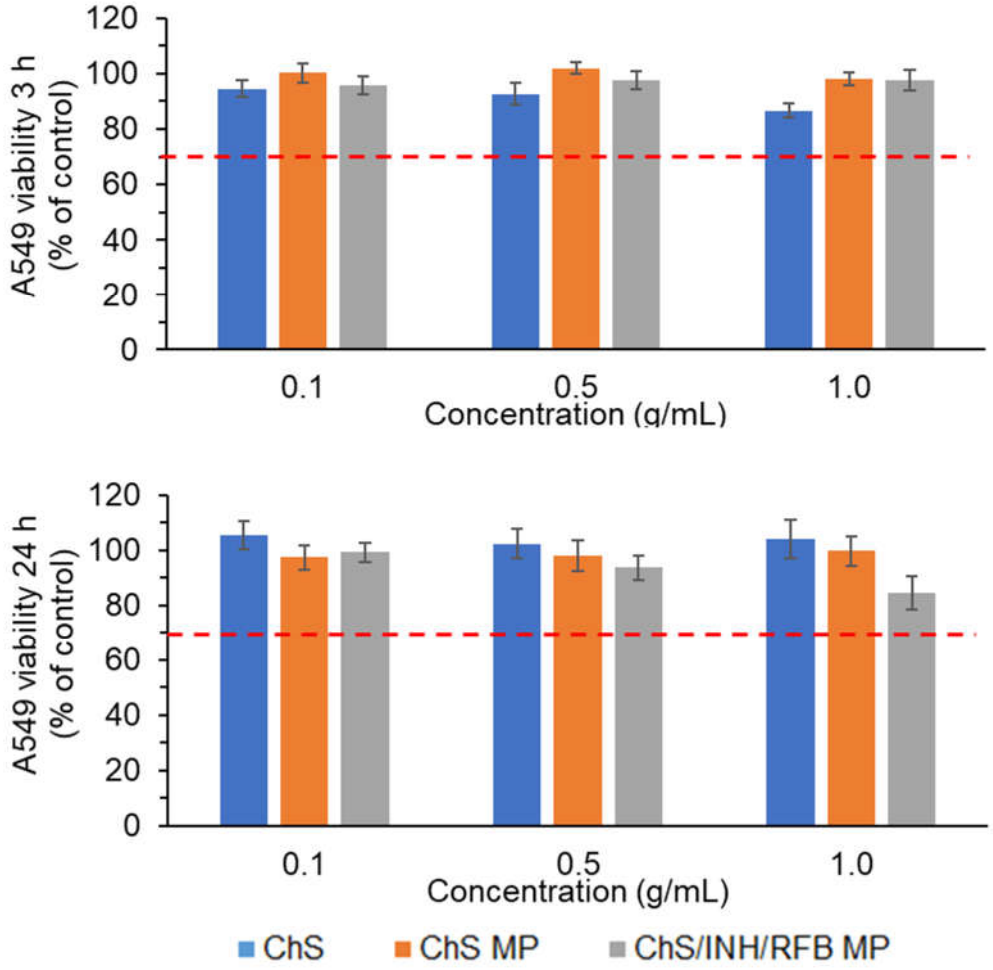

Figure 5.5 – Viability of A549 incubation with chondroitin sulphate (ChS) polymer, ChS unloaded and drug-loaded (ChS/INH/RFB) microparticles (MP). Dashed line indicates 70% cell viability. Data represent mean ± SEM (n = 3).

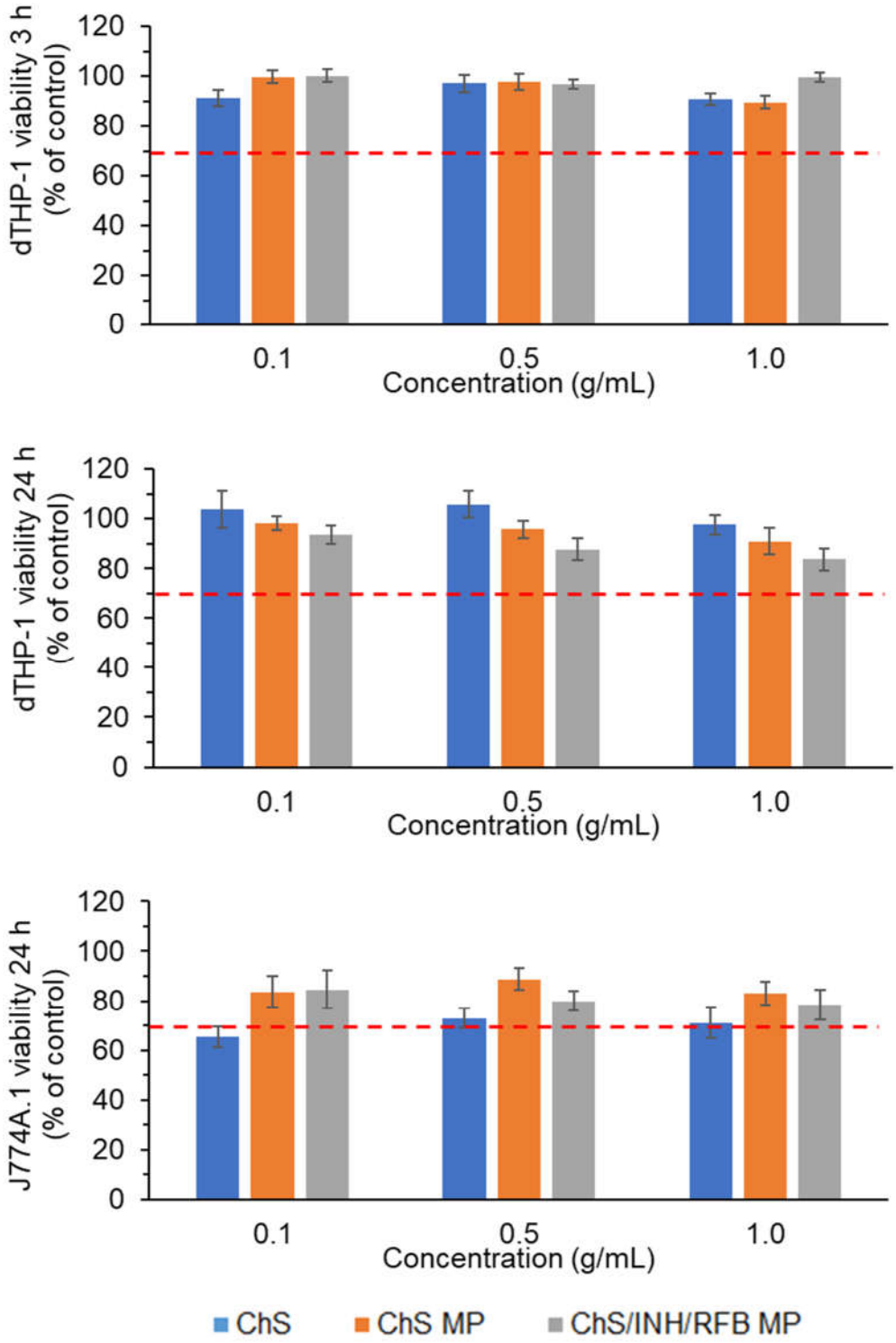

Figure 5.6 – Viability of macrophage-differentiated THP-1 (dTHP-1) and J774A.1 cells after 3 and 24 h incubation with chondroitin sulphate (ChS) polymer, ChS unloaded and drug-loaded (ChS/INH/RFB) microparticles (MP). Dashed line indicates 70% cell viability. Data represent mean ± SEM (n = 3).

An evaluation of the cytoplasmic enzyme LDH releasing from the cells after 24 h exposure to the samples was performed to complement the results of metabolic activity, providing an indication on the integrity of cell membrane after contact with microparticles. This assay was performed in A549 and dTHP-1 cells incubated with 1.0 mg/mL of test substances, which is the highest concentration tested in the MTT assay. The results are shown in Figure 5.7. ChS was found to elicit an increased response in this assay. Unexpectedly, independently of the cell line, ChS-based samples generally registered higher release of LDH comparing with CCM ($p < 0.05$). Moreover, free RFB, although also eliciting increased release of LDH comparing with CCM in dTHP-1 cells ($p < 0.05$), displayed statistically lower values than those registered for ChS/INH/RFB microparticles, in both cell lines. In fact, these results were not expected, especially considering what was observed in the MTT assay, where only RFB induced a significant decrease in cell viability. The authors believe that this increase in LDH observed for all samples containing ChS is the result of a reaction occurring between the polymer and the reagents of the assay kit, leading to overestimated values. The wells containing samples with ChS were observed to have visible turbidity, thus interfering in the measurements.

In any case, it was observed that ChS elicited similar release of LDH in the form of polymer and microparticles, either with or without loaded drugs. Furthermore, A549 cells were less sensitive to sample exposure, registering no statistical differences in unloaded ChS microparticles and free drugs when compared with CCM. On the contrary, dTHP-1 cells evidenced increased LDH release for all the tested conditions, when compared with CCM ($p < 0.05$).

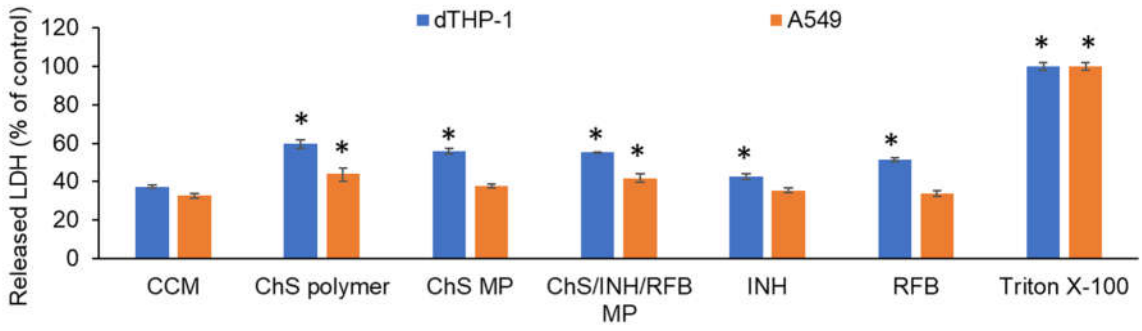

Figure 5.7 – Lactate dehydrogenase (LDH) released after 24 h incubation of A549 and macrophage-differentiated (dTHP-1) cells with chondroitin sulphate (ChS) polymer, unloaded and drug-loaded ChS microparticles (MP) at 1 mg/mL, free isoniazid (INH, 0.1 mg/mL) and free rifabutin (RFB, 0.05 mg/mL). Triton X-100 (10%, v/v) was used as positive control and cells incubated with cell culture medium (CCM) were used as negative control. The released LDH was calculated based on 100% assumed for positive control. Data represent mean ± SEM (n = 3, three replicates per experiment). *$p < 0.05$ compared with respective CCM.

Establishing a general comparison with the results obtained for microparticles composed by starch/CRG it can be said that those comprised of ChS demonstrated to be better tolerated by the tested cell lines. Due to the ambiguous results observed herein between the MTT and LDH release assays for the microparticles composed of ChS, it was considered necessary to perform a deeper evaluation of these microparticles in order to further clarify the safety of ChS as matrix material of inhalable microparticles. The results of that study are presented in the next section.

5.5. High content analysis (HCA) to assess J774A.1 response to subtoxic concentrations of ChS microparticles

Poorly soluble compounds, as well as some micro- and nanoparticle systems have been shown to elicit various responses in macrophages at subtoxic concentrations. For example, cationic amphiphilic drugs, such as amiodarone are known to induce a phospholipid accumulation disorder, termed phospholipidosis [16], while polymeric nanoparticles comprised of polyvinyl

acetate-co-alcohol and polystyrene have been shown to induce increased vacuolation in macrophage cells via a mechanism that is currently unknown [220]. It is important to investigate macrophage responses at subtoxic concentrations, as these might occur *in vivo* during preclinical toxicology investigations and, depending on their prevalence, they may be considered an adverse response to the drug vehicle [221].

Mouse macrophages (J774A.1 cells) were used in this assay and ChS microparticles produced with ethanol were selected to perform the assay. Six parameters were investigated simultaneously using fluorescence microscopy-based HCA (Table 5.3): mitochondrial activity, cell area, nucleus area, membrane permeability, phospholipid content (phospholipidosis), and neutral lipid content (steatosis). In order to focus solely on the subtoxic concentration range, the number of adherent cells remaining in the well following treatment was assessed. All treatment concentrations resulting in a reduction of the cell number >50% of the mean value of the untreated cell population were not taken forward into the HCA. Therefore, microparticles and ChS polymer were analysed at concentrations < 350 µg/mL, INH < 250 µg/mL and RFB < 25 µg/mL.

The heatmap in Figure 5.8 depicts the percentage of the cell population with abnormal values in any of the six categories tested. Abnormality was defined as an output higher than two standard deviations from the mean value of the untreated cell population. This means that any cell counted within the abnormal population can be considered to show a robust response compared to untreated cells. Therefore, it is expected that all treatments tested at the subtoxic concentration levels should show low percentages of cells with abnormal mitochondrial activity, membrane permeability and nuclear area, which was confirmed in Figure 5.12. Considering that phagocytosis may lead to an expanded cell area, it was hypothesised that the microparticle carriers could lead to a dose-dependent increase in cell area, which was not observed in the study. Finally, assessment of both neutral and phospholipid content showed an interesting result in that RFB induced a dose-dependent increase in phospholipid content, although phospholipidosis has not been reported in the RFB literature as a common observation in toxicology studies. Interestingly, ChS microparticle formulations which containing ~15 µg/mL RFB and 30 µg/mL INH in 350 µg/mL total solids, did not show cells with abnormal phospholipid content, indicating that

the encapsulation of the drug prevented phospholipid accumulation, at least over the 48 h time period of this experiment.

Table 5.3 - Parameters assessed at subtoxic concentration levels.

Number	Parameter
1	Mitochondrial activity
2	Cell area
3	Nucleus area
4	Membrane permeability
5	Phospholipid content
6	Neutral lipid content

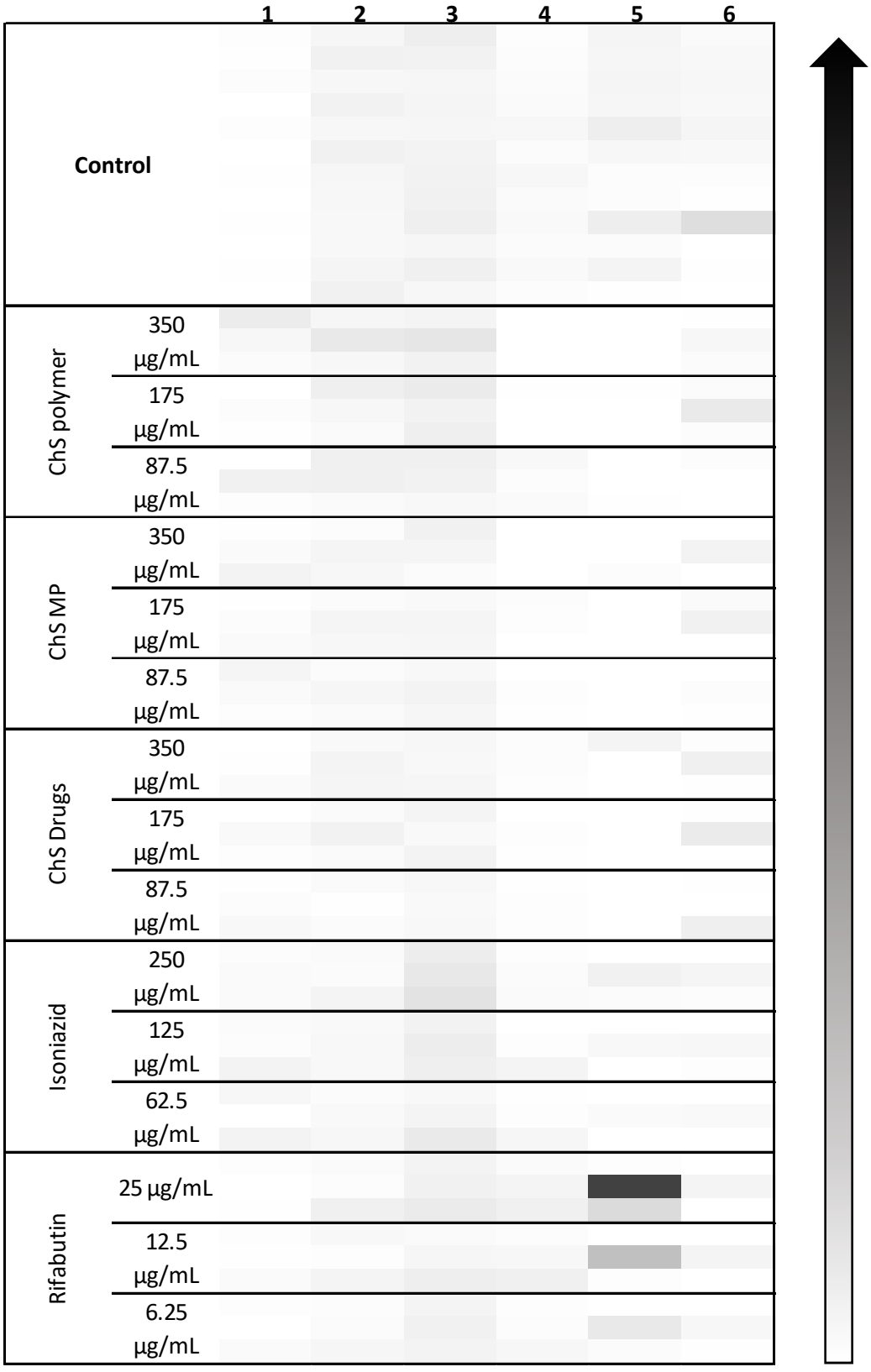

Figure 5.8 - Heat map showing individual results of n=3 experiments. (each square represents one experiment). The colour gradient sets the lowest value (0% cells in the population) for each given parameter in the heat map (white),

highest value (black) and midrange values (grey) with a corresponding gradient between these extremes.

5.6. Macrophage capture of ChS microparticles

The capacity of microparticles to be phagocytised by macrophages was assessed by flow cytometry. Different concentrations of fluorescently-labelled unloaded ChS microparticles were aerosolised onto a monolayer of macrophage-like cells, differentiated from THP-1 monocytes. Unexposed cells (incubation with CCM only) were taken as negative control (0% of phagocytosis) and the increase in fluorescence was considered to correspond to cells that phagocytose microparticles. As depicted in Figure 4.9, the increase in the fluorescence intensity of macrophages was dose-dependent. ChS microparticles were found to have high affinity for macrophages, with 60% - 80% of the cells showing to have phagocytosed microparticles in a dose-dependent manner. The higher dose led to significantly higher percentage of cells phagocytosing ChS microparticles ($p < 0.05$). The composition of microparticles possibly favoured the uptake, with sulphate groups and *N*-acetylgalactosamine residues of ChS being potentially recognized by several macrophage receptors [10, 222]. The observed values were higher than those reported for fucoidan microparticles [101], but lower than those observed for locust bean gum [223], a polymer with galactose and mannose moieties and for chitosan [195], which bears *N*-acetylglucosamine groups. These differences in macrophage uptake of different microparticles may be explained by polymeric compositions, which certainly influence the affinity for macrophage receptors. Different moieties from each polymeric chain will target different macrophage receptors with different bidding affinities. However, using an antibody stain, the present study eliminates any possible interference of non-phagocytosed microparticles in the quantifications, which was not addressed in the previous studies. In fact, in the present study only the events presenting a double fluorescent signal (APC from the antibody and FITC from fluorescent microparticles) were considered to have phagocytosed microparticles, avoiding possible microparticles aggregates to count as positive phagocytic macrophage events.

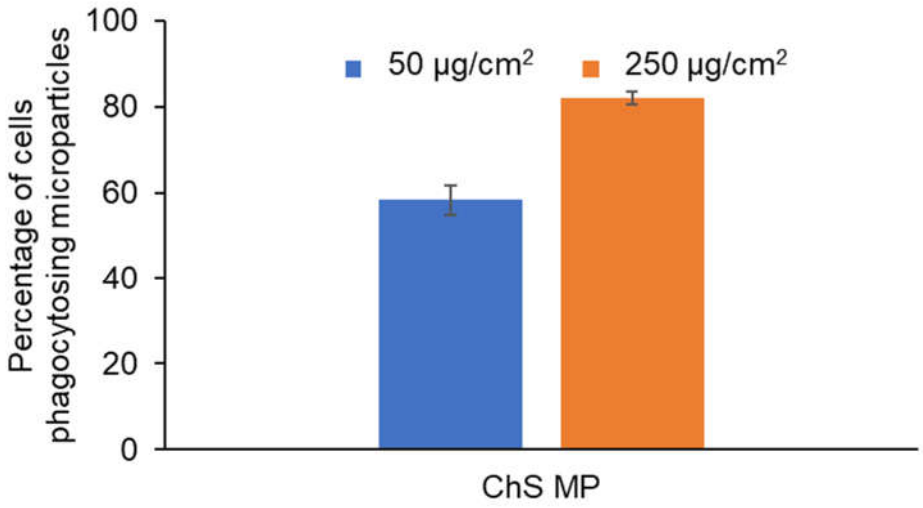

Figure 5.9 – Percentage of macrophage-like THP-1 cells undergoing phagocytosis, after 2 h exposure to different doses of fluorescently-labelled unloaded chondroitin sulphate microparticles (ChS MP), as analysed by flow cytometry. Data represent mean ± SEM (n = 3).

In order to validate the flow cytometry results regarding microparticle uptake, a cell imaging assay was performed. Macrophages were exposed to fluorescent ChS particles during 24 h and imaged after several stain-washing steps. As dTHP-1 cells were too sensitive and easily detached from the plates after a washing step, J774A.1 cells were chosen for this experiment. The setup of this assay differed from the previous one in that cells were exposed to a suspension of microparticles and not to the dry powder directly. According to particle kinetics, the deposition depends on several characteristics like particle size, concentration and density [224]. These ChS-based microparticles evidenced a polydisperse size ranging from 250 nm to 10 µm, despite the Dv50 of 4.1 µm. The rationale of establishing an incubation time of 24 h relied on the need to allow most of the particles to deposit in the bottom of the well. The cells were exposed to different microparticle concentrations. Fluorescence intensity of each well was measured at the wavelength of the different fluorochromes and the normalised FITC signal per well is depicted in Figure 5.10. It was observed that the fluorescence signal increased with the increase of microparticle concentration. Figure X further shows the observation of a FITC area accumulation was also observed in the images of the cells incubated with higher concentrations of microparticles. Indeed, small

green spots observed on the image corresponding to the concentration of 0.125 mg/mL became large green areas within the cell at the concentration of 1.00 mg/mL (indicated with arrows). The FITC signal from ChS microparticles revealed to be within the CellMask (entire cell dye: cytoplasm and nucleus) signal, indicating that the microparticles were associated with the cells, and that the washing steps removed the unbound particles, since no FITC signal was found out of the cellular area. The FITC signal increased with the increase in microparticle concentration, corroborating the flow cytometry result of a dose-dependent interaction.

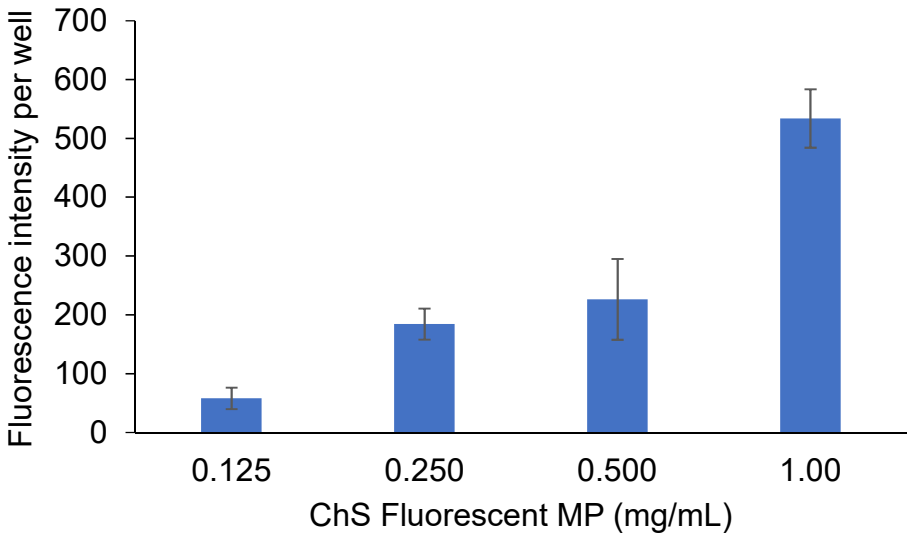

Figure 5.10 – FITC fluorescence intensity (a.u.) per well of J774A.1 cells after 24 h of exposure to different concentrations of fluorescently-labelled chondroitin sulphate (ChS) microparticles (MP). Data represent mean ± SEM (n = 3).

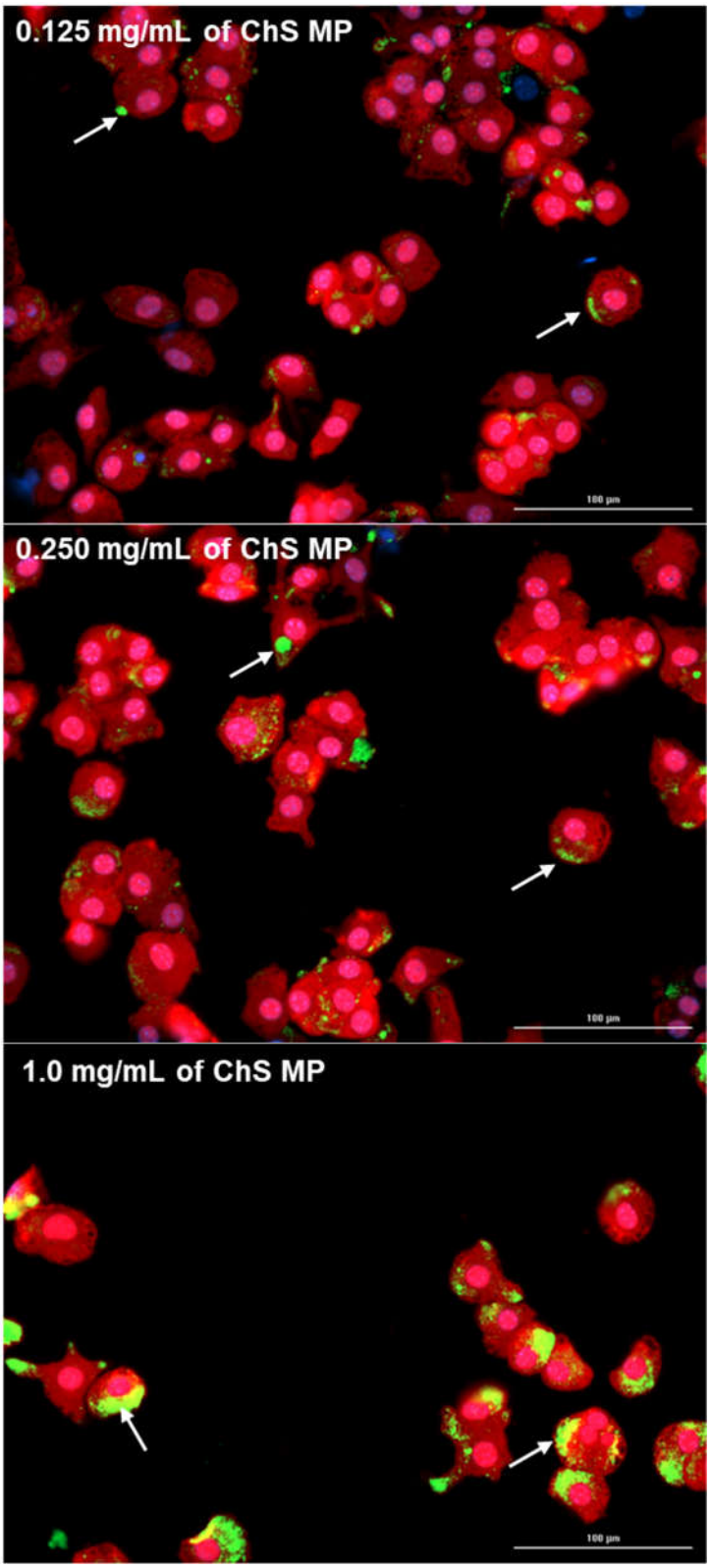

Figure 5.11 – Representative micrographs of J774A.1 cells after 24 h of exposure to different concentrations of fluorescently-labelled chondroitin sulphate (ChS) microparticles (MP). Nuclei were stained with Hoechst (blue), cytoplasm with deep red HCS CellMask and microparticles with FITC (green). Scale bar represents 100 µm. Arrows indicate the FITC signal within the cell.

As another parameter of microparticle interaction with macrophages, the release of pro-inflammatory interleukins by the cells upon 24 h exposure to the microparticles (1 mg/mL) was evaluated.

As before, negative control consisted of cells incubated only with CCM and positive control comprised an exposure to LPS. The obtained results are presented in Figure 5.12, evidencing a moderate induction of both proinflammatory interleukins (IL-8 ≈ $3.9x10^3$ pg/mL and TNF-α ≈ 300 pg/mL) upon contact with ChS-based samples. No statistical differences were observed between the effect induced by the polymer and drug-loaded microparticles, suggesting a polymer-driven effect. The observed values were approximately a fifth of those resulting from exposure to LPS for IL-8 and a tenth for TNF-α. A previous work from our group has shown the ability of another sulphated polysaccharide, fucoidan, to elicit the release of interleukins by macrophages [101]. However, that polymer induced TNF-α similarly to an LPS stimulation, which could raise concerns on the hyper responsiveness of macrophages. In fact, very high stimulation may result in uncontrolled or dysregulated release of mediators that exacerbate acute tissue injury and/or promote the development of chronic diseases, such as fibrosis and cancer [225, 226]. ChS has been reported to bind and stabilise IL-8 leading to an increase in biological half-life and extended proinflammatory activity [227], especially in the lung [228]. This fact needs to be taken into account, since a small activation in the production of this cytokine could lead to an extended effect *in vivo*. ChS is also reported to possess anti-inflammatory characteristics and to act as a protective in LPS induced inflammation [150, 229].

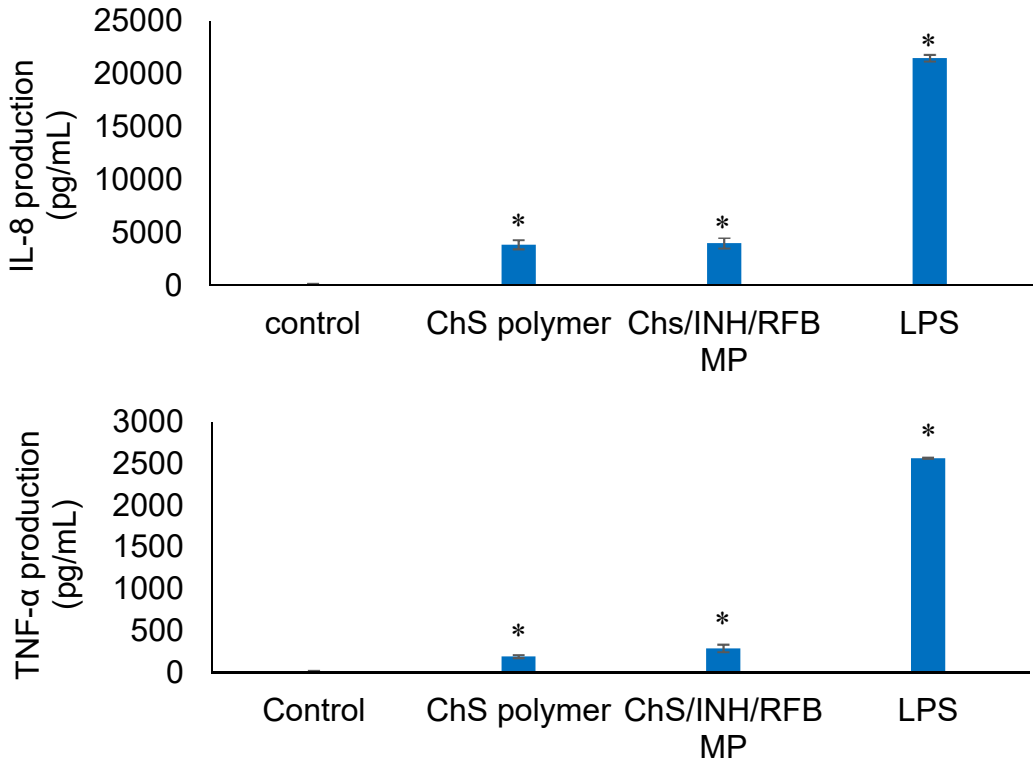

Figure 5.12 – IL-8 and TNF-α released by macrophage-differentiated THP-1 cells after 24 h incubation with chondroitin sulphate (ChS) polymer, ChS/INH/RFB microparticles (MP) and lipopolysaccharide (LPS), the latter used as positive control. Data represent mean ± SEM (n = 3). INH: isoniazid, RFB: Rifabutin. * $p < 0.05$ compared with control (cell culture medium).

As referred in the previous chapter, these results must be taken cautiously, considering recent findings suggesting that the generation of an inflammatory response can benefit bacterial growth rather than potentiating the elimination of the pathogen [25]. Importantly, the hypothesis of that study was confirmed based on ROS production and a possible role of TNF-α or IL-8 was not unveiled. However, it is prudent to consider a possible effect of these mediators, considering that they all have a role in inflammation.

Notwithstanding these remarks, when comparing ChS-based microparticles with starch/CRG counterparts, the former were generally observed to promote higher levels of macrophage uptake and induce a lower production of interleukins, especially TNF-α. It should be stressed, additionally, that the cells were exposed to a concentration of ChS microparticles that doubles that of starch/CRG microparticles. As a whole, the results observed for ChS-based microparticles

regarding macrophage interaction are considered more favourable for an application in tuberculosis therapy.

5.7. Conclusions

ChS microparticles were able to successfully associate a combination of INH and RFB, with efficiency between 60% and 95%, either using ethanol or HCl as co-solvent in the spray-drying process. The process selected for microencapsulation (spray-drying) did not induce any alterations in the antitubercular efficacy of the drugs. Despite the obtained microparticles revealed similar aerodynamic properties and *in vitro* respirability, the powder prepared using ethanol as co-solvent showed a better ability to sustain the release of RFB. Regarding the objective of associating INH and RFB, two drugs of opposite aqueous affinity, in the same formulation of ChS-based microparticles aimed at lung delivery, the use of ethanol as co-solvent revealed to be more advantageous. Considering the performed set of tests, the microparticles demonstrated a satisfactory biocompatibility in the three used cell lines, representing both the alveolar epithelium and macrophages. High content analysis revealed that RFB induced a dose-dependent elevation in phospholipid content, which could be prevented by formulation in ChS microparticles. Microparticles were further demonstrated to be phagocytosed by macrophages in a dose-dependent manner and to induce a moderate production of pro-inflammatory interleukins by macrophage-like cells. The results obtained in this work provide good indications on the suitability of ChS/INH/RFB microparticles as inhalable antitubercular drug carriers for tuberculosis therapy, justifying progression to *in vivo* studies focusing on safety and therapeutic efficacy.

Chapter VI - *In vivo* safety evaluation

This page was intentionally left in blank

6. In vivo safety evaluation

6.1. Introduction

Immunological and inflammatory reactions are common responses of the lungs to exogenous materials that come into contact with the organ, usually upon normal breathing. When the purpose of the inhalation is, however, therapeutic, such effects are not desirable. The safety of inhalable therapeutic formulations, thus, needs to be ensured. A very narrow list of excipients is approved for lung delivery, and currently for this route there is a tremendous lack of options. ChS, starch and CRG, the materials used and evaluated for drug delivery in this thesis, have limited exploration in the lung delivery field.

Mouse is normally the first animal model chosen to perform *in vivo* safety tests of new excipients, and evaluate the immune response despite the differences with humans [230, 231]. Allergic reactions are commonly associated to an increase in the levels of IgE (the primary antibody involved in exacerbating allergic diseases) and IgG (the main immunoglobulin isoform of the secondary immune response) [232]. IgG comprise 70–75 of the serum antibodies and four subclasses of immunoglobulin G are distinguished: the IgG1, IgG2, IgG3, and IgG4 that amount to 66%, 23%, 7%, and 4% of the IgG antigen pool, respectively [233-235]. The concentration of IgE in the serum is the lowest of the five immunoglobulin isotypes (constituting 0.004% of total serum immunoglobulin) [236]. In addition, the IgE serum half-life is short, 12h in mice and 2 days in humans, compared with 6-8 days in mice and 21-23 days in humans for IgG [237, 238]. However, when IgE binds to the surface of mast cells via the high affinity IgE receptor an extended tissue half-life of 3-weeks is possible [239]. IgE has been reported to play a role in the recruitment of eosinophils to the affected region [240-242], which represents a typical step of allergic asthma, for instance. If IgE stimulation and eosinophil recruitment to the lung is prolonged, it could lead to organ damage and also affect other tissues and can be used as an indicator of toxicity [243].

LDH is an enzyme found in almost all body tissues, although its blood levels are normally low. It is a marker of common injuries and diseases, because it is released during tissue damage, namely in lung cellular damage and inflammation [244]. Therefore, it has been used as a complementary indicator of toxicity, along with the MTT assay, when testing the microparticle formulations developed and evaluated in this thesis. The liver is another organ that is frequently affected after

the exposure to some toxicants. In this context, aspartate aminotransferase (AST) and alanine aminotransferase (ALT) are widely used as serum enzyme biomarkers of liver injury [245, 246]. Taking into consideration the importance of avoiding immune stimulation and inflammation by vehicles used for drug delivery, it was deemed relevant to perform a study, although preliminary, to determine parameters linked to the safety of ChS and starch/CRG when delivered by inhalation, in the form of microparticles, to mice.

6.2. Methods

6.2.1. Animals

BALB/c mice (6–8 weeks old) were obtained from the Gulbenkian Institute of Science (Oeiras, Portugal). The animals were kept under standard hygiene conditions, fed commercial chow and given acidified drinking water *ad libitum*. All animal experiments were carried out with the permission of the local ethical committees of the Faculty of Pharmacy and of the Institute of Molecular Medicine in accordance with the EU Directive (2010/63/UE) and Portuguese laws (DR 113/2013, 2880/2015 and 260/2016). The Portuguese Direção Geral de Alimentação e Veterinária further approved the animal assays (reference 0421/000/000/2013) to be conducted under the project PTDC/DTP-FTO/0094/2012.

6.2.2. Pulmonary administration

Animals were divided into 3 groups, Control, ChS and Starch/CRG. Each group had 4 animals (excluding the control without treatment that only had 2 animals) that were exposed to a daily dose (30 mg) for 2 weeks with 5 administrations per week of the unloaded microparticles composed of the formulated polymers. The control group received no treatment. For the pulmonary administration of spray dried microparticles, a simple apparatus fabricated with a 15 mL centrifuge tube where the powder was inserted, was used. A small hole was made in the bottom of the tube that was used for the delivery of the powder to mice. A plastic pump connected to the upper part of the tube allowed the production of a turbulent air stream for fluidising the powder. Mice were restrained in a 50 mL tube that

contained a small hole in the bottom, which was connected to the 15 mL tube using a baby bottle teat. Thirty mg of the dry powder were inserted in the device and each animal received the formulation by inhalation during 2 min.

6.2.3. Safety evaluation of inhaled microparticles in healthy mice

On the first day of treatment, before powder inhalation, blood samples (100– 200 µL) were collected from the tail vein into tubes with no anticoagulant. Following centrifugation, serum aliquots (30 – 50 µL) were prepared and stored at - 30 °C. Three days after the last administration of the microparticles, mice were anaesthetised with isoflurane, samples of blood were collected from the retinal blood vessels and a few drops of peripheral blood were used to prepare blood smears (three slides per mouse). Moreover, the remaining blood samples were then centrifuged to separate the serum, which was stored at -30°C for further analysis. Organs of interest such as liver, spleen and lung were removed. The respective tissue indexes were determined according to the formula below and compared to naïve mice:

$$\text{Tissue index} = \sqrt{\frac{\text{organ weight}}{\text{animal weight}}} \times 100 \qquad (6.1)$$

6.2.4. Tissue integrity and liver function

Serum samples were analysed with kits for quantification of aspartate aminotransferase (ALT) [GPT (ALAT) kit]; alanine aminotransferase (AST) [GOT (ASAT) kit]; and LDH, according to the manufacturers recommendations (Hospitex Diagnostics S.r.l., Italy).

6.2.5. Eosinophil count on blood smears

Slides with blood smears were stained using the Wright staining method [247, 248]. A minimum of 100 leucocytes were counted in each blood smear with the use of a light microscope (Microscope TR 500, VWR International, Belgium). Twelve slides (blood smears) were included in the count, considering three slides per mouse in each of the groups (n = 4).

6.2.6. Ouchterlony double immunodiffusion to detect serum immunoglobulin E (IgE)

Ouchterlony double immunodiffusion technique was performed to determine if IgE was present in sera from mice treated with unloaded ChS and Starch/CRG microparticles. To obtain a positive control samples, C57BL/6J mice (Charles River, France) were sensitised to ovalbumin (0.1 mg/mL in PBS). The intraperitoneal injection of ovalbumin (200 µL) was performed twice with an interval of 2 weeks between administrations. A pool of mouse serum (8 µL) was prepared by combining the serum collected from the OVA-sensitised animals. Likewise, equal volumes of serum collected from the treated mice of each group were combined to prepare a pool.

For the Ouchterlony assay, agar gel/phosphate saline buffer 1.5% (w/v) was poured to a depth of 3 mm onto glass slides (25 x 75 mm) coated with 1% (w/v) agar gel/water and dried. Wells were made using a template and gel punch; the agar plugs were removed from wells using a water vacuum pump. The assay format consisted of a central well surrounded by three equidistant wells. Horseradish peroxidase-conjugated IgG fraction of polyclonal goat antiserum to mouse IgE, Fc specific and goat anti mouse IgG1 (subclass specific), conjugated with Horseradish peroxidase (Nordic Immunology, Netherlands) were used as the antibodies to detect IgE and IgG in the serum samples. The antibodies were diluted (1:2) with Tris-base (Nzytech, Portugal). Each individual antibody solution (8 µL) was placed in the central well and the peripheral wells were filled with the pools of treated mouse sera and the positive control (8 µL). Slides were set on a horizontal surface and incubated in a moist chamber at 4°C for two days. Afterwards, they were washed with PBS buffer several times and stained with Coomassie Brilliant Blue G 250 (Serva, Germany). The slides were destained in 10% methanol (v/v) / 10% acetic acid (v/v) for 5 min and then washed with distilled water. Results were scored based on the observation of a visible line of precipitation.

6.2.7. Statistical analysis

The student t-test and the one-way analysis of variance (ANOVA) with the pairwise multiple comparison procedures (Holm-Sidak method) were performed

to compare two or multiple groups. All analysis was run using Sigmaplot (version 12.5) and differences were considered to be significant at a level of $p < 0.05$.

6.3. Results/Discussion

6.3.1. Safety evaluation of microparticles in healthy mice

Animals received the microparticles by the pulmonary route for two weeks, in a total of 10 administrations, as described in the methods. Mice were monitored daily and physical conditions evaluated in terms of mobility and weight variation. Three days after the last pulmonary administration, mice were sacrificed and the organs of interest, such as liver, kidney and lungs, were removed. These were then macroscopically analysed and the respective tissue index determined and compared to naïve mice. The tissue index allows the evaluation of changes in specific organs that may occur in relation to the whole-body weight. These changes have long been accepted as a sensitive indicator of toxicity [243].

The obtained results are shown in Table 6.1. No significant differences in tissue indexes for mice receiving the pulmonary administration of the two different microparticles in comparison to naïve mice were observed, which suggests the polymers were safe for inhalation under the established schedule.

Table 6.1. Tissue indexes of mice receiving pulmonary administration of microparticles in comparison to naïve mice (mean ± SD, n = 4). Different letters represent significant differences in each parameter ($p < 0.05$).

Group of mice	Liver	Lung	Kidney
Naïve (n = 2)	23.4 ± 0.1^{a}	7.7 ± 0.6^{b}	12.6 ± 0.3^{c}
ChS	24.4 ± 0.4^{a}	7.7 ± 0.2^{b}	13.0 ± 0.5^{c}
Starch/CRG	24.3 ± 0.4^{a}	7.9 ± 0.5^{b}	12.7 ± 0.4^{c}

6.3.2. Eosinophil count on blood smears

After staining of blood smears, white blood cells were counted. The results are depicted in Figure 1, and no significant differences were observed between the different groups. Focusing specifically on eosinophils, both the microparticle formulations and the naïve mice presented a similar number of these cells, which

was approximately 1%. This indicates that no immune response was elicited in response to the inhalation of any of the formulations of microparticles.

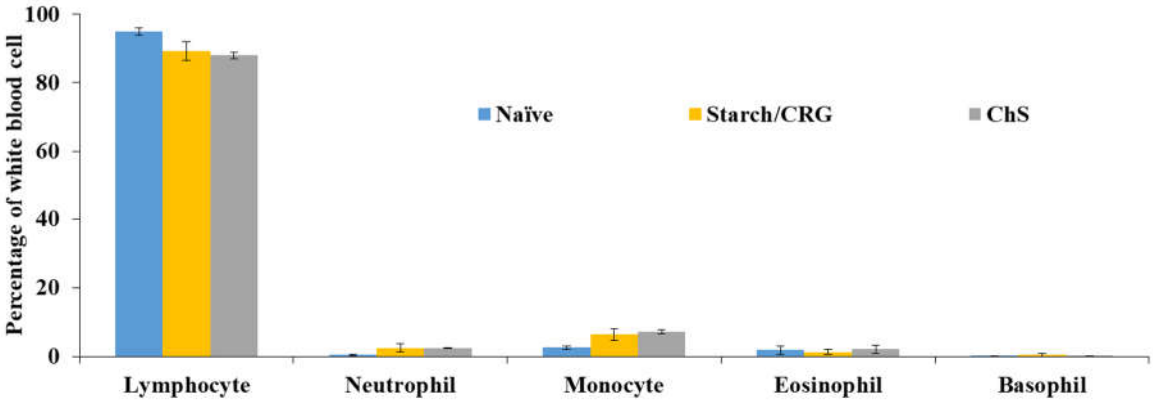

Figure 6.1 - Percentage of white blood cells counted in the mice blood smears. Results represent mean ± SEM, n = 3x4.

6.3.3. Tissue integrity and liver function

Serum of the animals was analysed using different kits to determine the levels of LDH, ALT and AST, and the results are depicted in Table 2. The levels of ALT and AST were similar to those reported in the literature for healthy animals [249]. No statistical differences were observed when comparing naïve and exposed animals, indicating tolerance of the mice to the inhalable microparticles. The experimental design should include more animals per group in a future investigation in order to reduce the fairly large standard deviations.

Table 6.2. Serum levels of ALT, AST, and LDH in mice receiving pulmonary administration of microparticles, in comparison to naïve mice (mean ± SEM, n≥2). Different letters represent significant differences in each parameter ($p < 0.05$).

	ALT (U/L)	AST (U/L)	LDH (U/L)
Naïve (n = 2)	2.9 ± 2.9^{a}	32.0 ± 2.9^{b}	2978 ± 1975^{c}
ChS	3.9 ± 1.7^{a}	21.3 ± 4.4^{b}	2811 ± 999^{c}
Starch/CRG	4.4 ± 1.4^{a}	13.6 ± 1.9^{b}	1851 ± 812^{c}

6.3.4. IgG and IgE detection in the serum samples

To complement the eosinophil count, the possible increase in immunoglobulin due to the treatment was investigated. As the antibodies available in the laboratory were polyclonal, an Ouchterlony double immunodiffusion test was conducted to evaluate the immunological response. In this assay, the serum and antibody solutions diffuse away from the original wells through the agar gel, toward one another. At the point where they meet in the agarose, if “equivalence” between the antigen and antisera occurs, a visible line of precipitation is formed. No reaction was detected between antibody-antigen in this assay, as the test samples (serum of mice before and after inhalation of microparticles) did not precipitate in contact with antibodies IgE and IgG_1, despite using a range of concentrations. Nevertheless, a suitable control was needed to confirm that the reaction worked properly. Sera obtained from OVA-sensitised mice was used in this context as a positive control, but it did not cause an immunoprecipitation when used in the Ouchterlony assay, possibly due to protein degradation. A commercial imunoglobulin sample or other positive control would be a better control to be used in the future, in order to adequately obtain clear observations. The literature also indicates trimellitic anhydride as a good positive control in the identification of potential chemical respiratory allergens [250].

Western-blot assays were also attempted, as they are more sensitive, but as the available antibodies were not monoclonal, a cross reaction was found in most of the samples, leading to a smudged result. Together with the lack of a proper positive controls, the immunoglobulin assessment was not feasible. Western-blot is possibly the most adequate for use in the future, but requires the application of a monoclonal antibody to improve specificity and reduce the likelihood of cross-reaction between different immunoglobulin isoforms, and a better positive control should also be applied.

6.4. Conclusions

The tissue index of mice remained unaltered after exposure, by inhalation, to ChS and starch/CRG microparticles, similarly the levels of ALT, AST and LDH were also unchanged. Eosinophilia was also not observed in any of the test groups. These preliminary assays indicate that, in the tested schedule, the inhalation of the developed microparticles did not apparently elicit an immunological or

inflammatory response in the analysed organs. A preliminary indication of the safety of the tested materials, under the specific schedule, is, thus, provided. However, the study needs to be deepened, not only by increasing the duration of the exposure, but also by using a higher number of animals and a positive control that validates the analysis.

This page was intentionally left in blank

Chapter VII - Final considerations and future perspectives

This page was intentionally left in blank

7.1. Final considerations

In the present work, we proposed the use of polysaccharide-based carriers for pulmonary tuberculosis therapy. Alveolar macrophages act as the trojan horse in tuberculosis disease, offering *Mtb* a place to hide and replicate. Developing a therapeutic strategy that permits targeting these cells in a direct manner and co-localising the antibacterial drugs in the same compartment of the bacteria, would, expectedly, lead to better and more efficient therapy of tuberculosis. In this context, we believe that natural materials and, namely, polysaccharides, may have advantage over other materials. The composition of some of these natural molecules resembles that of some moieties undergoing recognition by macrophage receptors, which are reported to naturally target macrophages and induce an immune response at some level. With these ideas in mind, ChS and starch/CRG microparticles associating simultaneously two first-line antitubercular drugs (INH and RFB) were proposed as inhalable therapy of tuberculosis with particular emphasis on pulmonary tuberculosis.

Microparticles composed of either ChS or starch/CRG were successfully produced by spray-drying, associating INH and RFB with efficacy varying within 54% and 96%. Microparticles composed of ChS were studied regarding the effect of using different co-solvents to provide the solubilisation of RFB, which resulted in having the solvents present during the spray-drying process. Ethanol or HCl were tested for this effect and, despite similar aerodynamic diameter around 4 µm was calculated, several differences were found among the resulting microparticles:

- The association efficiency of RFB was higher for microparticles produced with HCl (68% *versus* 59% in microparticles produced with ethanol);
- The use of ethanol resulted in microparticles with lower tap density (0.32 g/cm^3 *versus* 0.58 g/cm^3 in microparticles produced with HCl);
- FPD and, consequently, FPF was higher for microparticles prepared with ethanol (assuming RFB as reference, 1.5 mg were quantified *versus* 1.2 mg in microparticles produced with HCl);

- Release profiles were somewhat different; microparticles produced with ethanol showing a slightly slower release of RFB, although a similar profile was found for INH.

From these results, ChS microparticles prepared using ethanol as solvent were considered to have more favourable properties for the established objective, being, thus, selected to undergo the following biological assessment. Regarding the preparation of starch/CRG microparticles, the use of this solvent was hampered by the fact that ethanol would evaporate due to the high temperature used while heating CRG to avoid its gelation during the spray-drying process. Therefore, in starch/CRG microparticles HCl was added to solubilise RFB, which further contributed to a decrease of the viscosity of CRG solution. This had an effect in the spray-drying yield, which increased from 58% to 71%. In this manner, it was observed that different solvents benefited the microparticle formulations in a different way, both contributing for an improvement of the resulting characteristics. Starch/CRG microparticles were determined to have aerodynamic diameter of 3.3-3.9 μm and FPF of 32-37%, which were considered satisfactory. However, almost 50% of the microparticles were observed to be above 5 μm, which was considered a critical limitation requiring being addressed if the formulation is to be further explored.

The process of microencapsulation was shown to not affect the activity of the encapsulated drugs in any of the microparticle formulations, as the inhibitory action of the drugs against *M. bovis* BCG remained unaltered. This indicates the adequacy of spray-drying to produce the carriers.

Microparticles of starch/CRG and of ChS (produced with ethanol) were tested for biological interaction. The biocompatibility profile was determined by a metabolic assay (MTT) and the release of the enzyme LDH, upon incubation of microparticles with cell lines that are relevant for the application. The assessment was performed using human alveolar epithelial cells (A549), human derived macrophages (dTHP-1) and mouse macrophages (J7774A.1). In the first two cell lines, the 24 h exposure to 1 mg/mL of starch/CRG drug-loaded microparticles resulted in cell viability near the limit of 70%, while J774A.1 cells showed lower tolerability, with viability below 70%. On the contrary, ChS microparticles were well tolerated in all cell lines under the same conditions. Nevertheless, for ChS

microparticles the results of LDH release were not conclusive, possibly due to a cross-reaction occurring between ChS and the reagents of the LDH kit. This formulation was, thus, further evaluated in a high content analysis (HCA) assay that focused specifically on parameters including mitochondrial activity, areas of cell and nuclei and intracellular lipid accumulation. The assay revealed no toxic effects on J774A.1 cells after 48 h exposure. Free RFB demonstrated some phospholipid accumulation, but this was overpassed when the drug was encapsulated.

dTHP-1 cells were used to analyse the behaviour of macrophages when exposed to the contact with microparticles. On one hand, ChS-based microparticles evidenced higher ability for internalisation by macrophages, reaching values up to 82%, comparing with maximum 65% for starch/CRG microparticles. On the other hand, the production of pro-inflammatory interleukins (TNF-α and IL-8) was measured after a 24 h exposure to polymers and drug-loaded particles. A moderate level of activation was observed for ChS polymer and ChS microparticles, higher than the one observed for CRG polymer, but lower than that induced by starch polymer and starch/CRG microparticles. Importantly, the concentration of starch/CRG was half that of ChS. The results obtained for starch/CRG microparticles require a cautious analysis, as the high induction of interleukin production raises concern regarding the potential to generate an inflammatory response in the lung after the inhalation of the microparticles. It is believed that the observed effect was due to the higher size of starch/CRG microparticles and to the incomplete solubilisation of starch in cell culture medium, which could have increased the level of activation because of the particulate form. However, different starch/CRG mass ratio, of lower starch content, needs to be tested to confirm this hypothesis. Furthermore, recent findings indicating that an inflammatory response could be beneficial for bacterial growth need to be taken into account in the future consideration of both formulations of microparticles for an application in tuberculosis therapy.

Finally, a preliminary *in vivo* assay intended to evaluate the generation of a potential inflammatory and allergic response of the animals after inhalation of the carriers, providing some hints on the safety of the materials for an application in pulmonary delivery. No evidence of toxic effects was observed after exposure of the animals to any of the developed microparticles upon their delivery by

inhalation, in a schedule involving 10 inhalations performed within a period of 2 weeks. Values of serum ALT, AST and LDH remained unaltered compared with the control group, indicating absence of tissue damage. Additionally, this was in accordance with the maintenance of the tissue index of liver, lung and kidney. Moreover, no eosinophilia was observed in the blood of the exposed animals.

In summary, the produced microparticle formulations revealed suitable characteristics for the pulmonary administration of antitubercular drugs. Starch/CRG formulation would require further optimisation, but ChS-based microparticles produced with ethanol demonstrated to have suitable characteristics for an application as inhalable drug carriers with a specific focus on the treatment of pulmonary tuberculosis. Additionally, the obtained results unveiled the possibility of using these microparticles in other clinical situations requiring targeting cells of the mononuclear phagocyte system, which encompasses other macrophage intracellular diseases and vaccination approaches.

7.2. Future perspectives

The work presented in this thesis comprises a considerable amount of data that, in its essence, establishes the foundations of the hypothesis created initially around the project. The obtained results were very satisfactory, but the developed drug-loaded microparticles require further investigation to demonstrate their efficacy as inhalable therapy of pulmonary tuberculosis and consider a possible translation to clinics. Essentially, a more realistic view of the safety of the proposed carriers in inhalable application and a therapeutic proof-of-concept that could demonstrate their efficacy are considered the most helpful and relevant issues. However, other intermediate steps of evaluation are also considered relevant, for instance regarding storage stability or the determination of the specific mechanisms used by macrophages to recognise the microparticles.

The conversion of these ideas into concrete actions would involve:

a. To optimise starch/CRG microparticles to display higher fine particle content;

b. To evaluate the physical stability of the carriers upon storage, regarding the maintenance of their aerodynamic characteristics but also the drug loading;

c. Further investigate if phagocytosis is mediated by the chemical groups available on the polymeric structures and determine the specific receptor that is mediating the particles/macrophage interaction;

d. To determine the biocompatibility of the carriers *in vivo*, in order to evaluate the safety of microparticles for inhalable application, namely regarding the generation of immune and inflammatory reactions;

e. To evaluate *in vivo* the antibacterial efficacy of drug-loaded microparticles.

This page was intentionally left in blank

References

1. Martin, C., N. Aguilo, and J. Gonzalo-Asensio, *Vaccination against tuberculosis.* Enfermedades infecciosas y microbiologia clinica (English ed.), 2018. **36**(10): p. 648-656.
2. (WHO), W.H.O. *Global tuberculosis report 2018*. 2018 [cited 2019 20 July]; Available from: http://www.who.int/tb/publications/global_report/en.
3. Ranjita, S., A. Loaye, and M. Khalil, *Present Status of Nanoparticle Research for Treatment of Tuberculosis.* Journal of Pharmacy and Pharmaceutical Sciences, 2011. **14**(1): p. 100-116.
4. Floyd, K., et al., *The global tuberculosis epidemic and progress in care, prevention, and research: an overview in year 3 of the End TB era.* The Lancet Respiratory Medicine, 2018. **6**(4): p. 299-314.
5. (DGS), D.-G.d.S. *Programa Nacional para a Tuberculose. Tuberculose em Portugal: Desafios e Estratégias*. 2018 [cited 2019 20 July]; Available from: https://www.dgs.pt/documentos-e-publicacoes/tuberculose-em-portugal-desafios-e-estrategias-2018-.aspx.
6. Timmins, G.S. and V. Deretic, *Mechanisms of action of isoniazid.* Molecular Microbiology, 2006. **62**(5): p. 1220-1227.
7. Sousa, M., A. Pozniak, and M. Boffito, *Pharmacokinetics and pharmacodynamics of drug interactions involving rifampicin, rifabutin and antimalarial drugs.* Journal of Antimicrobial Chemotherapy, 2008. **62**(5): p. 872-878.
8. Levitz, S.M., *Overview of Host Defenses in Fungal Infections.* Clinical Infectious Diseases, 1992. **14**(Supplement 1): p. S37-S42.
9. van Rooijen, N., et al., *Macrophages in host defense mechanisms.* Current topics in microbiology and immunology, 1996. **210**: p. 159-165.
10. Rodrigues, S. and A. Grenha, *Activation of macrophages: Establishing a role for polysaccharides in drug delivery strategies envisaging antibacterial therapy.* Current pharmaceutical design, 2015. **21**(33): p. 4869-4887.
11. Italiani, P. and D. Boraschi, *From monocytes to M1/M2 macrophages: phenotypical vs. functional differentiation.* Frontiers in immunology, 2014. **5**(514): p. 1-22.
12. Ovchinnikov, D.A., *Macrophages in the embryo and beyond: Much more than just giant phagocytes.* genesis, 2008. **46**(9): p. 447-462.
13. Gordon, S. and P.R. Taylor, *Monocyte and macrophage heterogeneity.* Nature reviews. Immunology, 2005. **5**(12): p. 953-964.
14. Ferenbach, D. and J. Hughes, *Macrophages and dendritic cells: what is the difference?* Kidney International, 2008. **74**(1): p. 5-7.
15. Janeway, C.J., et al., *Immunobiology: The Immune System in Health and Disease*. 5th edition ed. 2001, New York: Garland Science.
16. Silva, M.T. and M. Correia-Neves, *Neutrophils and macrophages: The main partners of phagocyte cell systems.* Frontiers in immunology, 2012. **3**: p. 1-6.
17. Stow, J.L., et al., *Cytokine secretion in macrophages and other cells: Pathways and mediators.* Immunobiology, 2009. **214**(7): p. 601-612.

18. Parkin, J. and B. Cohen, *An overview of the immune system.* The Lancet, 2001. **357**(9270): p. 1777-1789.
19. Liu, Y.C., et al., *Macrophage polarization in inflammatory diseases.* International journal of biological sciences, 2014. **10**(5): p. 520-529.
20. Sieweke, M.H. and J.E. Allen, *Beyond Stem Cells: Self-Renewal of Differentiated Macrophages.* Science, 2013. **342**(6161): p. 1242974.
21. Gordon, S., *The macrophage: Past, present and future.* European Journal of Immunology, 2007. **37**: p. S9-S17.
22. Gordon, S.B. and R.C. Read, *Macrophage defences against respiratory tract infections.* British medical bulletin, 2002. **61**: p. 45-61.
23. Benoit, M., B. Desnues, and J.-L. Mege, *Macrophage Polarization in Bacterial Infections.* The Journal of Immunology, 2008. **181**(6): p. 3733-3739.
24. Geissmann, F., et al., *Development of monocytes, macrophages and dendritic cells.* Science (New York, N.Y.), 2010. **327**(5966): p. 656-661.
25. Dallenga, T., et al., *M. tuberculosis-induced necrosis of infected neutrophils promotes bacterial growth following phagocytosis by macrophages.* Cell host & microbe, 2017. **22**(4): p. 519-530. e3.
26. Peiser, L. and S. Gordon, *Phagocytosis: Enhancement*, in *eLS*. 2001, John Wiley & Sons, Ltd.
27. Krombach, F., et al., *Cell size of alveolar macrophages: an interspecies comparison.* Environmental Health Perspectives, 1997. **105 Suppl 5**: p. 1261-1263.
28. Hoffbrand, A.V., et al., *Postgraduate Haematology*. 2011: Wiley.
29. Vasselon, T. and P.A. Detmers, *Toll Receptors: a Central Element in Innate Immune Responses.* Infection and immunity, 2002. **70**(3): p. 1033-1041.
30. Doyle, S.L. and L.A.J. O'Neill, *Toll-like receptors: From the discovery of NFκB to new insights into transcriptional regulations in innate immunity.* Biochemical Pharmacology, 2006. **72**(9): p. 1102-1113.
31. Beutler, B., et al., *GENETIC ANALYSIS OF HOST RESISTANCE: Toll-Like Receptor Signaling and Immunity at Large.* Annual review of immunology, 2006. **24**(1): p. 353-389.
32. Peiser, L., S. Mukhopadhyay, and S. Gordon, *Scavenger receptors in innate immunity.* Current Opinion in Immunology, 2002. **14**(1): p. 123-128.
33. Geijtenbeek, T.B.H. and S.I. Gringhuis, *Signalling through C-type lectin receptors: shaping immune responses.* Nature Reviews Immunology, 2009. **9**(7): p. 465-479.
34. Sankala, M., et al., *Characterization of recombinant soluble macrophage scavenger receptor MARCO.* The Journal of Biological Chemistry, 2002. **277**(36): p. 33378-33385.
35. PrabhuDas, M., et al., *Standardizing Scavenger Receptor Nomenclature.* The Journal of Immunology, 2014. **192**(5): p. 1997-2006.
36. Cummings, R.D. and R.P. McEver, *C-type Lectins*, in *Essentials of Glycobiology*, A. Varki, et al., Editors. 2009: Cold Spring Harbor (NY).
37. Kerrigan, A.M. and G.D. Brown, *C-type lectins and phagocytosis.* Immunobiology, 2009. **214**(7): p. 562-575.
38. Chavez-Santoscoy, A.V., et al., *Tailoring the immune response by targeting C-type lectin receptors on alveolar macrophages using*

"pathogen-like" amphiphilic polyanhydride nanoparticles. Biomaterials, 2012. **33**(18): p. 4762-4772.
39. East, L. and C.M. Isacke, *The mannose receptor family.* Biochimica et Biophysica Acta (BBA) - General Subjects, 2002. **1572**(2–3): p. 364-386.
40. Lewis, C. and J.D. McGee, *The macrophage*. The natural immune system. 1992, Oxford: IRL Press.
41. Taylor, P.R., et al., *The β-Glucan Receptor, Dectin-1, Is Predominantly Expressed on the Surface of Cells of the Monocyte/Macrophage and Neutrophil Lineages.* The Journal of Immunology, 2002. **169**(7): p. 3876-3882.
42. Coombs, P.J., M.E. Taylor, and K. Drickamer, *Two categories of mammalian galactose-binding receptors distinguished by glycan array profiling.* Glycobiology, 2006. **16**(8): p. 1C-7C.
43. Wang, N., H. Liang, and K. Zen, *Molecular Mechanisms That Influence the Macrophage M1–M2 Polarization Balance.* Frontiers in immunology, 2014. **5**(614): p. 1-9.
44. Cavaillon, J.M., *Cytokines and Macrophages.* Biomedicine & Pharmacotherapy, 1994. **48**(10): p. 445-453.
45. Goodman, S.B., et al., *Novel biological strategies for treatment of wear particle-induced periprosthetic osteolysis of orthopaedic implants for joint replacement.* Journal of the Royal Society Interface, 2014. **11**(93): p. 1-12.
46. Mantovani, A., et al., *The chemokine system in diverse forms of macrophage activation and polarization.* Trends in Immunology, 2004. **25**(12): p. 677-686.
47. Wang, N., H. Liang, and K. Zen, *Molecular mechanisms that regulate the macrophage M1/M2 polarization balance.* Frontiers in immunology, 2014. **5**.
48. Mills, C., *M1 and M2 Macrophages: Oracles of Health and Disease.* 2012. **32**(6): p. 463-488.
49. Hiraiwa, K. and S.F. van Eeden, *Contribution of Lung Macrophages to the Inflammatory Responses Induced by Exposure to Air Pollutants.* Mediators of Inflammation, 2013: p. 1-10.
50. Jaguin, M., et al., *Polarization profiles of human M-CSF-generated macrophages and comparison of M1-markers in classically activated macrophages from GM-CSF and M-CSF origin.* Cellular Immunology, 2013. **281**(1): p. 51-61.
51. Chanmee, T., et al., *Tumor-Associated Macrophages as Major Players in the Tumor Microenvironment.* Cancers, 2014. **6**(3): p. 1670-1690.
52. Wijesundera, K.K., et al., *M1-and M2-macrophage polarization in thioacetamide (TAA)-induced rat liver lesions; a possible analysis for hepato-pathology.* Histology and Histopathology, 2014. **29**(4): p. 497-511.
53. Yadav, M. and J.S. Schorey, *The β-glucan receptor dectin-1 functions together with TLR2 to mediate macrophage activation by mycobacteria.* Blood, 2006. **108**(9): p. 3168-3175.
54. Fujihara, M., et al., *Molecular mechanisms of macrophage activation and deactivation by lipopolysaccharide: roles of the receptor complex.* Pharmacology & Therapeutics, 2003. **100**(2): p. 171-194.
55. Gordon, S.B., et al., *Intracellular Trafficking and Killing of Streptococcus pneumoniae by Human Alveolar Macrophages Are Influenced by Opsonins.* Infection and immunity, 2000. **68**(4): p. 2286-2293.

56. Aderem, A. and D.M. Underhill, *MECHANISMS OF PHAGOCYTOSIS IN MACROPHAGES.* Annual review of immunology, 1999. **17**(1): p. 593-623.
57. Conner, S.D. and S.L. Schmid, *Regulated portals of entry into the cell.* Nature, 2003. **422**(6927): p. 37-44.
58. Dermine, J.-F. and M. Desjardins, *Survival of intracellular pathogens within macrophages.* Protoplasma, 1999. **210**(1-2): p. 11-24.
59. Rosenberger, C.M. and B.B. Finlay, *Phagocyte sabotage: disruption of macrophage signalling by bacterial pathogens.* Nat Rev Mol Cell Biol, 2003. **4**(5): p. 385-396.
60. Thi, E.P., U. Lambertz, and N.E. Reiner, *Sleeping with the Enemy: How Intracellular Pathogens Cope with a Macrophage Lifestyle.* PLoS Pathogens, 2012. **8**(3): p. e1002551.
61. Fratti, R.A., et al., *Mycobacterium tuberculosis glycosylated phosphatidylinositol causes phagosome maturation arrest.* Proceedings of the National Academy of Sciences, 2003. **100**(9): p. 5437-5442.
62. Vergne, I., et al., *Cell biology of mycobacterium tuberculosis phagosome.* Annual review of cell and developmental biology, 2004. **20**: p. 367-394.
63. Kang, P.B., et al., *The human macrophage mannose receptor directs Mycobacterium tuberculosis lipoarabinomannan-mediated phagosome biogenesis.* The Journal of Experimental Medicine, 2005. **202**(7): p. 987-999.
64. *Molecular Mechanisms in Legionella Pathogenesis Preface*. Current Topics in Microbiology and Immunology, ed. H. Hilbi. Vol. 376. 2014, New York Springer.
65. Newton, H.J., et al., *A Screen of <italic>Coxiella burnetii</italic> Mutants Reveals Important Roles for Dot/Icm Effectors and Host Autophagy in Vacuole Biogenesis.* PLoS Pathog, 2014. **10**(7): p. e1004286.
66. Makino, K., et al., *Phagocytic uptake of polystyrene microspheres by alveolar macrophages: effects of the size and surface properties of the microspheres.* Colloids and Surfaces B: Biointerfaces, 2003. **27**(1): p. 33-39.
67. Pacheco, P., D. White, and T. Sulchek, *Effects of Microparticle Size and Fc Density on Macrophage Phagocytosis.* Plos One, 2013. **8**(4): p. e60989.
68. Carter, C.A. and L.S. Ehrlich, *Cell biology of HIV-1 infection of macrophages.* Annual Review of Microbiology, 2008. **62**: p. 425-443.
69. Kumar, A. and G. Herbein, *The macrophage: a therapeutic target in HIV-1 infection.* Molecular and Cellular Therapies, 2014. **2**(1): p. 1-15.
70. Taylor, P.R., et al., *Macrophage receptors and immune recognition.* Annual review of immunology, 2005. **23**: p. 901-944.
71. Sinai, A.P. and K.A. Joiner, *SAFE HAVEN: The Cell Biology of Nonfusogenic Pathogen Vacuoles.* Annual Review of Microbiology, 1997. **51**(1): p. 415-462.
72. Sharma, M., et al., *Intracellular survival of Mycobacterium tuberculosis in macrophages is modulated by phenotype of the pathogen and immune status of the host.* International Journal of Mycobacteriology, 2012. **1**(2): p. 65-74.
73. Vergne, I., et al., *Mechanism of phagolysosome biogenesis block by viable Mycobacterium tuberculosis.* Proceedings of the National Academy of Sciences of the United States of America, 2005. **102**(11): p. 4033-4038.

74. Aldwell, F.E., et al., *In vitro control of Mycobacterium bovis by macrophages.* Tuberculosis, 2001. **81**(1–2): p. 115-123.
75. Agdestein, A., et al., *Intracellular growth of Mycobacterium avium subspecies and global transcriptional responses in human macrophages after infection.* BMC genomics, 2014. **15**(58): p. 1-14.
76. Barker, L.P., *Mycobacterium leprae interactions with the host cell: recent advances.* The Indian journal of medical research, 2006. **123**(6): p. 748-759.
77. Van Assche, T., et al., *Leishmania–macrophage interactions: Insights into the redox biology.* Free Radical Biology and Medicine, 2011. **51**(2): p. 337-351.
78. Koziel, J., et al., *Phagocytosis of Staphylococcus aureus by Macrophages Exerts Cytoprotective Effects Manifested by the Upregulation of Antiapoptotic Factors.* Plos One, 2009. **4**(4): p. e5210.
79. Hanawa, T., T. Yamamoto, and S. Kamiya, *Listeria monocytogenes can grow in macrophages without the aid of proteins induced by environmental stresses.* Infection and immunity, 1995. **63**(12): p. 4595-4599.
80. Forest, C.G., et al., *Intracellular survival of Salmonella enterica serovar Typhi in human macrophages is independent of Salmonella pathogenicity island (SPI)-2.* Microbiology, 2010. **156**(12): p. 3689-3698.
81. Pilonieta, M.C., et al., *Salmonella enterica Infection Stimulates Macrophages to Hemophagocytose.* mBio, 2014. **5**(6): p. 1-10.
82. Sun, H.S., et al., *Chlamydia trachomatis vacuole maturation in infected macrophages.* Journal of Leukocyte Biology, 2012. **92**(4): p. 815-827.
83. Kuwae, A., et al., *Shigella Invasion of Macrophage Requires the Insertion of IpaC into the Host Plasma Membrane: FUNCTIONAL ANALYSIS OF IpaC.* Journal of Biological Chemistry, 2001. **276**(34): p. 32230-32239.
84. Bi, Y., et al., *Yersinia pestis and host macrophages: immunodeficiency of mouse macrophages induced by YscW.* Immunology, 2009. **128**(1 Pt 2): p. e406-e417.
85. Ramarao, N. and T.F. Meyer, *Helicobacter pylori Resists Phagocytosis by Macrophages: Quantitative Assessment by Confocal Microscopy and Fluorescence-Activated Cell Sorting.* Infection and immunity, 2001. **69**(4): p. 2604-2611.
86. Ribeiro-Gomes, F.L., M.F. Lopes, and G.A. DosReis, *Negative Signaling and Modulation of Macrophage Function in Trypanosoma cruzi Infection*, in *Madame Curie Bioscience Database [Internet]*. 2000-2013, Landes Bioscience: Austin (TX).
87. Boschiroli, M.L., et al., *The Brucella suis virB operon is induced intracellularly in macrophages.* Proceedings of the National Academy of Sciences of the United States of America, 2002. **99**(3): p. 1544-1549.
88. Escoll, P., et al., *From Amoeba to Macrophages: Exploring the Molecular Mechanisms of Legionella pneumophila Infection in Both Hosts*, in *Molecular Mechanisms in Legionella Pathogenesis*, H. Hilbi, Editor. 2014, Springer Berlin Heidelberg. p. 1-34.
89. Ali, F., et al., *Streptococcus pneumoniae–Associated Human Macrophage Apoptosis after Bacterial Internalization via Complement and Fcγ Receptors Correlates with Intracellular Bacterial Load.* Journal of Infectious Diseases, 2003. **188**(8): p. 1119-1131.

90. Hunter, S.W. and P.J. Brennan, *Evidence for the presence of a phosphatidylinositol anchor on the lipoarabinomannan and lipomannan of Mycobacterium tuberculosis.* The Journal of biological chemistry, 1990. **265**(16): p. 9272-9279.
91. Fratti, R.A., et al., *Role of phosphatidylinositol 3-kinase and Rab5 effectors in phagosomal biogenesis and mycobacterial phagosome maturation arrest.* The Journal of cell biology, 2001. **154**(3): p. 631-644.
92. Vergne, I., J. Chua, and V. Deretic, *Tuberculosis toxin blocking phagosome maturation inhibits a novel Ca2+/calmodulin-PI3K hVPS34 cascade.* Journal of Experimental Medicine, 2003. **198**(4): p. 653-659.
93. Costa, H. and A. Grenha, *Natural carriers for application in tuberculosis treatment.* Journal of Microencapsulation, 2013. **30**(3): p. 295-306.
94. Germano, G., et al., *Role of Macrophage Targeting in the Antitumor Activity of Trabectedin.* Cancer Cell, 2013. **23**(2): p. 249-262.
95. Alexandru-Flaviu, T., *Macrophages Targeted Drug Delivery as a Key Therapy in Infectious Disease* Biotechnology, Molecular Biology and Nanomedicine, 2014. **2**(1): p. 17-20.
96. Tiwari, S., et al., *Macrophage-Specific Targeting of Isoniazid Through Mannosylated Gelatin Microspheres.* Aaps Pharmscitech, 2011. **12**(3): p. 900-908.
97. Saraogi, G.K., et al., *Mannosylated gelatin nanoparticles bearing isoniazid for effective management of tuberculosis.* Journal of Drug Targeting, 2011. **19**(3): p. 219-227.
98. Nimje, N., et al., *Mannosylated nanoparticulate carriers of rifabutin for alveolar targeting.* Journal of Drug Targeting, 2009. **17**(10): p. 777-787.
99. Smola, M., T. Vandamme, and A. Sokolowski, *Nanocarriers as pulmonary drug delivery systems to treat and to diagnose respiratory and non respiratory diseases.* International Journal of Nanomedicine, 2008. **3**(1): p. 1-19.
100. Rodrigues, S., et al., *Dual antibiotherapy of tuberculosis mediated by inhalable locust bean gum microparticles.* Int J Pharm, 2017. **529**(1-2): p. 433-441.
101. Cunha, L., et al., *Inhalable Fucoidan Microparticles Combining Two Antitubercular Drugs with Potential Application in Pulmonary Tuberculosis Therapy.* Polymers, 2018. **10**(6): p. 636.
102. Alahari, S.V., S. Dong, and S.K. Alahari, *Are macrophages in tumors good targets for novel therapeutic approaches?* Molecules and cells, 2015. **38**(2): p. 95-104.
103. Engströms, A., et al., *Conditioned media from macrophages of M1, but not M2 phenotype, inhibit the proliferation of the colon cancer cell lines HT-29 and CACO-2.* International Journal of Oncology, 2014. **44**(2): p. 385-392.
104. Deegan, P.B. and T.M. Cox, *Imiglucerase in the treatment of Gaucher disease: a history and perspective.* Drug Design Development and Therapy, 2012. **6**: p. 81–106.
105. Desnick, R.J. and E.H. Schuchman, *Enzyme replacement therapy for lysosomal diseases: lessons from 20 years of experience and remaining challenges.* Annual review of genomics and human genetics, 2012. **13**: p. 307-335.

106. Van Patten, S.M., et al., *Effect of mannose chain length on targeting of glucocerebrosidase for enzyme replacement therapy of Gaucher disease.* Glycobiology, 2007. **17**(5): p. 467-478.
107. Chong, A.S. and C.R. Parish, *Cell surface receptors for sulphated polysaccharides: a potential marker for macrophage subsets.* Immunology, 1986. **58**(2): p. 277-284.
108. Ahsan, F., et al., *Targeting to macrophages: role of physicochemical properties of particulate carriers—liposomes and microspheres—on the phagocytosis by macrophages.* Journal of Controlled Release, 2002. **79**(1–3): p. 29-40.
109. Kelly, C., C. Jefferies, and S.-A. Cryan, *Targeted Liposomal Drug Delivery to Monocytes and Macrophages.* Journal of Drug Delivery, 2011. **2011**: p. 1-11.
110. Gupta, A., et al., *Inhalable Particles Containing Rapamycin for Induction of Autophagy in Macrophages Infected with Mycobacterium tuberculosis.* Molecular Pharmaceutics, 2014. **11**(4): p. 1201-1207.
111. Chiellini, F., et al., *Micro/nanostructured polymeric systems for biomedical and pharmaceutical applications.* Nanomedicine, 2008. **3**(3): p. 367-393.
112. Raes, G., et al., *Macrophage galactose-type C-type lectins as novel markers for alternatively activated macrophages elicited by parasitic infections and allergic airway inflammation.* Journal of Leukocyte Biology, 2005. **77**(3): p. 321-327.
113. Shakya, A.K. and K.S. Nandakumar, *Applications of polymeric adjuvants in studying autoimmune responses and vaccination against infectious diseases.* Journal of The Royal Society Interface, 2012. **10**(79): p. 1-16.
114. Schleifer, K.H. and O. Kandler, *Peptidoglycan types of bacterial cell walls and their taxonomic implications.* Bacteriological Reviews, 1972. **36**(4): p. 407-477.
115. Yuriev, E., et al., *Three-dimensional structures of carbohydrate determinants of Lewis system antigens: Implications for effective antibody targeting of cancer.* Immunol Cell Biol, 2005. **83**(6): p. 709-717.
116. Rowe, R., P. Sheskey, and S. Owen, *Handbook of Pharmaceutical Excipients*. 5th ed. 2006, London: Pharmaceutical Press.
117. Li, L., et al., *Carrageenan and its applications in drug delivery.* Carbohydr Polym, 2014. **103**: p. 1-11.
118. Inic-Kanada, A., et al., *Effects of iota-carrageenan on ocular Chlamydia trachomatis infection in vitro and in vivo.* Journal of Applied Phycology, 2018. **30**(4): p. 2601-2610.
119. Baba, M., et al., *Sulfated polysaccharides are potent and selective inhibitors of various enveloped viruses, including herpes simplex virus, cytomegalovirus, vesicular stomatitis virus, and human immunodeficiency virus.* Antimicrobial Agents and Chemotherapy, 1988. **32**(11): p. 1742-1745.
120. Derby, N., et al., *Griffithsin carrageenan fast dissolving inserts prevent SHIV HSV-2 and HPV infections in vivo.* Nature Communications, 2018. **9**(1): p. 3881.
121. Magnan, S., et al., *Efficacy of a Carrageenan gel Against Transmission of Cervical HPV (CATCH): interim analysis of a randomized, double-blind, placebo-controlled, phase 2B trial.* Clinical Microbiology and Infection, 2018. **25**(2): p. 210–216.

122. Koenighofer, M., et al., *Carrageenan nasal spray in virus confirmed common cold: individual patient data analysis of two randomized controlled trials.* Multidisciplinary respiratory medicine, 2014. **9**(1): p. 57-57.
123. Graf, C., et al., *Development of a nasal spray containing xylometazoline hydrochloride and iota-carrageenan for the symptomatic relief of nasal congestion caused by rhinitis and sinusitis.* International journal of general medicine, 2018. **11**: p. 275-283.
124. Kraan, S., *Algal Polysaccharides, Novel Applications and Outlook*. Carbohydrates - Comprehensive Studies on Glycobiology and Glycotechnology. 2012.
125. Morris, C., *Carrageenan-Induced Paw Edema in the Rat and Mouse*, in *Inflammation Protocols*, P. Winyard and D. Willoughby, Editors. 2003, Humana Press. p. 115-121.
126. van de Velde, F. and A.D.R. Dr. Gerhard, *Carrageenan*, in *Biopolymers Online*. 2005, Wiley-VCH Verlag GmbH & Co. KGaA.
127. Sugita-Konishi, Y., et al., *Effects of carrageenans on the binding, phagocytotic, and killing abilities of macrophages to salmonella.* Bioscience, biotechnology, and biochemistry, 2003. **67**(6): p. 1425-1428.
128. Platt, N., et al., *Role for the class A macrophage scavenger receptor in the phagocytosis of apoptotic thymocytes in vitro.* Proceedings of the National Academy of Sciences of the United States of America, 1996. **93**(22): p. 12456-12460.
129. Tsuji, R.F., et al., *Suppression of allergic reaction by λ-carrageenan: Toll-like receptor 4/MyD88-dependent and -independent modulation of immunity.* Clinical & Experimental Allergy, 2003. **33**(2): p. 249-258.
130. McKim Jr, J.M., et al., *The common food additive carrageenan is not a ligand for Toll-Like- Receptor 4 (TLR4) in an HEK293-TLR4 reporter cell-line model.* Food and Chemical Toxicology, 2015. **78**(0): p. 153-158.
131. Bak, S.P., et al., *Scavenger Receptor-A–Targeted Leukocyte Depletion Inhibits Peritoneal Ovarian Tumor Progression.* Cancer Research, 2007. **67**(10): p. 4783-4789.
132. Kitchens, W.H., et al., *Macrophage Depletion Suppresses Cardiac Allograft Vasculopathy in Mice.* American Journal of Transplantation, 2007. **7**(12): p. 2675-2682.
133. Shigeaki, I., K. Shigeki, and T. Tadasu, *In vivo depletion of macrophages by desulfated ι-carrageenan in mice.* Journal of Immunological Methods, 1989. **124**(1): p. 17-24.
134. Chen, H., et al., *Degraded λ-carrageenan activates NF-κB and AP-1 pathways in macrophages and enhances LPS-induced TNF-α secretion through AP-1.* Biochimica et Biophysica Acta (BBA) - General Subjects, 2014. **1840**(7): p. 2162-2170.
135. Kalitnik, A., et al., *Oligosaccharides of κ/β-carrageenan from the red alga Tichocarpus crinitus and their ability to induce interleukin 10.* Journal of Applied Phycology, 2015: p. 1-9.
136. Rodrigues, S., et al., *Hybrid nanosystems based on natural polymers as protein carriers for respiratory delivery: Stability and toxicological evaluation.* Carbohydrate Polymers, 2015. **123**(0): p. 369-380.

137. Dionísio, M., et al., *Pullulan-based nanoparticles as carriers for transmucosal protein delivery.* European Journal of Pharmaceutical Sciences, 2013. **50**: p. 102-113.
138. Haijin, M., J. Xiaolu, and G. Huashi, *A κ-carrageenan derived oligosaccharide prepared by enzymatic degradation containing anti-tumor activity.* Journal of Applied Phycology, 2003. **15**(4): p. 297-303.
139. Raman, M. and M. Doble, *κ-Carrageenan from marine red algae, Kappaphycus alvarezii – A functional food to prevent colon carcinogenesis.* Journal of Functional Foods, 2015. **15**(0): p. 354-364.
140. Weiner, M.L., et al., *An infant formula toxicity and toxicokinetic feeding study on carrageenan in preweaning piglets with special attention to the immune system and gastrointestinal tract.* Food and Chemical Toxicology, 2015. **77**(0): p. 120-131.
141. Devi, N. and T.K. Maji, *Microencapsulation of isoniazid in genipin-crosslinked gelatin-A–κ-carrageenan polyelectrolyte complex.* Drug Development and Industrial Pharmacy, 2010. **36**(1): p. 56-63.
142. Grenha, A., et al., *Development of new chitosan/carrageenan nanoparticles for drug delivery applications.* Journal of Biomedical Materials Research Part A, 2010. **92A**(4): p. 1265-1272.
143. Yamada, K., et al., *Carrageenans can regulate the pulmonary absorption of antiasthmatic drugs and their retention in the rat lung tissues without any membrane damage.* International Journal of Pharmaceutics, 2005. **293**(1-2): p. 63-72.
144. Kaur, J., et al., *Cereal Starch Nanoparticles- A Prospective Food Additive: A Review.* Critical Reviews in Food Science and Nutrition, 2016: p. 1097-1107.
145. Le Corre, D., J. Bras, and A. Dufresne, *Starch nanoparticles: a review.* Biomacromolecules, 2010. **11**(5): p. 1139-53.
146. Rachmilewitz, J. and M.L. Tykocinski, *Differential effects of chondroitin sulfates A and B on monocyte and B-cell activation: evidence for B-cell activation via a CD44-dependent pathway.* Blood, 1998. **92**(1): p. 223-229.
147. Leteux, C., et al., *The Cysteine-Rich Domain of the Macrophage Mannose Receptor Is a Multispecific Lectin That Recognizes Chondroitin Sulfates a and B and Sulfated Oligosaccharides of Blood Group Lewis(a) and Lewis(x) Types in Addition to the Sulfated N-Glycans of Lutropin.* The Journal of Experimental Medicine, 2000. **191**(7): p. 1117-1126.
148. Ronca, F., et al., *Anti-inflammatory activity of chondroitin sulfate.* Osteoarthritis and Cartilage, 1998. **6**: p. 14-21.
149. Trif, M., et al., *Liposome formulations of chondroitin sulphate: Characterisation and in vitro evaluation of anti-inflammatory activity.* European Journal of Clinical Investigation, 2008. **38**: p. 68-69.
150. Lovu, M., G. Dumais, and P. du Souich, *Anti-inflammatory activity of chondroitin sulfate.* Osteoarthritis and Cartilage, 2008. **16**: p. S14-S18.
151. Tan, G.-K. and Y. Tabata, *Chondroitin-6-sulfate attenuates inflammatory responses in murine macrophages via suppression of NF-κB nuclear translocation.* Acta Biomaterialia, 2014. **10**(6): p. 2684-2692.
152. Surapaneni, L., et al., *Examination of Chondroitin Sulfate Molecular Weights on In Vitro Anti-inflammatory Activity.* Faseb Journal, 2013. **27**(Meeting Abstract Supplement): p. 846.15.

153. Orlowsky, E.W., et al., *Monosodium urate crystal induced macrophage inflammation is attenuated by chondroitin sulphate: pre-clinical model for gout prophylaxis?* Bmc Musculoskeletal Disorders, 2014. **15**: p. 1-6.
154. Suzuki, Y. and T. Yamaguchi, *Effects of Hyaluronic-Acid on Macrophage Phagocytosis and Active Oxygen Release.* Agents and actions, 1993. **38**(1-2): p. 32-37.
155. Geiser, M., *Update on macrophage clearance of inhaled micro- and nanoparticles.* Journal of Aerosol Medicine and Pulmonary Drug Delivery, 2010. **23**(4): p. 207-217.
156. Champion, J. and S. Mitragotri, *Shape induced inhibition of phagocytosis of polymer particles.* Pharmaceutical Research, 2009. **26**(1): p. 244-249.
157. Tsuda, A., F.S. Henry, and J.P. Butler, *Particle transport and deposition: basic physics of particle kinetics.* Comprehensive Physiology, 2013. **3**(4): p. 1437-1471.
158. Hinds, W.C., *Aerosol technology : properties, behavior, and measurement of airborne particles*. second edition ed. 1999, New York: Wiley.
159. Borghardt, J.M., C. Kloft, and A. Sharma, *Inhaled Therapy in Respiratory Disease: The Complex Interplay of Pulmonary Kinetic Processes.* Canadian respiratory journal, 2018. **2018**: p. 2732017-2732017.
160. Fahr, A., *Voigt's Pharmaceutical Technology*. 2018: John Wiley & Sons.
161. Bell, J.H., P.S. Hartley, and J.S.G. Cox, *Dry Powder Aerosols I: A New Powder Inhalation Device.* Journal of Pharmaceutical Sciences, 1971. **60**(10): p. 1559-1564.
162. Wang, S. and T. Langrish, *A review of process simulations and the use of additives in spray drying.* Food Research International, 2009. **42**(1): p. 13-25.
163. Vehring, R., *Pharmaceutical particle engineering via spray drying.* Pharmaceutical Research, 2008. **25**(5): p. 999-1022.
164. Gebreselassie, N., et al., *Tuberculosis research questions identified through the WHO policy guideline development process.* European Respiratory Journal, 2019. **53**(3): p. 1802407.
165. Alves, A., et al., *Inhalable antitubercular therapy mediated by locust bean gum microparticles* Molecules, 2016. **21**(702): p. 1-22.
166. Grenha, A., B. Seijo, and C. Remuñán-López, *Microencapsulated chitosan nanoparticles for lung protein delivery.* European Journal of Pharmaceutical Sciences, 2005. **25**: p. 427-437.
167. Muttil, P., et al., *Inhalable microparticles containing large payload of anti-tuberculosis drugs.* Eur J Pharm Sci, 2007. **32**(2): p. 140-50.
168. Lan, N.T., et al., *Randomised pharmacokinetic trial of rifabutin with lopinavir/ritonavir-antiretroviral therapy in patients with HIV-associated tuberculosis in Vietnam.* PLOS ONE, 2014. **9**(1): p. e84866.
169. Kumar, A.H., V. Sudha, and G. Ramachandran, *Simple and rapid liquid chromatography method for determination of rifabutin in plasma.* SAARC Journal of Tuberculosis, Lung Diseases and HIV/AIDS, 2012. **9**(2): p. 26-29.
170. Agency, E.M., *Guideline on quality of oral modified release products*. 2014, European Medicines Agency. p. 1-16.
171. Hiremath, P.S. and R.N. Saha, *Controlled release hydrophilic matrix tablet formulations of isoniazid: design and in vitro studies.* AAPS PharmSciTech, 2008. **9**(4): p. 1171-8.

172. Shah, V.P., et al., *In Vitro Dissolution Profile Comparison—Statistics and Analysis of the Similarity Factor, f2.* Pharmaceutical Research, 1998. **15**(6): p. 889-896.
173. USP, *United States Pharmacopeia USP-38*, U.S.P. Convention, Editor. 2015: Rockville.
174. *European Pharmacopoeia*, E.D.f.t.Q.o. Medicines, Editor. 2014.
175. Buttini, F., et al., *Aerodynamic Assessment for Inhalation Products: Fundamentals and Current Pharmacopoeial Methods*, in *Inhalation Drug Delivery*. 2013, John Wiley & Sons, Ltd. p. 91-119.
176. Zgoda, J. and J. Porter, *A convenient microdilution method for screening natural products against bacteria and fungi.* Pharmaceutical Biology, 2001. **39**(3): p. 221-225.
177. Caviedes, L., J. Delgado, and R.H. Gilman, *Tetrazolium Microplate Assay as a Rapid and Inexpensive Colorimetric Method for Determination of Antibiotic Susceptibility of Mycobacterium tuberculosis.* Journal of Clinical Microbiology, 2002. **40**(5): p. 1873-1874.
178. Vipra, A., et al., *Determining the minimum inhibitory concentration of bacteriophages: potential advantages.* Advances in Microbiology, 2013. **3**(02): p. 181.
179. Hoffman, E., et al., *Morphometric Characterization of Rat and Human Alveolar Macrophage Cell Models and their Response to Amiodarone using High Content Image Analysis.* Pharmaceutical Research, 2017.
180. Moritaka, H., et al., *Effects of pH, Potassium Chloride, and Sodium Chloride on the Thermal and Rheological Properties of Gellan Gum Gels.* Journal of Agricultural and Food Chemistry, 1995. **43**(6): p. 1685-1689.
181. Stanley, N., *Production, properties and uses of carrageenan.* Production and utilization of products from commercial seaweeds. FAO Fisheries Technical Paper, 1987. **288**: p. 116-146.
182. Tecante, A. and M.d.C.N. Santiago, *Solution properties of κ-carrageenan and its interaction with other polysaccharides in aqueous media*, in *Rheology*. 2012, IntechOpen.
183. Myneedu, L., *Effect of salts on the structure-function relationships of sodium kappa-carrageenan*. 2015, Purdue University.
184. Belotti, S., et al., *Spray-dried amikacin sulphate powder for inhalation in cystic fibrosis patients: The role of ethanol in particle formation.* European Journal of Pharmaceutics and Biopharmaceutics, 2015. **93**: p. 165-172.
185. Maretti, E., et al., *Solid lipid nanoparticle assemblies (SLNas) for an anti-TB inhalation treatment: A Design of Experiments approach to investigate the influence of pre-freezing conditions on the powder respirability.* International Journal of Pharmaceutics, 2016. **511**(1): p. 669-679.
186. Gardenhire, D.S., *Rau's Respiratory Care Pharmacology*. 9th ed. 2015: Elsevier Health Sciences.
187. Kyle, H., J. Ward, and J. Widdicombe, *Control of pH of airway surface liquid of the ferret trachea in vitro.* Journal of Applied Physiology, 1990. **68**(1): p. 135-140.
188. Griese, M., *Pulmonary surfactant in health and human lung diseases: state of the art.* European Respiratory Journal, 1999. **13**(6): p. 1455-1476.
189. Guerreiro, F., et al., *Spray-drying of konjac glucomannan to produce microparticles for an application as antitubercular drug carriers.* Powder Technology, 2019. **342**: p. 246-252.

190. Costa, P. and J.M. Sousa Lobo, *Modeling and comparison of dissolution profiles.* Eur J Pharm Sci, 2001. **13**(2): p. 123-33.
191. Ritger, P.L. and N.A. Peppas, *A simple equation for description of solute release II. Fickian and anomalous release from swellable devices.* Journal of Controlled Release, 1987. **5**(1): p. 37-42.
192. Ritz, N., et al., *Susceptibility of Mycobacterium bovis BCG Vaccine Strains to Antituberculous Antibiotics.* Antimicrobial Agents and Chemotherapy, 2009. **53**(1): p. 316-318.
193. Shishido, Y., et al., *Anti-tuberculosis drug susceptibility testing of Mycobacterium bovis BCG Tokyo strain.* International Journal of Tuberculosis and Lung Disease, 2007. **11**(12): p. 1334-1338.
194. Gaspar, D.P., et al., *Microencapsulated Solid Lipid Nanoparticles as a Hybrid Platform for Pulmonary Antibiotic Delivery.* Molecular Pharmaceutics, 2017. **14**(9): p. 2977-2990.
195. Cunha, L., et al., *Inhalable chitosan microparticles for simultaneous delivery of isoniazid and rifabutin in lung tuberculosis treatment.* Drug Development and Industrial Pharmacy, 2019: p. 1-35.
196. ISO, *Biological evaluation of medical devices Part 5: Tests for in vitro cytotoxicity*, in *10993-5*, I.O.f. Standardization, Editor. 2009.
197. Artursson, P., D. Johansson, and I. Sjöholm, *Receptor-mediated uptake of starch and mannan microparticles by macrophages: relative contribution of receptors for complement, immunoglobulins and carbohydrates.* Biomaterials, 1988. **9**(3): p. 241-246.
198. Toossi, Z., *The inflammatory response in Mycobacterium tuberculosis infection.* Arch Immunol Ther Exp (Warsz), 2000. **48**(6): p. 513-9.
199. Smith, S., et al., *Local role for tumor necrosis factor alpha in the pulmonary inflammatory response to Mycobacterium tuberculosis infection.* Infect Immun, 2002. **70**(4): p. 2082-9.
200. Gray, M.A., et al., *Phagocytosis Enhances Lysosomal and Bactericidal Properties by Activating the Transcription Factor TFEB.* Curr Biol, 2016. **26**(15): p. 1955-1964.
201. Inoue, H., et al., *Pseudomonas stimulates interleukin-8 mRNA expression selectively in airway epithelium, in gland ducts, and in recruited neutrophils.* American journal of respiratory cell and molecular biology, 1994. **11**(6): p. 651-663.
202. Laichalk, L.L., et al., *Tumor necrosis factor mediates lung antibacterial host defense in murine Klebsiella pneumonia.* Infection and immunity, 1996. **64**(12): p. 5211-5218.
203. Chanput, W., et al., *Transcription profiles of LPS-stimulated THP-1 monocytes and macrophages: a tool to study inflammation modulating effects of food-derived compounds.* Food Funct, 2010. **1**(3): p. 254-61.
204. Sakeer, K., et al., *Starch materials as biocompatible supports and procedure for fast separation of macrophages.* Carbohydrate Polymers, 2017. **163**: p. 108-117.
205. Sharma, R., et al., *Uptake of inhalable microparticles affects defence responses of macrophages infected with Mycobacterium tuberculosis H37Ra.* Journal of Antimicrobial Chemotherapy, 2007. **59**(3): p. 499-506.
206. Arpagaus, C., N. Schafroth, and A.G. Büchi Labortechnik, *Spray dried biodegradable polymers as target material for controlled drug delivery.* Best@ Büchi, 2007.

207. Lee, E.S., et al., *Protein complexed with chondroitin sulfate in poly(lactide-co-glycolide) microspheres.* Biomaterials, 2007. **28**(17): p. 2754-2762.
208. Lim, J.J., et al., *Development of nano- and microscale chondroitin sulfate particles for controlled growth factor delivery.* Acta Biomaterialia, 2011. **7**(3): p. 986-995.
209. Huang, L., et al., *Preparation of chitosan/chondroitin sulfate complex microcapsules and application in controlled release of 5-fluorouracil.* Carbohydrate Polymers, 2010. **80**(1): p. 168-173.
210. Hirota, K., et al., *Optimum conditions for efficient phagocytosis of rifampicin-loaded PLGA microspheres by alveolar macrophages.* Journal of Controlled Release, 2007. **119**(1): p. 69-76.
211. Audran, R., et al., *Encapsulation of peptides in biodegradable microspheres prolongs their MHC class-I presentation by dendritic cells and macrophages in vitro.* Vaccine, 2003. **21**(11): p. 1250-1255.
212. Reddy, S.T., M.A. Swartz, and J.A. Hubbell, *Targeting dendritic cells with biomaterials: developing the next generation of vaccines.* Trends in Immunology, 2006. **27**(12): p. 573-579.
213. Zhou, Q.T., et al., *Improving aerosolization of drug powders by reducing powder intrinsic cohesion via a mechanical dry coating approach.* International Journal of Pharmaceutics, 2010. **394**(1): p. 50-59.
214. Deng, Q., et al., *Particle deposition in the human lung: Health implications of particulate matter from different sources.* Environmental Research, 2019. **169**: p. 237-245.
215. Heyder, J., et al., *Deposition of particles in the human respiratory tract in the size range 0.005–15 μm.* Journal of Aerosol Science, 1986. **17**(5): p. 811-825.
216. Vostrikov, V.V., et al., *Distribution coefficient of rifabutin in liposome/water system as measured by different methods.* European Journal of Pharmaceutics and Biopharmaceutics, 2008. **68**(2): p. 400-405.
217. Gupta, K.C. and F.H. Jabrail, *Effect of molecular weight and degree of deacetylation on controlled release of isoniazid from chitosan microspheres.* Polymers for Advanced Technologies, 2008. **19**(5): p. 432-441.
218. Martinez, A.W., et al., *Effects of crosslinking on the mechanical properties, drug release and cytocompatibility of protein polymers.* Acta Biomaterialia, 2014. **10**(1): p. 26-33.
219. Fronius, M., W.G. Clauss, and M. Althaus, *Why Do We have to Move Fluid to be Able to Breathe?* Frontiers in physiology, 2012. **3**: p. 146-146.
220. Hoffman, E., et al., *In Vitro Multiparameter Assay Development Strategy toward Differentiating Macrophage Responses to Inhaled Medicines.* Molecular Pharmaceutics, 2015. **12**(8): p. 2675-2687.
221. Forbes, B., et al., *Challenges for inhaled drug discovery and development: Induced alveolar macrophage responses.* Advanced Drug Delivery Reviews, 2014. **71**: p. 15-33.
222. Higashi, N., et al., *The Macrophage C-type Lectin Specific for Galactose/N-Acetylgalactosamine Is an Endocytic Receptor Expressed on Monocyte-derived Immature Dendritic Cells.* Journal of Biological Chemistry, 2002. **277**(23): p. 20686-20693.
223. Alves, A.D., et al., *Inhalable Antitubercular Therapy Mediated by Locust Bean Gum Microparticles.* Molecules, 2016. **21**(6).

224. Hinderliter, P.M., et al., *ISDD: a computational model of particle sedimentation, diffusion and target cell dosimetry for in vitro toxicity studies.* Particle and fibre toxicology, 2010. **7**(1): p. 36.
225. Laskin, D.L., et al., *Macrophages and tissue injury: agents of defense or destruction?* Annual review of pharmacology and toxicology, 2011. **51**: p. 267-288.
226. David, J.M., et al., *The IL-8/IL-8R Axis: A Double Agent in Tumor Immune Resistance.* Vaccines, 2016. **4**(3): p. 22.
227. Pichert, A., et al., *Characterization of the interaction of interleukin-8 with hyaluronan, chondroitin sulfate, dermatan sulfate and their sulfated derivatives by spectroscopy and molecular modeling.* Glycobiology, 2011. **22**(1): p. 134-145.
228. Frevert, C.W., et al., *Binding of interleukin-8 to heparan sulfate and chondroitin sulfate in lung tissue.* Am J Respir Cell Mol Biol, 2003. **28**(4): p. 464-72.
229. Vallières, M. and P. du Souich, *Modulation of inflammation by chondroitin sulfate.* Osteoarthritis and Cartilage, 2010. **18**: p. S1-S6.
230. Guillon, A., et al., *Insights on animal models to investigate inhalation therapy: Relevance for biotherapeutics.* International Journal of Pharmaceutics, 2018. **536**(1): p. 116-126.
231. Mestas, J. and C.C.W. Hughes, *Of Mice and Not Men: Differences between Mouse and Human Immunology.* The Journal of Immunology, 2004. **172**(5): p. 2731.
232. Galli, S.J., M. Tsai, and A.M. Piliponsky, *The development of allergic inflammation.* Nature, 2008. **454**(7203): p. 445-454.
233. Dullaers, M., et al., *The who, where, and when of IgE in allergic airway disease.* Journal of Allergy and Clinical Immunology, 2012. **129**(3): p. 635-645.
234. van de Veen, W. and M. Akdis, *Role of IgG4 in IgE-mediated allergic responses.* Journal of Allergy and Clinical Immunology, 2016. **138**(5): p. 1434-1435.
235. Gocki, J. and Z. Bartuzi, *Role of immunoglobulin G antibodies in diagnosis of food allergy.* Postepy dermatologii i alergologii, 2016. **33**(4): p. 253-256.
236. Prussin, C. and D.D. Metcalfe, *4. IgE, mast cells, basophils, and eosinophils.* Journal of Allergy and Clinical Immunology, 2003. **111**(2): p. S486-S494.
237. Male, D.K., *Immunology*. Seventh Edition ed. 2006: Mosby Elsevier.
238. Vieira, P. and K. Rajewsky, *The half-lives of serum immunoglobulins in adult mice.* European journal of immunology, 1988. **18**(2): p. 313-316.
239. Shade, K.T., M.E. Conroy, and R.M. Anthony, *IgE Glycosylation in Health and Disease*, in *Current Topics in Microbiology and Immunology*. 2019, Springer.
240. Calheiros, A.S., et al., *Role of the IgE-Mediated System in Eosinophil Recruitment Triggered by Two Consecutive Cycles of Sensitisation and Challenge in Rats.* International Archives of Allergy and Immunology, 2001. **126**(4): p. 325-334.
241. Platts-Mills, T.A., *The role of immunoglobulin E in allergy and asthma.* Am J Respir Crit Care Med, 2001. **164**(8 Pt 2): p. S1-5.

242. Cheng, L.E., et al., *IgE-activated basophils regulate eosinophil tissue entry by modulating endothelial function.* The Journal of experimental medicine, 2015. **212**(4): p. 513-524.
243. Michael, B., et al., *Evaluation of Organ Weights for Rodent and Non-Rodent Toxicity Studies: A Review of Regulatory Guidelines and a Survey of Current Practices.* Toxicologic Pathology, 2007. **35**(5): p. 742-750.
244. Drent, M., et al., *Usefulness of lactate dehydrogenase and its isoenzymes as indicators of lung damage or inflammation.* European Respiratory Journal, 1996. **9**(8): p. 1736.
245. Kochar, R. and M.B. Fallon, *Pulmonary Diseases and the Liver.* Clinics in Liver Disease, 2011. **15**(1): p. 21-37.
246. Colldahl, H., *A Study of Serum Enzymes in Patients Suffering from Periods of Respiratory Insufficiency, Especially Asthma and Emphysema: Preliminary Report.* Acta Medica Scandinavica, 1960. **166**(5): p. 399-400.
247. O'Connell, K.E., et al., *Practical murine hematopathology: a comparative review and implications for research.* Comparative medicine, 2015. **65**(2): p. 96-113.
248. Dunning, K. and A.O. Safo, *The ultimate Wright-Giemsa stain: 60 years in the making.* Biotechnic & Histochemistry, 2011. **86**(2): p. 69-75.
249. Shi, Z.D., A.E. Wakil, and D.C. Rockey, *Strain-specific differences in mouse hepatic wound healing are mediated by divergent T helper cytokine responses.* Proceedings of the National Academy of Sciences of the United States of America, 1997. **94**(20): p. 10663-10668.
250. Hilton, J., et al., *The mouse IgE test for the identification of potential chemical respiratory allergens: considerations of stability and controls.* Journal of Applied Toxicology, 1996. **16**(2): p. 165-170.
251. Rani, A., R. Baruah, and A. Goyal, *Physicochemical, antioxidant and biocompatible properties of chondroitin sulphate isolated from chicken keel bone for potential biomedical applications.* Carbohydrate Polymers, 2017. **159**: p. 11-19.
252. Imeson, A., *Food stabilisers, thickeners and gelling agents*. 2010, Oxford, UK: Wiley Online Library.

Supplementary information

Impact of spray-drying on polymer characteristics

Methods

Molecular mass distribution

High Performance Size Exclusion Chromatography (HPSEC) was selected to define the molar mass profile of ChS, both in the form of polymer and microparticles (unloaded). High performance liquid chromatography (HPLC) equipment used was 1100 series Agilent (Germany) supplied with two columns (300 × 7.8 mm) in series TSKGel G3000PW$_{XL}$ and TSKGel G2500PW$_{XL}$ (Tosoh Bioscience, Stuttgart, Germany), and with a PWX-guard column (40 x 6 mm). Both samples were filtered (0.45 µm) and analysed using a refractive index (RI) detector, under the following conditions: 70 °C, Milli-Q water as mobile phase and flow rate of 0.4 mL/min. The used standards were dextrans (DX) with molecular weight ranging from 12 to 80 kg/mol (Fluka, MO, USA). Analyses were performed at least in duplicate.

Rheology: Steady-state shear measurements

A rheological study was performed on ChS polymer, unloaded ChS microparticles and ChS/INH/RFB microparticles prepared with either ethanol or HCl. Aqueous dispersions at 10 g/L were prepared in all cases, dispersing the corresponding amount of sample in distilled water, under stirring for 15 min, at room temperature. Steady-shear flow curves in terms of apparent viscosity *vs.* shear rate were conducted on a controlled-stress rheometer (MCR 302, Paar Physica, Austria) using a plate-plate geometry (25 mm diameter, 0.5 mm gap). Flow measurements were obtained by decreasing and, then, increasing shear rate following a logarithmic ramp to assess the presence of hysteresis. All trials were made at 25 ºC and were controlled by a Peltier system (± 0.01). In all cases, aqueous dispersions were sealed with light paraffin oil to avoid water loss during measurements and were rested for 10 min in the measuring system to allow sample structural equilibration. All trials were performed at least in triplicate.

Results and discussion

Spray-drying was the technique selected to produce the microparticles, as it permits tailoring their properties for deep lung delivery. Nevertheless, it was deemed important to study the impact of the process on the polymer properties. The molecular mass distribution of ChS was investigated as raw material and after the spray-drying process, and the obtained profiles are exhibited in the Figure S1. In both samples, the molecular mass was greater than 80 kDa, which was the highest standard used. The peaks of the two samples evidenced similar distribution profiles and, although showing a slight difference, the molecular mass was considered similar. Rani et al. (2017) isolated chondroitin sulfate from the cartilage of chicken keel bone and reported the peak of molecular mass at 100 kDa [251].

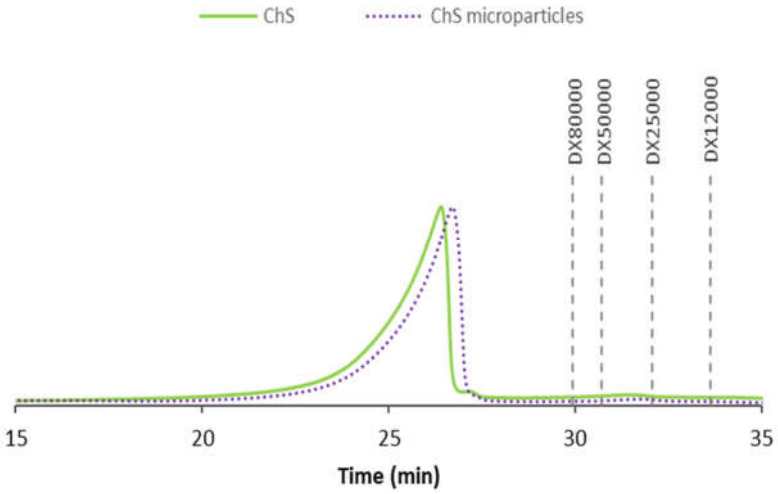

Figure S1. HPSEC profiles of chondroitin sulphate (ChS) as raw material, represented by continuous line, and after processing by spray-drying (microparticles), illustrated by dotted line.

A rheological study was also performed, evaluating the rheological behaviour of the polymer before and after spray-drying and further determining the effect of associating the drugs. Figure S2 displays the steady shear flow curves for tested aqueous dispersions (10 g/L) at 25 ºC. In all cases, a shear-thinning behaviour was observed, with the apparent viscosity decreasing with increasing shear rate (about 2 decades). The apparent viscosity drop can be explained by the

alignment of long chain molecules with each other at the highest shear rates, leading to easier flows. This behaviour is characteristic of pseudoplastic fluids, which may be described by the power law model, and the viscosity trend is consistent with a typical non-entangled polymer behaviour in the dilute regime [252]. At a fixed shear rate, it can be clearly observed that ChS polymer exhibited the lowest apparent viscosity over the tested range. After processing by spray-drying, higher apparent viscosity values were observed (about 2-fold), suggesting an effect of the process on polymer characteristics. Since slight differences were identified in the HPSEC profiles, this behaviour suggests that some aggregates of the proper polymer chains may have formed during microparticle processing, which could involve higher flow resistance and, consequently, higher apparent viscosities. The samples corresponding to post-spraying drying products, all registered similar behaviour, indicating an absence of effect of both drug association and used solvents. It should be further highlighted that no hysteresis was observed in the tested samples, with the consequent advantage from the industrial point of view.

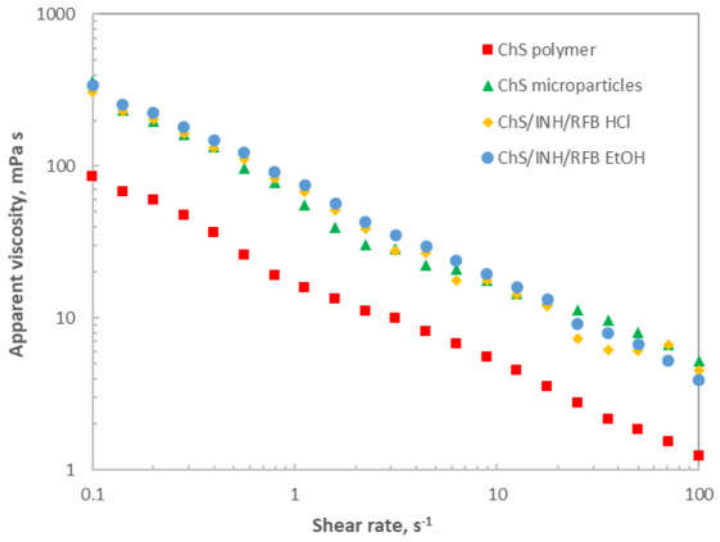

Figure S2. Steady shear flow curves for aqueous dispersions of ChS polymer, ChS unloaded microparticles and ChS/INH/RFB microparticles produced with ethanol (EtOH) or HCl, at polymer concentration of 10 g/L and 25 ºC.

Figures permissions

Copyright Clearance Center

Note: Copyright.com supplies permissions but not the copyrighted content itself.

1 PAYMENT 2 REVIEW 3 CONFIRMATION

Step 3: Order Confirmation

Thank you for your order! A confirmation for your order will be sent to your account email address. If you have questions about your order, you can call us 24 hrs/day, M-F at +1.855.239.3415 Toll Free, or write to us at info@copyright.com. This is not an invoice.

Confirmation Number: 11836131
Order Date: 07/28/2019

If you paid by credit card, your order will be finalized and your card will be charged within 24 hours. If you choose to be invoiced, you can change or cancel your order until the invoice is generated.

Payment Information

Ana Grenha
amgrenha@ualg.pt
+351 433512898001007556
Payment Method: n/a

Order Details

Current pharmaceutical design

Order detail ID:	71961847
Order License Id:	4637720734851
ISSN:	1381-6128
Publication Type:	Journal
Volume:	
Issue:	
Start page:	
Publisher:	BENTHAM SCIENCE PUBLISHERS LTD.

Permission Status: Granted
Permission type: Republish or display content
Type of use: Thesis/Dissertation

Requestor type	Author of requested content
Format	Electronic
Portion	chart/graph/table/figure
Number of charts/graphs/tables/figures	7
The requesting person/organization	Ana Grenha
Title or numeric reference of the portion(s)	Figure 1, 3, 4, 5, 6, 7, Table 1, 2
Title of the article or chapter the portion is from	Activation of Macrophages: Establishing a Role for Polysaccharides in Drug Delivery Strategies Envisaging Antibacterial Therapy
Editor of portion(s)	N/A
Author of portion(s)	Grenha, Ana ; Rodrigues, Susana

Volume of serial or monograph	21
Issue, if republishing an article from a serial	33
Page range of portion	4869-4879
Publication date of portion	Oct 1, 2015
Rights for	Main product
Duration of use	Life of current edition
Creation of copies for the disabled	no
With minor editing privileges	no
For distribution to	Worldwide
In the following language(s)	Original language of publication
With incidental promotional use	no
Lifetime unit quantity of new product	Up to 499
Title	Development of polysaccharide-based carriers for pulmonary tuberculosis therapy
Institution name	University of Algarve
Expected presentation date	Jul 2019

Note: This item will be invoiced or charged separately through CCC's **RightsLink** service. More info **$ 0.00**

This is not an invoice.

Total order items: 1

Order Total: 0.00 USD

Confirmation Number: 0

Special Rightsholder Terms & Conditions

The following terms & conditions apply to the specific publication under which they are listed

There are no special terms.

Close

Confirmation Number: 0

Citation Information

There are no Citations.

Close

Animal assay approval by DGAV

GOVERNO DE PORTUGAL | MINISTÉRIO DA AGRICULTURA E DO MAR

dgav Direção Geral de Alimentação e Veterinária

Exma Senhora
Doutora Maria Manuela Gaspar
Faculdade de Farmácia da Universidade de Lisboa
Departamento de Farmácia Galénica e Tecnologia Farmacêutica
Campus do Lumiar
Estrada do Paço do Lumiar, 22, Edifício F, R/C
1649 – 038 LISBOA

2013-09-02 023517

Nossa referência	Vossa referência	Vossa data
0421/000/000 /2013		

Assunto: **PROTEÇÃO DOS ANIMAIS UTILIZADOS PARA FINS EXPERIMENTAIS E/OU OUTROS FINS CIENTÍFICOS – PEDIDO DE AUTORIZAÇÃO PARA REALIZAÇÃO DE PROJECTO DE EXPERIMENTAÇÃO ANIMAL**

Na sequência do pedido efetuado por V. Exª no sentido de poder ser autorizada a realização do projeto experimental designado **"Development of microparticulate systems to target alveolar macrophages in tuberculosis therapy"**, tendo como investigadora responsável a **Doutora Ana Grenha**, cabe-me informar que o mesmo foi levado à consideração dos membros da Comissão Consultiva prevista na alínea b) do nº 49, da Portaria nº 1005/92, de 23 de Outubro, sendo que os mesmos não levantaram qualquer objeção à solicitação supra referida.

Mais se informa V. Exª que esta Direção Geral, depois de esclarecidas as dúvidas que a sua análise nos levantou, nada teve a opôr ao projeto apresentado, pelo que o mesmo foi autorizado, ao abrigo do nº 8º do mesmo diploma legislativo.

Com os melhores cumprimentos,

A Diretora Geral

As) Maria Teresa Villa de Brito

DBEA/APM